



The University of
Nottingham

UNITED KINGDOM • CHINA • MALAYSIA

Bio-molecular gradient surfaces for biological recognition

Enzo Fornari BSc, MSc (Hons)

Thesis submitted to the University of Nottingham for
the degree of Doctor of Philosophy

DECEMBER 2014

Acknowledgements

I would like first thanks my supervisors, Professor Clive Roberts, and my co-supervisors Professor Philip Williams and Professor Stephanie Allen, for the technical discussions on every aspect of the project, and for the funding to carry out this research.

Thanks to Professor James O'Shea to give me the possibility to be part of the Marie Curie SMALL project, an amazing experience that I will never forget.

Special thanks to my family and my partner to support and encourage me through this journey.

Abstract

The use of protein microfluidic systems is of growing interest for a variety of applications, including but not limited to tissue engineering, drug delivery and biosensors. The means by which to control chemistries on substrates for biological and medical applications is therefore in high demand.

Here the creation of a bio-functional gradient on silica and polymeric surfaces using a micro fluidic technique, for the guidance of cell adhesion and functionality, using AFM tools for protein imaging and force spectroscopy investigation is reported.

Atomic force microscopy (AFM) is a high resolution microscopic technique highly used in biological investigations, allowing conformational elucidation of protein deposition on the substrate.

In this work application of the techniques of AFM, fluorescence microscopy and cell adhesion studies were used to assess the protein deposition along the microfluidic system. From the fluorescence analysis, it was immediately observed that successful protein immobilization on both substrates was achieved. Differences in fluorescence intensity were also registered along the microfluidic channel (start and end point) suggesting a variation in protein adsorption along the channel. The AFM imaging analysis conducted on the same samples revealed a difference in surface coverage considering the injection and end point (from 70% to 14% respectively) of the protein pattern.

The difference in protein density registered along the fibronectin pattern was tested using a functionalised probe AFM technique, allowing molecular resolution of ligands in a physiological environment. A difference in the percentage of observed adhesion events was registered considering the start and end point of the microfluidic pattern, from 90% to 37% respectively. This is likely due to the fact that at the higher surface concentration there is a higher probability of the functionalised tip interacting with multiple fibronectin molecules, as confirmed from the presence of multiple adhesions at start point with a higher adhesion force of $82 \text{ pN} \pm 7.4 \text{ pN}$.

To complement the AFM force measurements, protein functionality was tested by investigating the cell adhesion, shape and migration on the protein pattern. The fibronectin protein gradient was shown to control cell adhesion and migration along the patterns, demonstrating that this system can be used for biological applications to monitor the cell behaviour using difference protein concentration and cell density all in the same microfluidic channel. The ability to control cell adhesion and migration on substrates could be of significant interest when researching possible applications in future tissue engineering and biological studies.

The combination of AFM and fluorescence microscopy techniques for protein density investigation used in this work demonstrated that protein deposition and arrangement on substrate play an important role in cell adhesion and migration studies.

Table of Contents

Acknowledgements	0
Abstract	1
List of Figures	6
List of tables	13
List of abbreviations	14
1. Introduction	16
1.1. Bio-molecular Gradients	16
1.1.1. Evolutionarily conserved signalling	16
1.1.2. Traditional gradient generating methods.....	17
1.1.3. Limits of traditional methods	20
1.1.4. Microfluidic methods.....	20
1.1.5. Review of biological studies using micro-fluidic gradient generators. 22	
1.1.6. Impact in biological community	23
1.2. Microfluidic device	25
1.2.1. Properties of PDMS (poly-dimethyl-siloxane)	25
1.2.2. Chemistry of PDMS.....	26
1.2.3. Optical properties PDMS	26
1.2.4. Fabrication microfluidic device using PDMS.....	27
1.2.5. Flow in micro-channels.....	28
1.2.6. Critique of PDMS for cell biological studies.....	29
1.3. Microfluidic tools for cell biology	31
1.3.1. Micro-environment control.....	31
1.3.2. Micro-fluidic precise spatial-temporal gradients	33
1.3.3. Liquid flow in channel for complex functionalization.....	34
1.3.4. Comments.....	35
1.4. Summary	36
1.5. Aims of work	38
1.6. Future perspectives	40
2. Materials and methods	42
2.1 Design of silicon master and PDMS micro-channel fabrication.	42
2.1.1. Materials.....	42

2.1.2.	Methods.....	42
2.2	Creation of protein patterns and surface analysis.....	48
2.2.1.	Materials.....	48
2.2.2.	Methods.....	48
2.3	Fibroblasts micro-patterning.....	54
2.3.1.	Materials.....	54
2.3.2.	Methods.....	54
2.4	Brief review of instrumental and photolithography methods.....	59
2.4.1.	Photolithography.....	59
2.4.2.	Atomic force microscopy.....	62
2.4.3.	Fluorescence microscopy.....	70
2.4.4.	Cell micro-patterning.....	72
3.	Protein patterning and surface characterization.....	75
3.1.	Introduction.....	75
3.2.	Methods: AFM analysis.....	76
3.2.1.	AFM Probe Functionalization.....	76
3.3.	Results and discussion.....	78
3.3.1.	Patterning of proteins using the microfluidic technique.....	78
3.3.2.	Protein pattern AFM characterization.....	84
3.3.3.	AFM functional studies.....	92
3.4.	Summary.....	98
4.	Micro-patterning of cells using fibronectin patterns.....	99
4.1.	Introduction.....	99
4.1.1.	Fibronectin as a protein component of the ECM and integrins role in cell proliferation, survival and migration.....	101
4.2.	Results and discussion.....	107
4.2.1.	Substrate functionalization using Pluronics F127.....	107
4.2.2.	3T3 mouse fibroblasts cells adhesion studies.....	112
4.2.3.	Immortalized mesenchymal stem cells (i-HMSC) adhesion studies..	118
4.3.	Summary.....	120
5.	Cell migration studies: Influence of protein adsorption on cell behaviour.....	121
5.1.	Introduction.....	121
5.2.	Results and discussion.....	123

5.2.1.	3T3 mouse fibroblasts migration on fibronectin patterns	123
5.2.2.	i-HMSC immortalised mesenchyme stem cells migration on fibronectin patterns.....	131
5.3.	Summary	137
6.	Reflections and remarks	138
6.1.	Brief overall summary of the surface characterisation and cell behaviour studies.....	138
6.2.	Surface characterization and protein functionality	142
6.2.1.	Fluorescence microscopy versus AFM functionalised probe technique. 142	
6.2.2.	Assessment of fibronectin influence in cell behaviour.....	145
7.	Conclusions and future work	147
	Reference List	151

List of Figures

FIGURE 1.1: TRADITIONAL METHODS REPRESENTATION, 1A BOYDEN CHAMBER, 1B ZIGMOND CHAMBER AND 1C DUNN CHAMBER.	19
FIGURE 1.2: MICROFLUIDICS DEVICES. IN FIGURE A PRE-MIXER GRADIENT GENERATOR, IN FIGURE B T-SENSOR.	22
FIGURE 1.3: SCHEMATIC REPRESENTATION OF FLOW IN MICRO-CHANNELS. IN A TURBULENCE TAKES PLACE INSIDE CHANNEL, IN B LAMINAR FLOW IS OCCURRING.	29
FIGURE 1.4: PRE-MIX MICRO-GRADIENT GENERATOR DEVICE THAT RESTRICTS ORTHOGONAL DIFFUSION OF CHEMICAL COMPOUNDS ⁽²⁾	34
FIGURE 2.1: REPRESENTATION OF THE MASK DESIGN REALISED USING THE CAD PROGRAMME. 9 SQUARES WITH DIMENSION 15 X 15 MM WERE DESIGNED CONTAINING DIFFERENT MICRO STRUCTURES. ON THE LEFT SIDE THE WIDTH DIMENSION OF EACH MICRO STRUCTURE IS REPORTED. THE ETCH DEPTH USED FOR THE REALISATION OF THE MICRO STRUCTURES WAS 10.5 ± 0.5 MICRONS. A, B AND C MICROSTRUCTURES REPORTED ON THE RIGHT SIDE SHOW DIFFERENT DESIGNS WITH WIDTH DIMENSIONS OF 100 AND 200 µM FOR A AND C AND IN B DIMENSIONS OF 100 µM IN THE THINNER CHANNEL AND 350 µM IN THE THICKER CHANNEL.	44
FIGURE 2.2: PROCEDURE FOR MASK DEVELOPMENT. A, B, C, D AND E REPRESENTED PHASES INVOLVED IN CHROME PROCESS. A) "BLANK" SAMPLE, B) LIGHT EXPOSURE, C) DEVELOPMENT, D) ETCHING, E) STRIPPING.	45
FIGURE 2.3: STEPS INVOLVED IN SILICON MASTER FABRICATION. A) SPUN COATED, B) BAKING, C) AND D) UV RADIATION EXPOSURE AND BAKING AFTER EXPOSURE RESPECTIVELY, E) DEVELOPMENT, F) MASTER FABRICATION.	46
FIGURE 2.4: ELASTOMERIC STAMP FABRICATION (PDMS) IN A) THE SILICON MASTER, B) MIXTURE OF ELASTOMERIC RUBBER BASE AND CROSS-LINKER ON TOP OF THE MASTER C) POLYMERIZATION, D) PEEL THE STAMP OFF.	47
FIGURE 2.5: IN A: SCHEMATIC REPRESENTATION OF THE MICROFLUIDIC CHANNEL SHAPE USED FOR THE CREATION OF THE PDMS TO GUIDE PROTEIN DEPOSITION (A ₂ , A ₃) AND CELL PATTERNING FORMATION (A ₁ , A ₃). THE WIDTH, LENGTH AND DEPTH OF THE MICROSTRUCTURES USED ARE	

ALSO REPORTED. IN B: SCHEMATIC REPRESENTATION OF THE PROCEDURE USED TO FUNCTIONALISE THE NON-TCP USING PLURONIC F127. STEP1: POURING A SOLUTION OF PLURONIC F127 IN THE PLASTIC PLATE (APPROX. 2ML). THIS WAS LEFT OVERNIGHT TO GET A THICK FILM ON THE SURFACE; STEP2 & 3: AFTER OXYGEN PLASMA TREATMENT OF SURFACE AND ELASTOMERIC STAMP, PUT IN CONTACT THE PDMS STAMP WITH THE PLASTIC SUBSTRATE AND INJECT FIBRONECTIN; STEP4: TAKE THE PDMS OFF AND STEP5: SEEDING FIBROBLASTS 3T3 WITH A CONCENTRATION OF 10^6 CELLS 56

FIGURE 2.6: AFM APPARATUS SCHEMATIC REPRESENTATION. IN THE FIGURE ARE REPORTED THE COMPONENTS OF ATOMIC FORCE MICROSCOPE: A PHOTODIODE DETECTOR, LASER, CANTILEVER AND A TIP ATTACHED TO THE CANTILEVER 64

FIGURE 2.7: SCHEMATIC REPRESENTATION OF FORCE VARIATION BETWEEN AN AFM TIP AND SAMPLE. 65

FIGURE 2.8: SCHEMATIC DEFLECTION VS Z-PIEZO DISPLACEMENT CURVE. IN REGION A, NO DEFLECTION OCCURS. IN REGION B, PROBE ADHERES TO THE SURFACE AND IN REGION C THE PROBE IS IN CONTACT WITH THE SURFACE AND THE CANTILEVER DEFLECTS..... 69

FIGURE 2.9: BASIC PRINCIPLE OF THE FLUORESCENCE MICROSCOPY. THE LIGHT SOURCE EMITS LIGHT THAT IS REFLECTED BY THE MIRROR THROUGH THE OBJECTIVE INTO THE SAMPLE. THE EXCITATION OF THE FLUOROPHORE WILL EMIT LIGHT OF A LONGER WAVELENGTH, WHICH WILL GO BACK THROUGH THE OBJECTIVE AND FORM THE FINAL IMAGE ON A DETECTOR..... 71

FIGURE 2.10: REPRESENTATION OF MICROFLUIDIC AND STENCIL PATTERNING METHODS. IN A NEGATIVE PHOTORESIST PATTERN, IN A_1, B_1, C_1 MICROFLUIDIC PATTERNING METHOD SHOWING PDMS SEALING TO THE SUBSTRATE, MICROFLUIDIC TECHNIQUE APPLICATION AND PATTERNING RESPECTIVELY. IN A_2, B_2, C_2 STENCIL PATTERNING METHOD SHOWING STENCIL DEPOSITION, EXPOSURE TO THE MATERIAL AND PATTERNING REALIZATION RESPECTIVELY 74

FIGURE 3.1: FN MONOMER COMPOSITION; ADOPTED FROM PATEL AND CO-WORKERS⁽¹²³⁾ 77

FIGURE 3.2: PROCEDURE TO CREATE PATTERNING OF PROTEINS ON SUBSTRATES. A) STAMP AND SUBSTRATES REPRESENTATION, B) OXYGEN-PLASMA TREATMENT OF PDMS, C) AND D) INJECTION OF PROTEIN SOLUTIONS IN THE MICROFLUIDIC CHANNELS, AND ABSORPTION, E) PATTERNING OF PROTEINS..... 81

FIGURE 3.3: PROTEIN PATTERNS ANALYSIS USING FLUORESCENCE MICROSCOPY TECHNIQUE. A) NOT GOOD ADHESION BETWEEN PDMS AND SILICA WAFER SUBSTRATE, BEFORE OXYGEN PLASMA TREATMENT, A_1) PROTEIN PATTERN ANALYSIS USING FLUORESCENCE MICROSCOPY, B) GOOD

ADHESION BETWEEN PDMS AND SILICA WAFER SUBSTRATE, AFTER OXYGEN PLASMA TREATMENT, B₁) PROTEIN PATTERN ANALYSIS AFTER OXYGEN PLASMA TREATMENT USING FLUORESCENCE MICROSCOPY TECHNIQUE. 82

FIGURE 3.4: REPRESENTATION OF PROTEIN FLUORESCENCE SURFACE ANALYSIS USING FLUORESCENCE MICROSCOPY TECHNIQUE. IN A AND B REPRESENTATION OF THE MICRO-STRUCTURE DESIGN, LENGTH AND DEPTH MEASUREMENTS USED FOR THE FIBRONECTIN AND ALBUMIN DEPOSITION ON SUBSTRATES RESPECTIVELY. AN EXAMPLE OF FLUORESCENCE IMAGES OF THE SILICON WAFER AFTER FN01 (A) AND BSA (B) IMMOBILIZATION WERE REPORTED. ANALYSIS OF THE FLUORESCENCE INTENSITY IS REPORTED ON BOTH SUBSTRATES (SILICON WAFER AND NOT-TCP) USING IMAGE J PROGRAMME SELECTING THE AREA OF INTEREST (THE CHANNEL) AND AN ANALYSIS OF THE FLUORESCENCE INTENSITY WAS REPORTED ON THE GRAPH, CONSIDERING THREE REPEATING MEASUREMENTS FOR EVERY SAMPLE. THE ERROR BAR REPORTED IN THE FLUORESCENCE INTENSITY GRAPH REPRESENTS THE AVERAGE VALUE OF \pm SD OBSERVED ON THREE REPEATING MEASUREMENTS. SCALE BAR 100 μ M..... 83

FIGURE 3.5: REPRESENTATION OF AFM IMAGES ACQUIRED ALONG THE MICRO-PATTERN CONSIDERING THE START, MIDDLE AND END POINT OF THE PATTERN AFTER ALBUMIN IMMOBILISATION ON SILICON WAFER SUBSTRATE USING TAPPING MODE AFM TECHNIQUE IN AIR. A SCREENING OF DIFFERENT PROTEIN CONCENTRATIONS WAS PERFORMED TO IDENTIFY THE IDEAL CONCENTRATION TO USE IN THE STUDY (FROM 100 μ G/ML TO 1 μ G/ML). THE AFM IMAGES REPORTED ARE AN EXAMPLE OF THE REPRESENTATION OF THE SURFACE AFTER ALBUMIN IMMOBILISATION, SHOWING PROTEIN AGGREGATION WHEN HIGHER CONCENTRATIONS ARE USED. 3 DIFFERENT AREAS FOR EVERY POINT FOR A TOTAL OF 9 IMAGES FOR EVERY CONCENTRATION USING DIFFERENT SCAN SIZE FROM 10 μ M TO 1 μ M WERE ACQUIRED..... 89

FIGURE 3.6: SCHEMATIC REPRESENTATION OF AFM SURFACE ANALYSIS CONDUCTED ON THE SILICA WAFER SUBSTRATE, BEFORE AND AFTER PROTEINS IMMOBILIZATION. IN IMAGE A, ANALYSIS OF THE SILICA WAFER BEFORE PROTEINS IMMOBILIZATION IS REPORTED. IN IMAGE B AND C ANALYSIS OF THE SILICA WAFER AFTER FN AND BSA IMMOBILISATION RESPECTIVELY IS REPORTED. 1 μ G/ML OF PROTEIN SOLUTION WAS DEPOSITED ON THE SILICA WAFER SUBSTRATE AND IMAGES ACQUIRED USING TAPPING MODE AFM IN AIR. MORE IMAGES WERE ACQUIRED TO SHOW THE PROTEIN DEPOSITION ALONG THE CHANNEL AND HERE REPORTED. THE ANALYSIS OF THE AFM IMAGES WAS CONDUCTED USING THE NANOSCOPE PROGRAMME. AFM IMAGES WERE COLLECTED ANALYSING THREE DIFFERENT POINTS ON THE SAMPLES FOR A TOTAL OF 12 IMAGES, USING DIFFERENT SCAN SIZE FROM 10 μ M TO 1 μ M AND AN EXAMPLE REPORTED. ... 90

FIGURE 3.7: SCHEMATIC REPRESENTATION OF AFM SURFACE ANALYSIS CONDUCTED ON THE NOT-TCP SUBSTRATE, AFTER PLASMA OXYGEN TREATMENT AND AFTER PROTEIN IMMOBILISATION ON PLASMA TREATED NOT-TCP. IMAGES WERE ACQUIRED USING TAPPING MODE IN AIR .FIVE POINTS FOR EVERY SAMPLE WERE CONSIDERED USING DIFFERENT SCAN SIZE FROM 10 TO

0.5 μ m, ANALYSIS OF THE ROUGH VALUE AND THE 3D SURFACE REPRESENTATION WAS CONDUCTED USING THE NANOSCOPE PROGRAMME..... 91

FIGURE 3.8: REPRESENTATION OF THE FIBRONECTIN MULTIPLE AND SINGLE UNBINDING EVENTS DETECTED AT THE START AND END POINT OF THE PROTEIN PATTERN ON NOT-TCP AND SILICON WAFER SUBSTRATE. IN A, B AND C AN EXAMPLE OF THE NO EVENTS, SINGLE AND MULTIPLE UNBINDING EVENTS RESPECTIVELY REGISTERED DURING THE ANALYSIS ARE REPORTED. THE ANALYSIS OF THE SPECIFIC UNBINDING EVENTS IS REPORTED SHOWING THE HISTOGRAMS RELATIVE TO THE FORCES REGISTERED AT THE START AND END POINT. 1000 CURVES WERE ANALYSED FOR EVERY POINT IN TRIPLICATE AND AN EXAMPLE IS REPORTED HERE (\pm SD). IN D A CORRELATION BETWEEN THE SPECIFIC FORCE DETACHMENT MEASUREMENTS REGISTERED AT THE START AND END POINT IS REPORTED..... 97

FIGURE 4.1 : INTEGRIN FAMILY. ORGANIZATION AND GROUPING OF THE INTEGRIN SUBUNITS IN MAMMALIAN CELLS BASED ON THEIR MATRIX AFFINITY OR CELL SPECIFIC EXPRESSION⁽¹⁴¹⁾ ... 102

FIGURE 4.2 : PLURONICS F127 CHEMICAL STRUCTURE, A HYDROPHOBIC POLYPROPYLENE SEGMENT AND TWO POLYETHYLENE SEGMENTS MW: 12600DA 111

FIGURE 4.3 : REPRESENTATION OF THE PLURONIC BRUSH LIKE CONFORMATION (A) AND THE TWO APPROACHES USED TO CREATE 3T3 FIBROBLAST CELLS PATTERNING (B, B₁). THE FLUORESCENCE IMAGES REPORTED REPRESENT A SELECTION OF TWO IMAGES COLLECTED USING THE A₂ MICRO-CHANNEL SHAPE REPORTED IN FIGURE 2.5 USED FOR THE CELL MICRO-PATTERNING STUDIES. THE DENSITY OF CELLS USED WAS 10⁶ CELLS/ML. SCALE BAR 100 μ m. 111

FIGURE 4.4 : SCHEMATIC REPRESENTATION OF THE NOT-TCP SUBSTRATE AND 3T3 CELL ADHESION STUDIES PERFORMED ON IT. FLUORESCENCE IMAGES OF 3T3 CELL DEPOSITION ON THE SUBSTRATE BEFORE THE FUNCTIONALIZATION WITH PLURONICS F127 SURFACTANT IS REPORTED. IN A AND B CELL DEPOSITION ON THE SUBSTRATE BEFORE AND AFTER PLURONICS IMMOBILISATION IS REPORTED. IN C DESIGN OF THE MICRO-CHANNEL USED TO CREATE THE PROTEIN PATTERN ON THE NOT- TCP SUBSTRATE, BEFORE AND AFTER FUNCTIONALIZATION WITH PLURONICS. IN D AND E CELL DEPOSITION ON FIBRONECTIN PATTERN BEFORE AND AFTER PLURONICS DEPOSITION RESPECTIVELY. THE FLUORESCENCE IMAGES WERE ACQUIRED USING A NIKON ECLIPSE TS100 MICROSCOPE. ANALYSIS OF THE IMAGES WAS CONDUCTED USING VOLOCITY 5.2 SOFTWARE. FIVE IMAGES FOR EVERY POINT WERE CONSIDERED AND ANALYSED. 115

FIGURE 4.5: SCHEMATIC REPRESENTATION OF THE POSSIBLE MECHANISM INVOLVED IN THE CELL ADHESION ON THE FIBRONECTIN. CELLS ADHESION ON FIBRONECTIN IS REGULATED BY THE INTEGRIN-RECEPTOR RECOGNITION ON THE FN SURFACE. IN FIGURE A THE NATIVE FN CONFORMATION (FOLDED CONFORMATION; NOT INTEGRIN FIBRONECTIN RECEPTOR INTERACTION^(180,181,182)), BEFORE ADSORPTION ON THE SUBSTRATE IS REPORTED. IN FIGURE B

EXTENDED FN CONFORMATION AFTER ADSORPTION ON THE SUBSTRATE IS REPORTED WHERE INTEGRIN RECEPTOR RECOGNITION OCCURRED WITH CELL ADHESION (INTEGRIN RECEPTORS INTERACTION⁽¹⁸³⁾). IN FIGURE C MORE FIBRONECTIN MOLECULES ON THE SUBSTRATE IN THE EXTENDED CONFORMATION, MORE CELL ADHESION IS OBSERVED..... **116**

FIGURE 4.6 : SCHEMATIC REPRESENTATION OF 3T3 FIBROBLAST CELLS ADHESION STUDIES PERFORMED ON FIBRONECTIN PATTERNS DEPOSITED (FN01 1 μ G/ML PROTEIN CONCENTRATION USED) ON NON-TCP SUBSTRATE FUNCTIONALIZED WITH PLURONICS F127. IN A A REPRESENTATION OF THE MICRO-CHANNEL DESIGN USED IN THE STUDY IS REPORTED. IN B, C AND D MESENCHYMAL STEM CELL ADHESION AT START MIDDLE AND END POINT RESPECTIVELY (FLUORESCENT IMAGES REPORTED). IN THIS CASE DUE TO THE USE OF RHODAMINE FIBRONECTIN FOR THE CREATION OF THE PROTEIN PATTERNS 3T3 FIBROBLAST CELLS CARRYING THE GREEN FLUORESCENT PROTEIN (MGFP) COLOUR WERE USED (GREEN FLUORESCENT IMAGES REPORTED). IN FIGURE E SURFACE COVERAGE ANALYSIS ALONG THE CHANNEL IS REPORTED. THE FLUORESCENT IMAGES WERE ACQUIRED USING A NIKON ECLIPSE TS100 MICROSCOPE. ANALYSIS OF THE IMAGES WAS CONDUCTED USING VOLOCITY 5.2 SOFTWARE. FIVE IMAGES FOR EVERY POINT WERE CONSIDERED AND ANALYSED AND THE AVERAGE VALUE OF THE SURFACE COVERAGE REPORTED IN THE GRAPH (\pm SD). SCALE BAR 200 μ M..... **117**

FIGURE 4.7 : SCHEMATIC REPRESENTATION OF I-HMSC CELLS ADHESION STUDIES PERFORMED ON FIBRONECTIN PATTERNS (FN01 1 μ G/ML PROTEIN CONCENTRATION USED) DEPOSITED ON NON-TCP SUBSTRATE FUNCTIONALIZED WITH PLURONICS F127. IN A A REPRESENTATION OF THE MICRO-CHANNEL DESIGN USED IN THE STUDY IS REPORTED. IN B, C AND D MESENCHYMAL STEM CELL ADHESION AT START MIDDLE AND END POINT RESPECTIVELY (FLUORESCENT IMAGES REPORTED). IN THIS CASE THE USE OF RHODAMINE FIBRONECTIN FOR THE CREATION OF THE PROTEIN PATTERNS WAS REPLACED BY THE GREEN FLUORESCENT HiLYTE488 FIBRONECTIN DUE TO THE AVAILABILITY OF MESENCHYMAL STEM CELLS CARRYING THE RED FLUORESCENT PROTEIN (MRFP) COLOUR WERE USED (RED FLUORESCENT IMAGES REPORTED). IN FIGURE E SURFACE COVERAGE ANALYSIS ALONG THE CHANNEL IS REPORTED. THE FLUORESCENT IMAGES WERE ACQUIRED USING A NIKON ECLIPSE TS100 MICROSCOPE. ANALYSIS OF THE IMAGES WAS CONDUCTED USING VOLOCITY 5.2 SOFTWARE. FIVE IMAGES FOR EVERY POINT WERE CONSIDERED AND ANALYSED AND THE AVERAGE VALUE OF THE SURFACE COVERAGE REPORTED IN THE GRAPH (\pm SD). SCALE BAR 100 μ M..... **119**

FIGURE 5.1: REPRESENTATION OF THE 3T3 FIBROBLAST CELLS MIGRATION. THE MIGRATION ANALYSIS WAS CONDUCTED USING THE CHEMOTAXIS TOOL IBIDI PROGRAMME, USING THE VIDEOS OBTAINED FROM PICTURE FRAMES ACQUIRED EVERY 10 MINS FOR 24 HRS. 18 CELLS WERE CONSIDERED AS SAMPLE IN THE MIGRATION ANALYSIS TO HAVE MORE RELIABLE RESULTS. DATA WERE REPEATED IN TRIPLICATE AND HERE AN EXAMPLE REPORTED. IN A AND B AN EXAMPLE OF THE TIME LAPSE PICTURES COLLECTED AT START AND END POINT SHOWING THE TRACKING ANALYSIS PERFORMED USING THE TRACKING PROGRAMME USING IMAGE J PLUGS. IN A₂ AND B₂ THE TRACKING MIGRATION OF 18 CELLS IS REPORTED. IN FIGURE C AN EXAMPLE OF THE ANALYSIS CONDUCTED ON THE SAMPLE USING THE IBIDI CHEMOTAXIS TOOL AND CELL VELOCITY ANALYSIS IS REPORTED. THE CELL VELOCITY ANALYSIS WAS REPEATED IN TRIPLICATE.

STATISTICAL ANALYSIS USING A TWO VARIABLE T-TEST WAS CONDUCTED TO PROVE THE STATISTICAL SIGNIFICANCE DIFFERENCE BETWEEN START AND END POINT CELL VELOCITY AND CELL MIGRATION ANALYSIS WITH $P < 0.05$ **128**

FIGURE 5.2: ANALYSIS OF THE CELL SHAPE. BRIGHT-FIELD IMAGES A_1 AND B_1 WERE ACQUIRED CONSIDERING CELL DEPOSITION ON THE FIBRONECTIN PATTERNS USING 1×10^6 3T3 FIBROBLAST CELLS AND INCUBATED FOR TWO HOURS USING A DMEM MEDIUM WITHOUT FBS TO AVOID CELL INTERACTION WITH OTHER PROTEINS, AT START AND END POINT RESPECTIVELY. THE FLUORESCENT IMAGES A AND B WERE ACQUIRED USING A HIGHER MAGNIFICATION. 5 IMAGES OF THREE POINTS ALONG THE CHANNEL FOR EVERY POINT WERE ACQUIRED AND HERE AN EXAMPLE REPORTED..... **129**

FIGURE 5.3: BRIEF SUMMARY OF THE 3T3 FIBROBLAST CELLS BEHAVIOUR USING THE MICROFLUIDIC SYSTEM. AN ANALYSIS OF THE DATA OBTAINED CONSIDERING THE UNCONFINED (END POINT) AND CONFINED (START POINT) SPACE IS REPORTED..... **130**

FIGURE 5.4: REPRESENTATION OF THE I-HMSC MESENCHYMAL STEM CELLS MIGRATION. THE MIGRATION ANALYSIS WAS CONDUCTED USING THE CHEMOTAXIS TOOL IBIDI PROGRAMME, USING THE VIDEOS OBTAINED FROM PICTURE FRAMES ACQUIRED EVERY 10 MINS FOR 24 HRS. 18 CELLS WERE CONSIDERED AS SAMPLE IN THE MIGRATION ANALYSIS TO HAVE MORE RELIABLE RESULTS. DATA WERE REPEATED IN TRIPLICATE AND HERE AN EXAMPLE REPORTED. IN A AND B AN EXAMPLE OF THE TIME LAPSE PICTURES COLLECTED AT START AND END POINT SHOWING THE TRACKING ANALYSIS PERFORMED USING THE TRACKING PROGRAMME USING IMAGE J PLUGS. IN A_2 AND B_2 THE TRACKING MIGRATION OF 18 CELLS IS REPORTED. IN FIGURE C AN EXAMPLE OF THE ANALYSIS CONDUCTED ON THE SAMPLE USING THE IBIDI CHEMOTAXIS TOOL AND CELL VELOCITY ANALYSIS IS REPORTED. THE CELL VELOCITY ANALYSIS WAS REPEATED IN TRIPLICATE. STATISTICAL ANALYSIS USING A TWO VARIABLE T-TEST WAS CONDUCTED TO PROVE THE STATISTICAL SIGNIFICANCE DIFFERENCE BETWEEN START AND END POINT CELL VELOCITY AND CELL MIGRATION ANALYSIS WITH $P < 0.05$ **134**

FIGURE 5.5: REPRESENTATION OF THE POSSIBLE MECHANISM INVOLVED IN MESENCHYME STEM CELLS MIGRATION I-HMSC CELLS. THE ASSUMPTION THAT THE CONCENTRATION OF THE RGD COMPLEX EXPRESSED ON THE FIBRONECTIN MOLECULES IMMOBILISED ON THE NOT-TCP SUBSTRATE IN THE RIGHT CONFORMATION CAN INFLUENCE THE CELLS DENSITY AND SPREADING, SEEMS TO BE A POSSIBLE EXPLANATION ALSO TO CONFIRM DIFFERENCE IN CELL VELOCITY MIGRATION. **135**

FIGURE 5.6: FIBRONECTIN FLUORESCENCE ANALYSIS DURING THE I-HMSC STEM CELLS MIGRATION. THE ANALYSIS WAS CONDUCTED USING THE PICTURE FRAMES OF THE FIBRONECTIN TAKEN EVERY 10 MINUTES FOR 24 HOURS. IN FIGURE A AND B, A REPRESENTATION OF THE FLUORESCENCE ANALYSIS IS REPORTED..... **136**

FIGURE 6.1: CORRELATION BETWEEN FLUORESCENCE INTENSITY AND SPECIFIC AFM FORCE MEASUREMENTS (A) ON FIBRONECTIN PATTERN (B) CREATED ON NOT-TISSUE CULTURE PLATE SUBSTRATE. A TIP WAS FUNCTIONALIZED WITH AN ANTI-FIBRONECTIN ANTIBODY ABLE TO TARGET THE HISTAMINE GROUPS EXPOSED ON THE FIBRONECTIN SURFACE. FLUORESCENT FIBRONECTIN AT THE START POINT (C) EXHIBITS A HIGHER NUMBER OF SPECIFIC MULTIPLE UNBINDING EVENTS (RED LINE) WHEREAS FOR MOST OF THE LOWER FLUORESCENT FIBRONECTIN AT THE END POINT (D), NO EVENTS OR SOME FEW SPECIFIC SINGLE UNBINDING EVENTS CAN BE DETECTED CONFIRMING THE PRESENCE OF A LOWER PROTEIN DEPOSITION ALONG THE PATTERN. SCALE BAR 200 μ M. **144**

List of tables

TABLE 1: PDMS PHYSICAL AND CHEMICAL CHARACTERISTICS	27
TABLE 2: WATER CONTACT ANGLE MEASUREMENTS BEFORE AND AFTER OXYGEN PLASMA TREATMENT	79
TABLE 3: AFM IMAGES ANALYSIS AFTER PROTEINS IMMOBILIZATION ON SILICON WAFER SUBSTRATE	86
TABLE 4: ADHESION FORCE ANALYSIS	94
TABLE 5: WATER CONTACT ANGLE MEASUREMENTS BEFORE AND AFTER FUNCTIONALIZATION WITH PLURONICS F127.....	112

List of abbreviations

MDA-MB-231	Breast cancer cell line
ECM	Extra cellular matrix
PDMS	Poly-dimethyl-siloxane
CAD	Computer aided design
SU-8	Photoresist
PMMA	Poly-methyl-methacrylate
AFM	Atomic force microscope
i-HMSC	Immortalised mesenchymal stem cells
NIH-3T3	Mouse fibroblast cells
BSA	Bovine serum albumin
FN	Fibronectin
WCA	Water contact angle
Not-TCP	Not- Tissue culture plates polystyrene based
AMAS	N-(α -Maleimidoacetoxy) succinimide ester)
PBS	Phosphate buffer
DMEM	Dulbecco's modified eagle medium
FCS	Foetal calf serum
STM	Scanning tunnelling microscopy
DNA	Deoxyribonucleic acids
TEM	Transmission electron microscopy

SEM	Scanning electron microscopy
μCP	Micro-contact printing
TM	Tapping mode
UV	Ultraviolet

1. Introduction

1.1. Bio-molecular Gradients

Bio-molecular gradients play an important part in biological and pathological stages such as development, inflammation, cancer chemotaxis and embryogenesis^(1,3). The study of these phenomena requires the capability to expose cells to bio-molecular gradients in a controllable way that mimics *in vivo* conditions. Such gradients have been used for controlling growth, migration and differentiation of cells using quantitative methods^(4,5). Here, as a prelude to presenting work on the creation and characterisation of biomolecular gradients via microfluidic approaches a review of the traditionally used *in vitro* methods, and new microfluidic devices is given, focusing attention on the microfluidic technique devices and the impact that they have had in biological studies.

1.1.1. Evolutionarily conserved signalling

Bio-molecular gradients are an important evolutionarily conserved signalling mechanism for the growth, migration and differentiation of cells in the three dimensional environment of living tissue⁽²⁾. Because of the high efficiency with which developmental operations need to occur, the signalling protein gradients used for biological cell mechanisms are spatially temporally regulated. These gradients rarely act independently^(6,7,8) as evidenced from

the fact that many gradient-induced signalling cascades share, or have interactions with intracellular second messengers, which facilitate signalling modulation ^(9,10). The combination of *in vitro* methods to expose the cell to bio-molecular gradients and *in vivo* studies has revealed the presence of intricate and highly regulated signalling processes, in which the cell response is determined by the specific characteristics of the gradients ⁽²⁾. Traditional *in vitro* gradient methods have been used to improve our understanding of gradient signalling, but they are not ideal if quantitative or combinatorial gradients are used. The major limitation is due to their inability to produce defined gradients with a spatial-temporal profile. Using traditional methods chemical gradients often evolve unpredictably over space and time so become difficult to characterize quantitatively ⁽¹¹⁾. Using microfluidic devices, fluids can be controlled precisely and with automation at micrometre dimensions provides a strategy to control fluid flow for cellular studies.

1.1.2. Traditional gradient generating methods

Biological hydrogels were used to create bio-molecular gradient for *in vitro* studies ⁽¹²⁾. Normally agarose, fibrinogen and collagen are used in cell *in vitro* studies ^(12,13,14). Cells are homogenized and mixed with the liquid solution before gelation or exposed directly on the gel. Biomolecule gradients can be expressed using another cell source that release chosen biomolecule ⁽¹⁴⁾, or using droplets of biomolecule solutions that diffuse through a gel matrix ⁽¹⁵⁾. Biological hydrogels have the advantage of being easy to make, giving control

over position and a free diffusion of chemical species excluded movements around the gel. Unfortunately they offer a low reproducibility and a low spatial-temporal control ⁽²⁾.

In 1962 Stephen Boyden developed a gradient-generating system to study chemotaxis ⁽¹⁶⁾. The system consists of an upper compartment, a porous membrane where cells are seeded and a lower compartment filled with a chemo-attractant solution (Figure 1.1 A). The gradient induces cells to migrate through the porous membrane to the lower compartment, where migrated cells are fixed, stained and counted to quantify the degree of chemotaxis. Using the so-called Boyden chamber a quantitative measure of migration induced by chemotaxis can be provided. The inability to control directly the bio-molecular gradient and the observation of cells during the experiment makes this method unsuitable to study cell response under specific chemical signals.

In 1977 Sally Zigmond reported the first bio-molecular gradient generating system to study individual neutrophils responding to a specific gradient ⁽¹⁷⁾. The device consisted of two parallel channels mounted on a glass slide (Figure 1.1 B). Cells were seeded on a coverslip inverted over the etched surface where after injection of medium in the sink and bio-molecular solution in the source channel, changes in cell growth, differentiation or migration can be observed using a microscope. The Zigmond chamber is a good method for exposing cells to a predictable, reproducible bio-molecular gradient up to 1hr, but its inability to control the gradient over longer period and the evaporation

problem due to the design of the chamber, prevent its use in understanding how cells integrate multiple bio-molecular gradient signals.

In 1991 Graham Dunn and co-workers solved the problem of evaporation in the Zigmond chamber developing a new system similar in the concept, but in this case the source and the sink chambers were rearranged in concentric rings⁽¹⁸⁾. This strategy eliminates the liquid and air interface sealing both chambers when coverslip is inverted on the glass slide (Figure 1.1 C). The inability to control the gradient for longer periods of time, the presence of radial symmetric support and the use of polar coordinates makes cell visualisation difficult.

The *in vitro* methods described model the complexity of the gradient signal but cannot explain the mechanism of action due to the limitation of collecting quantitative knowledge about bio-molecular gradients present *in vivo*.

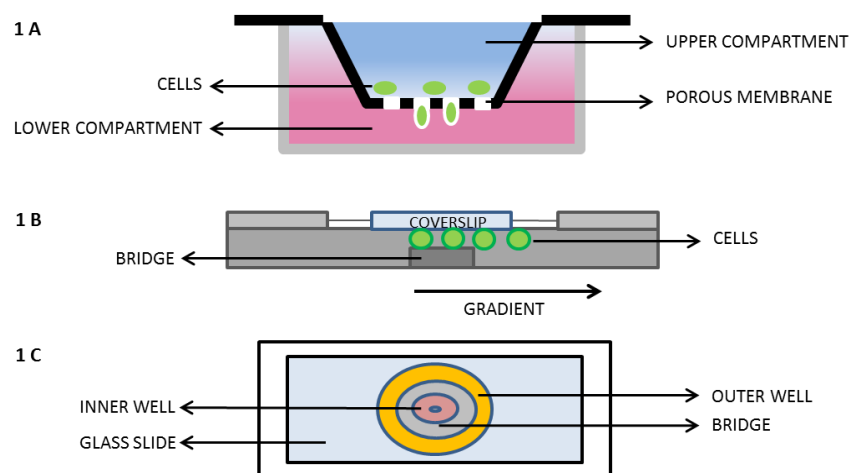


Figure 1.1: Traditional methods representation, 1A Boyden chamber, 1B Zigmond chamber and 1C Dunn chamber.

1.1.3. Limits of traditional methods

To understand the biological mechanisms involved in phenomena like growth, migration and cell development biochemical signals should mimic the *in vivo* environment. Biochemical signals *in vivo* such as growth factors, hormones and chemokines exist in form of gradients that vary in space and time ^(19,20). Disadvantages recorded using traditional *in vitro* methods are due to the low life span of the gradient and a low flexibility of the devices, in fact it is not possible to control or change molecules concentration during the experiment and observe cells interaction with multifunctional gradients. Using conventional assays such as the Boyden, Dunn, and Zigmond chambers, ^(16, 17,18) spatial gradients of molecule are typically limited to simple, non-quantitative gradients that cannot be precisely controlled in a reproducible fashion. To mimic cells environment in the last 30 years researchers provided a way to create predictable, reproducible and easily quantified biomolecule gradients *in vitro* controlling the fluid flow in a micro-meter scale.

1.1.4. Microfluidic methods

Microfluidic gradient methods produce spatial and temporal controlled biomolecular gradients by regulating diffusive transport process. The ability of fluids to pass through micro-channel or micrometre scale circuits is dominated by laminar flow regime. This specialized flow system is well understood mathematically and conceptually, allowing the movement of chemical species inside microfluidic device and calculated with great accuracy ⁽²¹⁾. Compared

to the traditional gradient generating methods microfluidic devices increase the throughput and reduce the cost of gradient experiments. One of the ways to create gradients suitable for cell culture studies, using microstructure tools is to absorb or tether molecules of interest on surfaces ^(22,23). Using micro-patterned gradients is possible to control the characteristics of the biomolecules, determined by the size and spacing of patterns. Another class of microfluidic generator consists of devices that control gradient along space and time called time evolving gradient generators. Micro-valve chemotaxis devices ⁽²⁴⁾ and microfluidic multi injectors systems ⁽²⁵⁾ effectively creates gradients capable of evoking responses from cells, with better reproducibility and quantitation due to the precise dimensions of the devices. To understand more in detail cell behaviour in *in vivo* studies steady state gradient generators provided important information, creating distinct regions of constant concentration to form gradients over cell culture area. This class of microfluidic generators included, T sensor, Pre-mixer gradient generators ⁽²⁶⁾, Universal gradient generators ⁽²⁷⁾ (Figure 1.2), with rapid formation of complex gradient profiles, allow correlations between cell response and specific gradient characteristics, including quantitative informations ^(28,29).

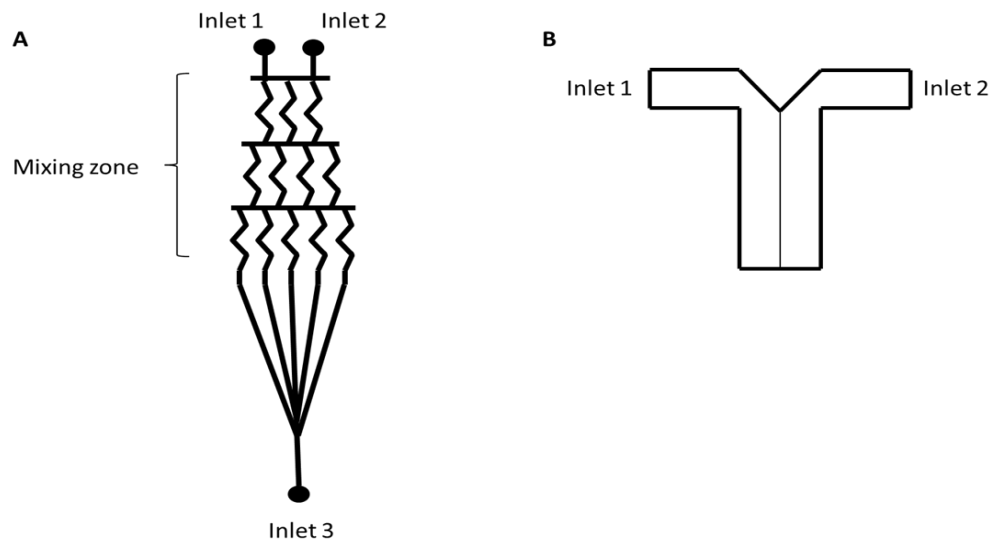


Figure 1.2: Microfluidics devices. In figure A Pre-mixer gradient generator, in figure B T-sensor.

1.1.5. Review of biological studies using micro-fluidic gradient generators

Microfluidic devices were used in the last ten years on a number of biological applications, like cancer metastasis, immune response and stem cells biology. Cancer metastasis originated from a multistep process of interactions between cells and surrounding stromal microenvironment. Utilising microfluidic generators, quantitative analysis has been performed to characterise the migratory behaviour of breast cancer cell line MDA-MB-231, indicated that tumour cell migration is influenced to the degree of concentration difference across cell body⁽³⁰⁾. Immune response is important to mitigate the response of infection; to recruit immune cells and rapidly migrate to the infection site. Applications of microfluidic technique in immune response studies have revealed quantitative information, between chemokines and their receptors understanding the relationship between

immune response and chemotaxis signals ⁽³¹⁾. Using microfluidic gradient generators, a complete understanding of how immune cells interpret the chemokine gradients ⁽³²⁾, and the mechanism of neutrophil chemotaxis has been revealed ⁽³³⁾. Due to the importance of stem cells to meet the clinical demands for repairing organs and treating important diseases, and their regulation under specific biochemical factors, microfluidic technique studies have been conducted to provide quantified correlation between biomolecular gradients and stem cell behaviour ^(34,35). The investigation of soluble factor gradients on the differentiation of human neural stem cells was conducted using a microfluidic generated stable gradient of growth factor, showed a clear dependence on gradient's concentration ⁽³⁶⁾. All these examples reported the applicability of microfluidic gradient technique in biological studies as cancer metastasis, immune response and stem cell biology; confirming the advantage in elucidating complex molecular interaction on the regulation of cells growth, migration and differentiation.

1.1.6. Impact in biological community

Micro-fabricated devices have received wide acceptance from the biology community due to their impact in fields such as developmental biology, immunology, stem cell biology, systems biology, and cancer research. In particular, microfluidics-based gradient devices are beginning to play an important role in cell migration research. Systemic investigations and quantitative analysis brought a new concept of understanding in the micro-

scale world, which was not available in the past ⁽²⁾. Micro-scale environment using microfluidic devices try to mimic complex *in vivo* biological mechanisms for a better understanding of the cell-cell and cell-ECM interactions in 3D micro-environment ⁽³⁵⁾. More work is required to integrate other cells including blood vessels control and mimic various pathological and physiological states, expanding the frontier of biological research.

1.2. Microfluidic device

Microfluidic devices have demonstrated that fluid components can be miniaturised and connected together to create a “lab on chip”⁽³³⁾. There has been interest in controlling the potential of this new approach and developing microfluidic devices using elastomeric material, such as PDMS (poly-dimethylsiloxane). A simplification in device fabrication and the possibility to integrate micro-valves⁽³⁷⁾ into the design opened the way to explore application in many different fields. In this section, a critical review of the PDMS as material for microfluidic devices is reported considering the advantages and limits in biological studies.

1.2.1. Properties of PDMS (poly-dimethyl-siloxane)

PDMS is an elastomeric compound, easy to deform and release from features of a mould without damage. PDMS is used to reproduce with high fidelity microfluidic channels or other features with micron scale dimensions⁽³⁷⁾. PDMS is compatible with water and polar solvent like methanol and glycerol; it swells however in non-polar organic solvents⁽³⁹⁾. To reduce swelling in the presence of non-polar organic solvents, PDMS can be modified with silica particles⁽⁴⁰⁾. PDMS is nontoxic to proteins and cells. It is permeable to oxygen and carbon dioxide, but only slowly permeable to water. It is suitable for biological studies for example; mammalian cells can be cultured on it⁽⁴¹⁾.

1.2.2. Chemistry of PDMS

The surface of PDMS is hydrophobic and presents units of $\text{-O-Si(CH}_3)_2\text{-}$ groups. When exposed to oxygen plasma silanol (Si-OH) groups are introduced, and methyl groups reduced rendering the polymer hydrophilic⁽³⁷⁾. By exposing the surface of PDMS and the surface of the substrate to oxygen-based plasma, PDMS channels can be sealed irreversibly to PDMS, glass, silicon and polystyrene⁽³⁸⁾. Heating a weak seal at 70°C can sometimes improve the strength of the seal⁽³⁷⁾. This characteristic makes PDMS versatile during experimentation, for example silylating oxidized PDMS with an aminosilane activates the surface for protein attachment. Another advantage of PDMS over glass, silicon, and hard plastics is that it makes reversible conformal contact (van der Waals contact) to smooth surfaces⁽³⁷⁾.

1.2.3. Optical properties PDMS

Optical transparency is important for the detection of particles or fluorescence detection. PDMS is classified like optically transparent material with a range from 240 to 1100nm⁽³⁷⁾, with a RI (refractive index value) around 1.4. PDMS can be used to study opto-fluidic components without significant loss during the absorption. To summarize, PDMS has demonstrated to be attractive and useful for a range of applications in laboratory, prototyping, used as material in large-scale manufacturing. Other polymers were tested like thermoplastic polymers and polycarbonates⁽⁴²⁾. Each material has

different characteristics, one more suitable than others depending on the applications. A summary of the PDMS characteristics are reported in **Table 1**.

Table 1: PDMS physical and chemical characteristics

Properties	Characteristics	Observations
Optical	Transparent, UV cut-off 240nm	Optical detection from 240 to 1100nm
Mechanical	Elastomeric	Reversible deformation, facilitate release from mould
Permeability	Low permeability to water, permeable to gases and non-polar solvents	Gas transport, not-compatible with many organic solvents
Reactivity	Can be oxidized with plasma	Reactive towards silanes, surface can be etched, can be modified to hydrophilic.
Toxicity	Non toxic	Supports mammalian cell growth.

1.2.4. Fabrication microfluidic device using PDMS

Microfluidic devices using PDMS are fabricated using soft lithography techniques. Soft lithography includes a large number of techniques where a moulded polymer is used. This is obtained by casting a pre-polymer on a rigid master with well-defined micro and nanostructures. Soft lithography techniques consist in the realisation of defined structures in photoresist which will be used to replicate the structures on a master. This replication on a master can be repeated in laboratory conditions, using a rapid, simple and inexpensive process. For the fabrication of the device, microfluidic channels CAD (Computer Aided Design) program and printed into high resolution photo-mask to produce a master, using SU-8 as photo-resist. The master

presents the positive stamp, which serves as a mould for PDMS. Preparation of the pre-polymer consists in pouring over the mask a solution of elastomeric rubber base and a curing agent, and cured for 2 hours at 80°C. The PDMS is peeled from the master and sealed using plasma oxidation treatment to a substrate to form microfluidic channel.

1.2.5. Flow in micro-channels

To develop a microfluidic device, an understanding of fluid dynamics in microsystems is important. Generally, as the length of the device decreases, surface forces become dominant while gravity becomes less important⁽⁴³⁾. In micro-channels flow is described by Reynolds number which describes the inclination of fluid to present turbulence. If Reynolds number is low than 2000, the flow in the channel is a laminar flow dominated by viscous forces, while if the number is above 2000 the flow tends to produce turbulence, dominated by inertial forces⁽⁴⁴⁾ (Figure 1.3). Due to the small scale of the microfluidic systems, normally less than 500 μm , the flow normally presents a Reynolds value around 10 indicating the presence of laminar flow and dominated viscous forces in the system. Liquids can be treated as uniform thickness the boundaries remain fixed and there is no turbulence that leads to mixing. Laminar flows have been used in studies for subcellular resolution and fast switching. Microfluidic systems were used to focus drug stream on a specific cell compartment to allow cell observation to study local stimuli in the cells^(45,46).

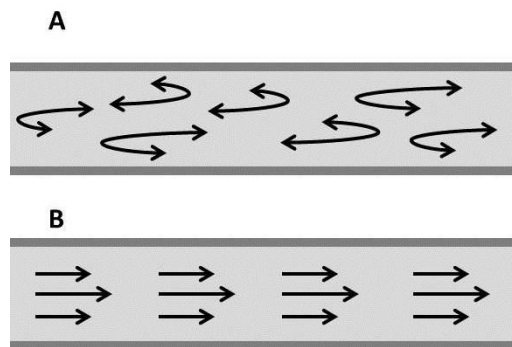


Figure 1.3: Schematic representation of flow in micro-channels. In A turbulence takes place inside channel, In B laminar flow is occurring.

1.2.6. Critique of PDMS for cell biological studies

A large number of materials have been used to fabricate microfluidic devices such as silicon, gelatine, PDMS and PMMA Poly-(methyl-methacrylate). Because of the characteristics and the simplicity of the technique PDMS has become the most popular material in microfluidic device fabrication. The possibility to produce a device in a few hours without expensive materials has attracted scientists exploring microfluidic techniques in cell biology studies. PDMS is cheap, transparent, and bio-compatible and can be bonded to glass and polystyrene substrates using oxygen plasma treatment. The deformability of the material and the permeability of gas make this material a useful tool in cell biology studies. However, using PDMS in biological studies can present problems. PDMS material can absorb/adsorb biomolecules and drug from the media due to its inherent hydrophobicity. To limit this problem many surface treatments have been used ^(40,41). PDMS is also water permeable leading to changes in medium osmolarity or drying effects ⁽³⁷⁾. Despite these limitations,

PDMS microfluidic devices are still popular in cell biological studies but it is necessary to study and understand these affects in micro-scale environment, comparing the results with traditional methods. The interdisciplinary application of microfluidic devices in biological studies, and the limitations of this technique have driven new research in microfluidics to understand more in details the micro-scale environment.

1.3. Microfluidic tools for cell biology

High throughput biological experiments can be processed using microfluidic chips, by miniaturisation of macroscopic systems and taking advantage of parallel processing and microfluidic knowledge. Exploiting effects of laminar flow in the microfluidic systems has helped the spatial control of liquid composition, temperature, changes in the media and single cell analysis. In this section a discussion about use of microfluidics to fabricate research tools in cell biology will be discussed considering micro-environmental composition control and the laminar flow in complex functionalization.

1.3.1. Micro-environment control

Chemical and mechanical parameters define the micro-environment of cells. The chemical environment is dependent on the composition of the media, in particular the molecules dissolved in the media that define the cell environment; while the culture substrate composition (ECM extracellular matrix) represents the mechanical environment. Normally these parameters can be controlled for a population of cells, but is more difficult to control it for individual cells. The major advantage of the micro-fluidic technique is that enables the control of the micro-environment changing parameters. The control of the parameters in the micro-environment is due to the speed of the process at the micro-scale. It is possible to control the medium composition and produce chemical gradients that mimic natural stimuli that are essential

in biological processes. Spatial control of chemical gradients concentration is important when cellular response studies are conducted, as the limit cellular response to chemical gradients is localized in a small region that represents the 2% of cell surface ⁽⁴⁷⁾. In this case macroscopic gradient generators show a poor spatio-temporal resolution not useful for cell biology studies. Micro-fluidic devices have demonstrated ability to create multiple bio-molecular gradients with controlled spatiotemporal distribution. Micro-fluidic devices offer faster response to immune cells, neural cells growth and differentiation ⁽²⁵⁾, endothelial cells migration ⁽⁴⁸⁾ and cancer cells chemo-taxis ⁽³⁰⁾.

Micro-fluidic devices also offer a great ability to control mechanical environment relating to the behaviour of cells in regulation of fundamental biological processes such as cell growth, ECM metabolism and gene expression. Using micro-technology to create mechanical deformation of cells, (depending on the geometry of cells and the forces applied) it is possible to: study the correlation between geometrical dependences and cytoskeleton behaviour extracting internal cell mechanisms ⁽⁴⁹⁾, study cell motility in constrained environment ⁽⁵⁰⁾, mimicking tissue organization ⁽⁵¹⁾. Deformability has also an implication in cancer cells, in fact was observed a different deformation in cancer cells comparing to healthy cells, which revealed a correlation in metastasis spreading over tissues ⁽⁵²⁾.

1.3.2. Micro-fluidic precise spatial-temporal gradients

One way to create gradients using micro-fluidic techniques is to take advantage of the laminar flow properties. The creation of molecular gradients based on laminar flow theory consists in the use of mixing between parallel laminar streams. The shape of the gradient is influenced on the flow rate, maintaining their shape at constant flow rate. The simplest device using this technology is T-sensor device composed by two micro-channels ⁽⁵³⁾.

Such T-sensors are easy to fabricate and conceptually with a known mathematical description. The constant diffusion inside the channel prevents cells accumulation and increases cell culture time. Limits of this technology are due to the cellular stress and removal of cell signalling caused by the flow stream and the limited portion of the channel which creates gradients. T-sensors devices found applications in bacteria chemotaxis ⁽⁵⁴⁾, or endothelial cell migration ⁽⁴⁸⁾.

Upgraded versions of the T-sensor device have been developed called Premix and Universal micro-gradient generators ⁽²⁾ (Figure 1.4). Using these devices more complex gradients can be generated, splitting the streams. In the Premixer device the idea is to split and recombine the fluids before mixing with the culture channel. Controlling the flow is possible to create smooth or step gradients. This device has been used in neutrophil ^(29, 55) and cancer cells chemo-taxis studies ⁽³⁰⁾. Universal gradient generators include a series of walls to split the streams. In this case the gradient is more difficult to describe mathematically and it shares the same problems of the T-sensor device. Major

limits with laminar flow micro-gradient generators are that they need precise flow control. Using flow resistive elements is possible to eliminate the cell stressing and preventing cell signalling loss. The idea of this device is to diffuse biomolecules through a barrier as a membrane⁽⁵⁶⁾ or micro-channels⁽⁵⁷⁾, to generate a gradient. Using flow or flow resistive micro-gradient methods is possible to create spatiotemporal gradients with better resolution. If a complex gradient and fast response is mandatory in the experiment a flow micro-gradient method is used, in other hand if cell stress or cell drifting must be controlled flow resistive method is suggested.

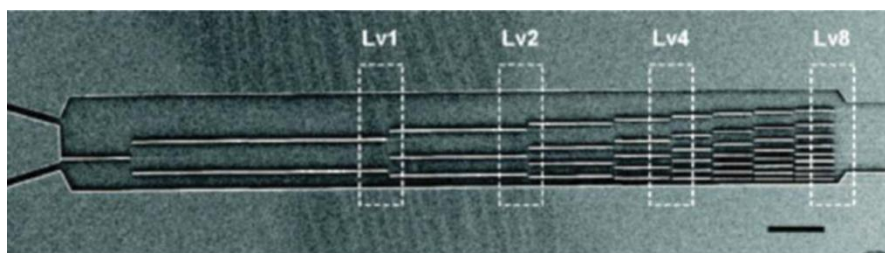


Figure 1.4: Pre-mix micro-gradient generator device that restricts orthogonal diffusion of chemical compounds⁽²⁾.

1.3.3. Liquid flow in channel for complex functionalization

Liquid flow can be used to achieve bio-molecular patterning on substrates. Using liquid flow it is possible to pattern substrates by confining the flow in micro-channels or on a stencil. One way to pattern molecules on substrates is to flow a bio-molecular solution in a micro-fluidic channel previously stuck on the substrate. Liquid flow permits the creation of biomolecules deposition on

substrates patterning them and enabling treatments on the patterned area. Microfluidic devices can be stuck permanently ⁽⁵⁹⁾, or temporarily ⁽⁵⁸⁾ on the substrate. Using this method it was demonstrated that is possible to pattern molecules on substrates like glass, polystyrene and gold with submicron resolution ⁽⁶⁸⁾. This liquid flow technique was used to deposit proteins on substrates and studies concerning cell adhesion were reported. The creation of multiple patterns or molecular gradients on substrates is possible by flowing different biomolecules on channels in parallel ⁽⁵⁹⁾, or using depletion effects of solution along channel generating a gradient ⁽⁶⁰⁾.

1.3.4. Comments

Microfluidic devices in cell-based assays have opened the way to exploring new microenvironments and new methods to control and observe cellular responses in important biological phenomena simulating the *in vivo* conditions. Analysis of the biological effects and physical differences in the creation of bio-molecular gradients for biological assays, were considered in the fabrication of new microfluidic devices.

It is clear that micro-fluidic devices still have some limitations in biological studies. In fact the lack of quantitative information makes it difficult to understand mechanisms such as cell proliferation. A better understanding of the effects of the micro-environments present in micro-devices from a cellular perspective is necessary.

1.4. Summary

Microfluidic devices have been designed to facilitate applied and fundamental research in tissue and cell biology. In biology it is essential to understand cellular mechanisms, by studying the interactions between intra and inter cellular mechanisms that coordinate cellular events. Developing a system that can study cellular mechanism is not an easy task due to the complexity of biological systems as summarized in this chapter. In the past, researchers have focused their attention on high-throughput tests using traditional methods to create bio-molecular gradients. These often lack the fidelity and number of details necessary to comprehend the signal propagation. In contrary biological experimentations which focus on a single signalling mechanism, these miss the throughput essential to reconstruct the biological system. In the last 20 years with the progress in the development of microfluidic devices, systematic studies have found some answers to these questions. Microfluidic devices provided for the first time the ability study cells at a single and multi-cellular level with biomimetic physiological conditions. In more detail the major benefits to use microfluidic devices in biological experiments are: micro-scale fluid flow enables precise and high-resolution microenvironment control; micro-fluidic devices are normally compatible with imaging and microscopy techniques; the ability of the technique to upscale microfluidic devices to understand complex biological systems. The microfluidic devices discussed in this chapter have demonstrated the ability to address experimental in systems biology, with the creation of a

specific spatial-temporal gradients investigating single or multiple cells signalling. In the last decade advances microfluidics approaches have been used to simplify complex analysis in systemic biology in a microfluidic device “lab on chip”. With the improvement of the technology and the highly integrated micro-fluidic devices in the future it will be possible to extend this technology in biomedical and pharmaceutical research in clinical settings.

1.5. Aims of work

The aim of this work is to create a bio-functional gradient on silica and polymeric surfaces using a micro fluidic technique, for the guidance of cell adhesion and functionality. In this study, we created protein gradients on silica wafer surface and cell plastic plate substrate and studied the morphology and density of cells on these gradients.

Two fluorescently tagged proteins, Texas Red-albumin, and Rhodamine-fibronectin were used in this investigation to study the surface adhesion and the behaviour of the proteins on the two surfaces, at different concentrations. Albumin and fibronectin are intimately involved in cell-surface adhesion to materials exposed to *in vivo* environments and also serve as carriers for important molecules in the body. Different proteins concentrations were used (from 1 mg/mL, to 1 µg/mL), to identify an optimal concentration able to form a suitable concentration gradient on each substrate. Atomic Force Microscopy (AFM) and Fluorescence Microscopy were used to monitor property changes before and after the protein immobilization on the surfaces.

A specific silica master was made with a photolithography technique to facilitate surface patterning in the desired geometries. The created fibronectin gradients were investigated for protein functionality (binding) using AFM probes functionalised with an antibody to fibronectin. The fibronectin patterns were also used to support specific cell cultures (fibroblasts). From the data obtained, and the analysis conducted we can confirm that we obtained a protein concentration gradient displaying different densities of

functional proteins (as determined by AFM force spectroscopy) along the line patterns formed by microfluidics. The most suitable concentration was 1 μ g/ml of proteins, where protein aggregation was lower compared to the higher concentrations. Studies investigating the behaviour (morphology, density and migration) of mouse 3T3 fibroblasts and immortalized mesenchymal stem cells (i-HMSC) on the fibronectin gradients were conducted. Such controllable cell growth on the defined areas of surface is important for potential applications in biosensor fabrication and tissue engineering.

1.6. Future perspectives

The microfluidic technique, due to its ability to create various bio-molecular gradients, from simple shapes to more complex architecture that can mimic the physiological environment, makes this technique perfectly suited for biological investigations. In this review, traditional methods for gradient generation and microfluidic system techniques were described with particular relevance to the investigation of cell biology studies.

In the second part of the review, recent and key information on how to fabricate a microfluidic device were highlighted. Using microfluidic techniques it is possible to control the environment and the biomolecules concentration working with micro scale, reducing the cost and increasing the efficiency of the biological processes. Patterning proteins on substrate using microfluidic technique showed that is possible to use proteins as substrate to conduct cell study investigations.

In terms of future perspectives, it is clear that the microfluidic technique based investigation of bio-molecular gradients has key application in tissue engineering and biosensors, particularly where the control and characterization of gradients can be used to identify specific targets on cell studies, to investigate the cellular response using specific chemotaxis signals. Using surface analysis techniques is possible to study the deposition of bio-molecules on substrate and study the interactions between substrates and bio-molecules.

In summary microfluidic technique offers a plethora of possible applications in cell biology and tissue engineering studies, combining surface analysis and cell interaction analysis.

2. Materials and methods

2.1 Design of silicon master and PDMS micro-channel fabrication.

2.1.1. Materials

Poly (dimethylsiloxane) was obtained from Dow Corning (Sylgard 184). Silicon wafers (p-type, 100 orientations), were obtained from Compart- Tech. SU-8 photoresist from MicroChem, Newton, MA, USA.

2.1.2. Methods

2.1.2.1. Silicon master design

The silicon master design is a crucial step during the development of masters. Choosing the photo-mask is the first step. A photo-mask is a film with transparent properties that allows light to shine through the designed patterns normally it is used in photolithography processes but also in other industrial processes. Materials used for mask fabrication include Soda Lime glass, Fused Silica or polystyrene films. The mask works as a template, and is designed to transfer patterns on to a substrate in order to fabricate devices.

The photolithography technique used projects light through a photo-mask; the light casts an image of the designed device on the substrate coated with a light sensitive material. Using negative photoresist the masked portion is

removed and can be etched to form channels or specific devices. Using positive photoresist the process is reversed.

A soda-Lime glass photo-mask was used in this work for the design of a master, with dimensions 3" x 3" with high resolution (64K dots per inch). The pattern information was created using an appropriate format AutoCAD (Figure 2.1) and transformed using JD Photo tools programme (photolithography tools) on the "mask writer" which then exposes the design onto the mask substrate.

The fabrication of the photo-mask requires the steps summarised in Figure 2.2. The crucial part in the mask realization is the chrome process. In step 2, the chrome process is summarised. The substrate Soda-Lime has a layer of chrome deposited on one side. The chrome is covered with a layer of anti-reflective coating and a layer of photoresist known as a "blank" (Figure 2.2 A). The light sensitive material absorbs the light when exposed and creates an image of the photoresist material (Figure 2.2 B). The development of the photo-sensitive material makes the unexposed parts of the "blank" soft and dissolves out the mask layer (Figure 2.2 C). The etching step removes the chrome part of the mask that is not necessary and after the final stripping of the photoresist material with a chemical treatment chrome patterns on Soda-Lime substrate with an anti-reflecting coating are formed (Figure 2.2 D,E). In this work the Soda-Lime mask was ordered from the JD photo tools website. The design of the microfluidic patterns were realised using Auto-CAD programme with various dimensions from 25 μm to 350 μm , as showed in

(Figure 2.1). The area that is useable on the mask is the central 50 mm x 50mm part so 9 squares with dimensions of 15mm x 15 mm were formed containing different designed microstructures for variable uses.

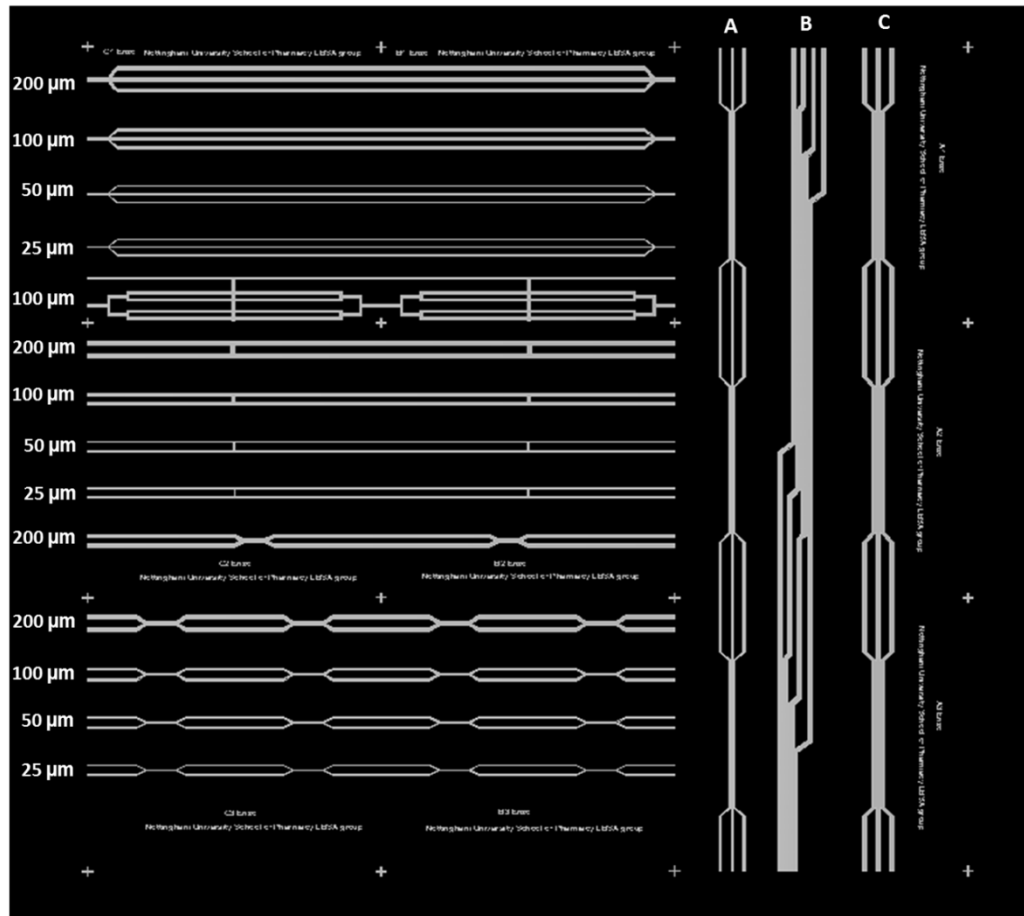


Figure 2.1: Representation of the mask design realised using the CAD programme. 9 squares with dimension 15 x 15 mm were designed containing different micro structures. On the left side the width dimension of each micro structure is reported. The etch depth used for the realisation of the micro structures was 10.5 ± 0.5 microns. A, B and C microstructures reported on the right side show different designs with width dimensions of 100 and 200 μm for A and C and in B dimensions of 100 μm in the thinner channel and 350 μm in the thicker channel. Section of the specific design used in the study is reported in the following pictures.

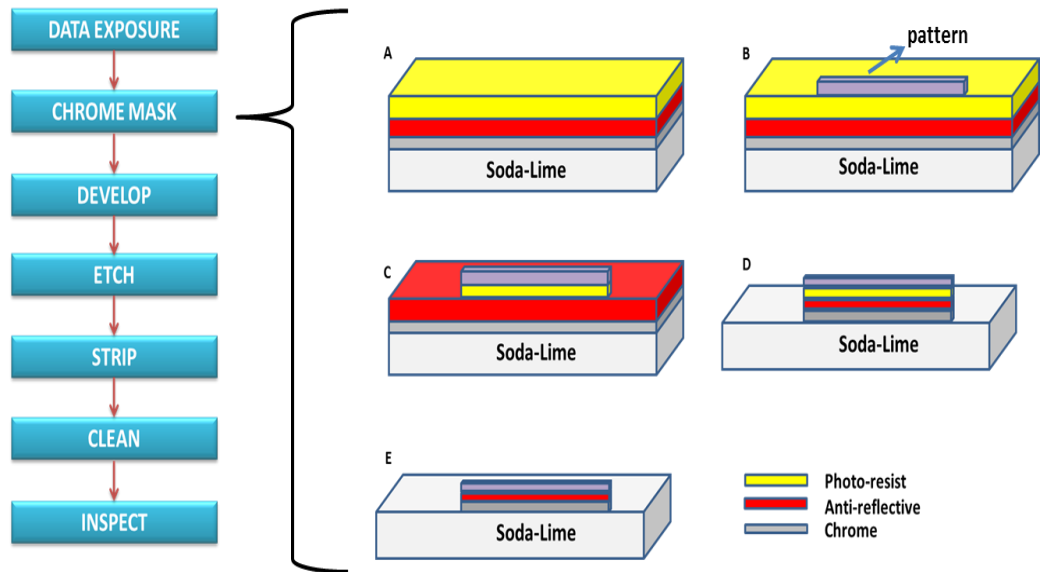


Figure 2.2: Procedure for mask development. A, B, C, D and E represented phases involved in chrome process. A) "Blank" sample, B) Light exposure, C) Development, D) Etching, E) Stripping.

2.1.2.2. Silicon master fabrication

A master silicon device was developed in SU-8 photoresist through photolithography. To begin, SU was spun coated and exposed to UV irradiation through a glass lime photo mask using a mask aligner. The mask, was created via laser direct writing ⁽⁶¹⁾, and is a positive replica of desired channel waveguide arrays. After post exposure, baking and photoresist development (as described in the previous section), the waveguide array master device was realized. Notably, SU8-patterns processed on silicon wafers are robust, durable and can be used indefinitely ⁽⁶¹⁾ (Figure 2.3).

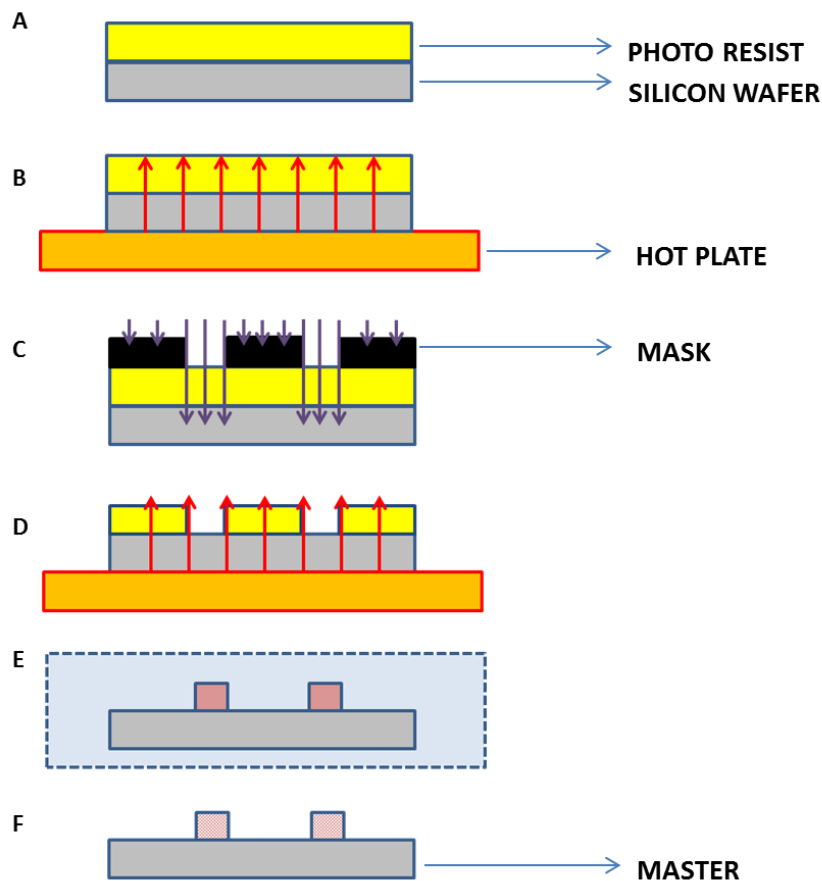


Figure 2.3: Steps involved in silicon master fabrication. A) Spun coated, B) baking, C) and D) UV radiation exposure and baking after exposure respectively, E) development, F) master fabrication.

2.1.2.3. Fabrication elastomeric mould

Poly (dimethyl siloxane) (PDMS) micro stamps were fabricated (Sylgard 184, Dow-Corning) through replica micro-moulding. A mixture of PDMS pre polymer and curing agent in a 10:1 (w/w) ratio was thoroughly stirred, degassed in a vacuum oven, poured onto the silicon master, and cured at 65°C in the oven overnight. The cured PDMS was then peeled away from the silicon master (Figure 2.4). The replica stamps can be used to create high-fidelity (nanometre scale) copies of the original master pattern. Additionally,

the stamps can be reused multiple times (up to 100 times) without degradation for mass replication. PDMS stamps with dimensions of approximately 1 cm x 1 cm were used to guide the microfluidic absorption of the proteins on the silicon wafer substrate.

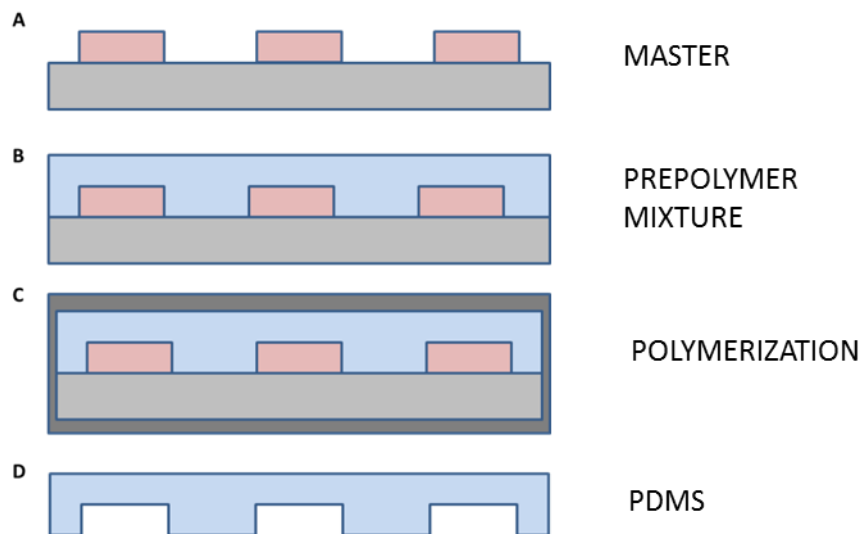


Figure 2.4: Elastomeric stamp fabrication (PDMS) in A) the silicon master, B) mixture of elastomeric rubber base and cross-linker on top of the master C) polymerization, D) peel the stamp off.

2.2 Creation of protein patterns and surface analysis

2.2.1. Materials

Poly (dimethylsiloxane) was obtained from Dow Corning (Sylgard 184). Silicon wafers (p-type, 100 orientations), were obtained from Compart- Tech. Texas red BSA (MW.69Kd), Rhodamine labelled fibronectin (MW.450Kd), green fluorescent HiLyte488 fibronectin and phosphate buffer were obtained from Sigma Gillingham, Dorset U.K. Anti-fibronectin antibody (Anti-Fibronectin (bovine) mouse monoclonal antibody) was purchased from the Antibody Shop (Denmark). AMAS cross-linker was obtained from Thermo Scientific (UK). RTESPA and DNP-S were purchased from Brucker (Coventry, UK).

2.2.2. Methods

2.2.2.1. Water contact angle measurements

Water contact angle (WCA) measurements were carried out on uniform samples with a CAM 200 Optical Contact Angle Meter. After placing the water drop on the PDMS, silica wafer and polystyrene based material (non-TCP), 10 images were captured at 1 second intervals. To determine the WCA at the initial contact of the drop with the surface, the first measurement was discarded and a linear regression was fitted to and the value at $t = 0$ was calculated.

2.2.2.2. Samples preparation

Spatial patterns of fluorescent proteins were created using a microfluidic technique to guide the protein injections on silica wafer and polystyrene substrates. PDMS devices were washed with streams of acetone, 2-propanol, and water and dried before using. Three different fluorescent proteins Texas Red labelled BSA, Rhodamine labelled fibronectin and green fluorescent HiLyte488 fibronectin were used. Dilutions were made using phosphate buffer at pH 7.4. Different protein concentrations were used from 1 mg/mL to 1 μ g/mL. The creations of spatial patterns of protein concentration gradient were achieved using the PDMS to guide the proteins injection inside the microfluidic channel on the silicon wafer and polystyrene supports. Briefly after washing the PDMS before use (to avoid contamination that can interfere with the analysis), it was put in to contact with the substrate. To promote a better adhesion of the PDMS stamp to the substrate, a Plasma Barrer Etcher (BIORAD) was used on the substrates and PDMS for 10sec with a power of 80W to create a temporarily hydrophilic substrate. A micropipette was used to inject 10 μ L of protein solutions inside the channels where through microfluidic diffusion protein was absorbed along the channel (the time to fill the microfluidic channel was around 50 seconds and not instantaneous), after 30 minutes of incubation the PDMS stamp was taken off, the sample washed with deionized water, dried under nitrogen flow and protein patterns revealed on the substrate. The features used in the creation of the PDMS stamp for the guidance of protein deposition on substrates are reported and described in Figure 2.5 A₂, A₃.

2.2.2.3. Fluorescence imaging

Fluorescence microscopy (Leica IRE2 time-lapse DIC and fluorescence microscope with full stage incubation (37°C, 5% CO₂) and a Hamamatsu OrcaER monochrome camera, for longer time-lapse and multi-channel acquisitions (filters for FITC/GFP, TRITC, DAPI) and image analysis). Briefly fluorescence analysis was conducted using a specific filter FITC/GFP, in our case considering the difference between excitation and emission value (535 nm excitation and 585 nm emission for Rhodamine labelled fibronectin; 528 nm excitation and 547 nm emission for Texas Red labelled BSA). In time lapse analysis fluorescence images were acquired every 10 minutes for 24 hours.

2.2.2.4. AFM imaging

AFM images were acquired in air in tapping mode at different scan sizes and rates, using a RTESPA (spring constant 20 N/m to 80 N/m, resonant frequency 300 kHz to 400 kHz) probe. . Quantitative imaging analysis of the substrates before and after protein immobilisation was performed using the Nanoscope Analysis program (Version 1.20, BrukerNano). Different scan size images were collected along the microfluidic channel before and after protein immobilisation from 5µm to 0.5µm scan sizes and an example is reported in Figure 3.6. The start, middle and end points of the microfluidic design used for the protein deposition reported in of the protein patterns were considered and three areas analysed at each of these points. The quantitative analysis of

the surface coverage after protein deposition was performed considering the differences observed between the bare and the functionalised substrate conducting a particle analysis with the Nanoscope Analysis programme. The analysis of the particle diameters and the surface coverage considered three areas for every point along the channel, and the average value of the analysis reported in **Table 3**. Analysis of the profile of the surface before and after protein immobilization was performed considering three sections of each area analysed along the protein patterns, and an average value of the roughness reported **Table 3**. Due to the relative roughness of the polystyrene substrate and the less repeatable features on its surface five different areas for every point (15 in total) were analysed and an example reported in Figure 3.7.

2.2.2.5. AFM probe functionalization

AFM probes were functionalised with anti-fibronectin antibody (Anti-Fibronectin (bovine) mouse monoclonal antibody), using AMAS (an amine-to-sulfhydryl cross-linker that contains NHS-ester and maleimide reactive groups at opposite ends of a very short 0.44 nm spacer arm) as cross-linker. Briefly, silica nitride DNP-S tips were cleaned using a UV cleaner for 45 minutes. 130 μ L of mercaptopropyl-trimethoxy-silane and 5 mL of dried toluene were mixed in a cleaned vial and immersed the tips in that solution for two hours at room temperature. Silanised tips were rinsed with toluene and put in the oven at 80°C overnight. 2.5 mg of AMAS were dissolved in 2 mL of DMSO and tips were immersed in the solution for two hours at room temperature, and

then rinsed with DMSO. Antibody (100 $\mu\text{g}/\text{mL}$) was added and left for two hours to be absorbed. Tips were rinsed with PBS pH 7.4 before start of the analysis. The analysis was conducted using a BrukerNano DI3000 AFM.

2.2.2.6. Binding force analysis

AFM force curves were acquired in liquid in contact mode at different scan size and rates, using a DNP-S probe (spring constant 0.06 N/m to 0.12 N/m, resonant frequency 10 kHz to 50 kHz). The concentration used for the analysis was 1 $\mu\text{g}/\text{mL}$ of fibronectin FN01 dissolved in PBS Ph 7.4. The Excel macros available in the School of Pharmacy in the University of Nottingham (created by Prof Xinyong Chen) were used for quantitative analysis of the force measurements. Force curves were carried out at a rate of 1 Hz with a force trigger of 0.25 V and a total travel distance of 1 μm . For each force experiment, between 500 and 1000 force curves were acquired. All force curves were taken under phosphate-buffered saline solution (PBS, Sigma Gillingham, Dorset, UK). Analysis of the single adhesion forces registered along the protein patterns are reported in **Table 4** 1000 force curves with the bare silicon tip were collected showing only 2% of specific adhesion (data not shown).

2.2.2.7. Proof of specificity

To verify probe-ligand specificity a blocking with free antigen or ligand can be done, interrupting interaction between the probe receptor and surface ligand which will remove signal due to specific interactions. For force spectroscopy, blocking was done by introducing fibronectin (100 µg/mL in PBS) into the fluid cell during measurements to block antibody sites on the surface of the sample.

2.3 Fibroblasts and mesenchymal stem cells micro-patterning

2.3.1. Materials

Pluronics F127, non-TCP (non-treated tissue culture plates Dow Corning®), Rhodamine labelled fibronectin (MW.450Kd), Green fluorescent HiLyte488 fibronectin and phosphate buffer were purchased from Sigma Gillingham, Dorset U.K.

2.3.2. Methods

2.3.2.1. Substrate functionalization

To obtain a uniform distribution of fibroblasts on the areas of the substrate exposed to the protein patterns and to reduce cell adhesion on the non-TCP (not treated tissue culture plastic plate), the substrate was coated with Pluronics F127. Non-TCP was treated with 3% (w/v) of Pluronics F127. The procedure used is summarised in (Figure 2.5). Briefly the non-TCP was first functionalised using Pluronics F127 with a concentration of 3% (w/v) and left for 24 hours to be absorbed. After 24 hours the substrate was treated using plasma oxygen and the PDMS stamp attached. The fluorescent fibronectin protein was injected inside the microfluidic channels and after 30 minutes the PDMS was peeled off and the protein deposition revealed (the design of the microfluidic channel used for the creation of the protein patterns, taken in examination in the fibroblasts and mesenchymal stem cells adhesion experiment are reported in Figure 2.5 A₁, A₂ respectively).

2.3.2.2. Cell culture and sample preparation

NIH-3T3 mouse embryonic fibroblasts and i-HMCS immortalized mesenchymal staminal cells (cell immortalization was achieved using same procedure described in Okamoto et al. 2002 ⁽⁶³⁾) were grown in Dulbecco's modified eagle medium (DMEM) with 10% FCS and standard additives. Details of reagents of the media can be found elsewhere ⁽⁶⁴⁾. Mouse embryonic fibroblasts were genetically labelled as previously described ⁽⁶²⁾ using transduction of lentiviruses expressing either enhanced monomeric red fluorescent protein (mRFP) and green fluorescent protein (mGFP) . Cells were selected with Puromycin (NIH-3T3: 3 mg/mL HMCS: 4mg/mL) for three passages. Flow cytometric analysis confirmed that cells were >95% labelled. For patterning, cell suspensions of 10^6 cells (in 4 mL per well), of both cell lines were seeded onto non-TCP (previously functionalised with pluronics F127), already patterned with Rhodamine labelled fibronectin in defined media conditions (lacking FCS). Cells were allowed to attach for a defined period of two hours. Non-adhered cells were removed by gently washing twice with PBS and replacing this with fresh growth media.

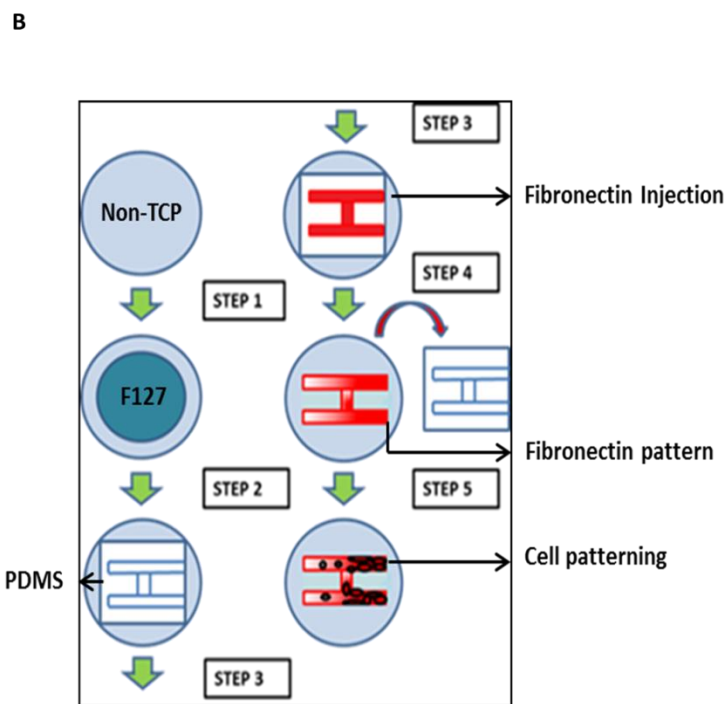
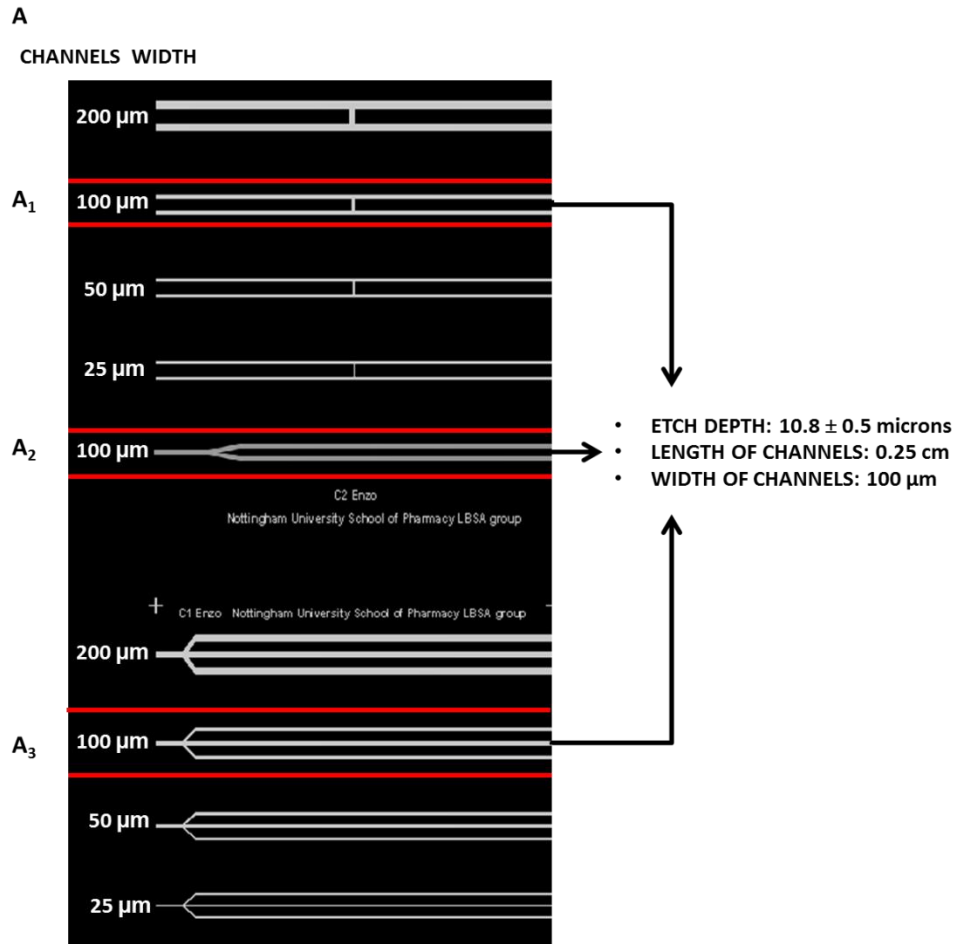


Figure 2.5: In A: Schematic representation of the microfluidic channel shape used for the creation of the PDMS to guide protein deposition (A_2 , A_3) and cell patterning formation (A_1 , A_3). The width, length

and depth of the microstructures used are also reported. In B: Schematic representation of the procedure used to functionalise the non-TCP using Pluronic F127. Step1: pouring a solution of Pluronic F127 in the plastic plate (approx. 2ml). This was left overnight to get a thick film on the surface; Step2 & 3: after oxygen plasma treatment of surface and elastomeric stamp, put in contact the PDMS stamp with the plastic substrate and inject fibronectin; Step4: take the PDMS off and Step5: seeding fibroblasts 3T3 with a concentration of 10^6 cells

2.3.2.3. Fluorescence imaging and time lapse analysis

Images of the patterns along the microfluidic channels were taken on a 0.5 s exposure using a red filter and signal intensity determined (Volocity 5.2 software; Improvion, UK). In the time lapse analysis images were collected every 10 minutes for 24 hours at 37°C with constant CO₂ and real time video recorded using Volocity 5.2 software. Analysis of the 3T3 fibroblast cells adhesion and i-HMSC cells were conducted analysing fluorescent images before and after cell deposition on the fibronectin pattern. The software Image J was used to evaluate the cell density in the channel comparing the channel before and after cell deposition. Three areas were analysed along the pattern and the average value reported in Figure 4.6 E and Figure 4.7 E.

3T3 fibroblast cells migration was evaluated analysing the videos collected using a time-lapse microscope every 10 minutes for 24hrs on a Nikon live imaging station (Nikon) equipped with a 10X phase-contrast objective, automated X-Y-Z-stage, a climate chamber and camera. Cell migration speed and directionality were analysed with the Chemotaxis and Migration tool plug-in (ibidi) for ImageJ. At least five independent analyses were considered for every point and an example of the analysis reported in Figure 5.1 and Figure 5.4. The two parameters that were considered to detect the cell

migration were the centre of mass (M_{end}), and the X, Y forward migration index as reported in the literature^(65,66,67).

$$M_{END} = \frac{1}{n} \sum_{i=1}^n (x_{i,end}, y_{i,end}) \quad 1 \leq i \leq n$$

“i” is the index of the different single cells. The first cell has the index value 1, the last one n.

$$X_{FMI} = \frac{1}{n} \sum_{i=1}^n \left(\frac{x_{i,end}}{d_{i,accum}} \right)$$

$$Y_{FMI} = \frac{1}{n} \sum_{i=1}^n \left(\frac{y_{i,end}}{d_{i,accum}} \right)$$

2.4 Introduction to the techniques

2.4.1 Photolithography

2.4.1.1 Applications and general consideration

Small micro-systems bring new applications and new capabilities to biotechnology and microelectronics ⁽⁶⁸⁾. Systems include microarrays, microfluidic devices such as ‘lab on chip’ for peptides analysis and microchips for cell culture investigation ⁽⁶⁹⁾. The work on micro-fabrication devices, and the advent of photolithography contributed in the fabrication of DNA arrays in late 1980s ⁽⁷⁰⁾. However, the commonly used photolithography techniques have shown a number of limitations in creating micro-architectures for biological systems. Although well suited for the mass manufacture of semiconductor based devices photolithography where light is used to create spatial patterns via light sensitive materials and subsequent etching is generally an expensive technique for the fabrication of bespoke micro-electronic devices, and is only applicable to a limited set of materials.

When bespoke micro or nano-devices are required on planar or curved surfaces so called soft-lithography offers an alternative approach ⁽⁷¹⁾. The idea behind soft-lithography technique is to use a moulded elastomeric stamp to create patterns on different substrates using micro-contact printing (μ CP) ⁽⁷²⁾, replica moulding ⁽⁷³⁾ or micro-fluidic patterning ⁽⁷⁴⁾ Soft-lithography offers access to a large range of materials, as well as experimental simplicity and flexibility.

Soft-lithography techniques consists of the creation of patterned copies using a PDMS stamp (itself created from a master) to fabricate structures on a surface and as a process consists of pattern design, fabrication of the mask and master, fabrication of the PDMS stamp and microstructures with this stamp. For the master pattern design, software can be used such as AutoCAD tools with higher capabilities to design patterns on chrome mask. Fabrication of the master is normally carried out using photolithography or e-beam lithography. Conventional photolithography is utilized for patterning structures with feature sizes larger than $1\ \mu\text{m}$ ⁽⁷¹⁾. E-beam lithography has the capacity to generate structures (20 nm to 30 nm in lateral dimensions) smaller than those available for photolithography, but is more expensive and a slower technique than photolithography. Fabrication of the PDMS stamp is typically achieved by casting a pre polymer and a cross-linker agent in a specific ratio on the master (normally silicon) with specific structure relief on its surface.

2.4.1.2. Operational mode

The term lithography comes from the Greek *lithos*, meaning stones, and *graphia*, meaning to write. It literally means writing on stones. In photolithography the stones are silicon wafers and the patterns are written in a light sensitive polymer called a photoresist. To build the complex structures requires lithography and pattern transfer steps to be repeated. Every pattern printed on a wafer is aligned to a previous one formed to build the final device. The fabrication of the devices using lithography technique requires a

variety of physical and chemical processes on semiconductor substrate like silicon.

Lithography as a photographic process consists of using a light sensitive polymer (photoresist), exposed to light to create 3D images on substrates. The sequence of processing steps is: preparation of substrate, photoresist spin coat, bake, light exposure, development and a final resist strip. Briefly, to prepare the substrate and improve the adhesion of photoresist material on the substrate, various cleaning steps are carried out to avoid contamination before the addition of an adhesion promoter. After substrate preparation, the coating process is carried out applying the photoresist to the wafer's surface, distributing a uniform thickness of resist on the wafer, in order to prevent problems during the expose process. During the exposure step, the photoresist layer is exposed when ultraviolet (UV) light travels through the mask to the resist. During the subsequent developing process, portions of the photoresist are dissolved by a chemical developer, leaving visible patterns within the resist (Figure 2.3).

2.4.2. Atomic force microscopy

2.4.2.1. Applications and general information

Atomic force microscope (AFM) has been used as tool to investigate micro-structural parameter and reveal complex intermolecular forces at the nano-scale level. Forces measured in the sub nano-Newton range and the ability to perform experiments under physiological conditions, make AFM the useful tool to study biological interaction (cell/cell, drug/proteins, cell/cell and cell/proteins), and to quantify molecular interactions in biological systems. An understanding of the interfacial adhesion from a molecular point of view is an important step that can be extremely beneficial in applications as drug design^(74,75), biomaterials development⁽⁷⁶⁾ and biosensor design. AFM has evolved from a simple tool for topographic imaging to one able to quantify a range of surface properties. The ability to detect very low forces (10 pN) and to work in simulated physiological conditions makes AFM an attractive technique to study biological systems. Using force spectroscopy it is possible to probe molecular interactions that include DNA⁽⁷⁷⁾, polysaccharides⁽⁷⁸⁾, proteins⁽⁷⁹⁾, and biopolymers on cellular surface⁽⁸⁰⁾. Probing single molecules on cell surface important phenomena as cell adhesion and chemo-taxis can be studied.

2.4.2.2. AFM Operational modes

A typical AFM system consists of a cantilever probe including a nanoscale sharp tip mounted to a piezoelectric actuator and a photo-detector to provide cantilever deflection feedback. Scanning the tip on, or close to a sample surface using the piezo scanner at a constant contact force and constant height above the surface allows the probe to experience tip-sample interactions that cause cantilever deflection. A laser beam reflected from the back of the cantilever allows this deflection to be monitored and a feedback loop to be set-up to control AFM tip position and provide an 'image' of a surface (Figure 2.6). The three main operational modes using an AFM technique are: non-contact mode, contact mode, and tapping mode. The non-contact mode is used by moving the cantilever from the sample surface and oscillating it near its resonance frequency, acquiring topographical information of the sample based on long range interaction between the surface and the tip⁽⁸¹⁾. Such interactions cause a shift in cantilever resonance amplitude or frequency which can be measured and used as the feedback signal. This mode provides minimal sample disturbance but lower spatial resolution. Using contact mode the cantilever tip remains in continuous contact with the sample, whilst cantilever deflection allows monitoring interaction forces on the sample surface⁽⁸²⁾. This mode provides the highest spatial resolution but the interaction forces can cause damage and deformation to soft samples, such as proteins. A combination of the qualities of both these operational modes is tapping mode where the oscillation of the cantilever near the resonance frequency allows the cantilever tip to impact on

the sample for a short time at the bottom of each oscillation cycle. This allows high spatial resolution to be achieved, without significant damage to the sample due to lateral scanning forces⁽⁸³⁾.

Interaction forces between the tip and the sample can be visualised on a force-displacement curve (Figure 2.7). When the distance between the tip and the sample surface is large (approx. 5 nm to 10 nm) weak attractive forces (van de Waals) are experienced. As the tip contact the sample, significant repulsive forces are experienced (Born repulsion).

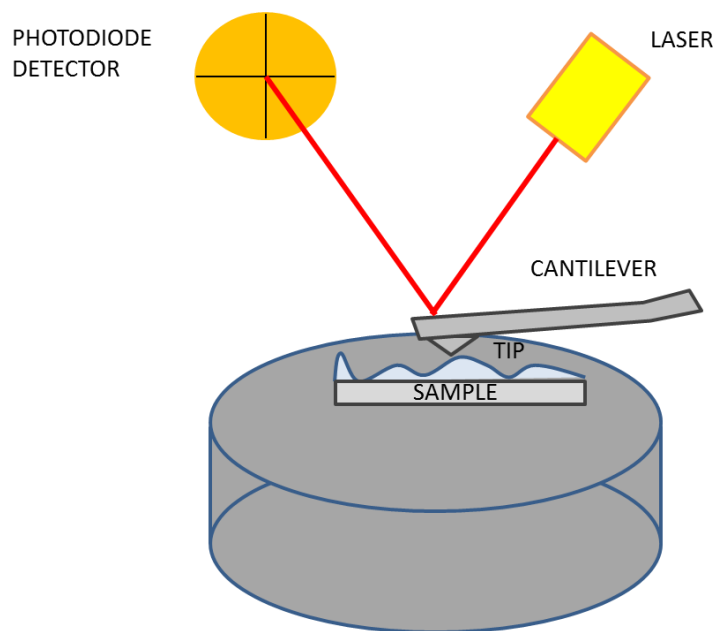


Figure 2.6: AFM apparatus schematic representation. In the figure are reported the components of Atomic Force Microscope: a photodiode detector, laser, cantilever and a tip attached to the cantilever

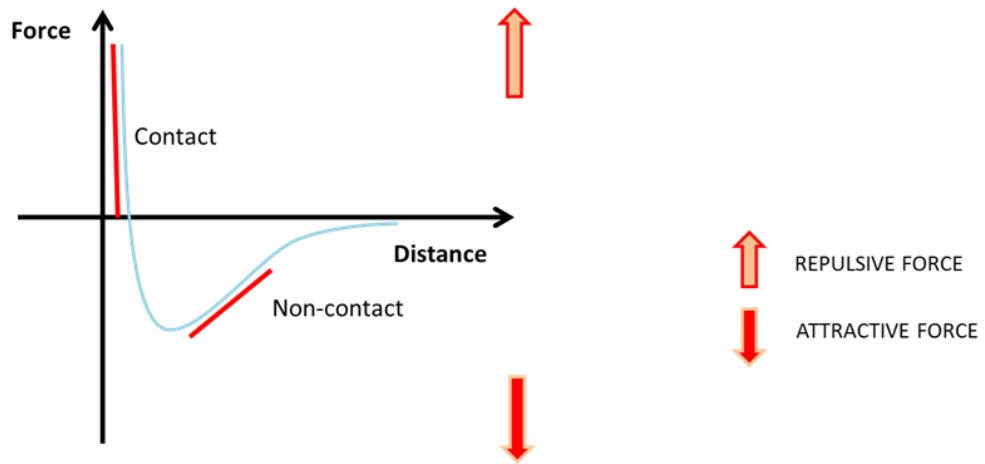


Figure 2.7: Schematic representation of Force variation between an AFM tip and sample.

2.4.2.3. AFM imaging system

2.4.2.3.1. Non-contact AFM imaging

Using non-contact mode AFM the attractive forces between the tip and the sample are initially weak comparing with the contact-mode. The tip in non-contact mode is oscillating to detect the small forces on the substrate by measuring changes in amplitude, phase or frequency of the cantilever. Non-contact AFM has been used for imaging large variety of materials as, semiconductor materials, polymers and biological materials ^(84,85), showing advantages over other scanning probe techniques (STM and contact AFM). With non-contact AFM is possible to imaging “soft” samples, providing topography of the sample surface with little or no contact between the tip and the sample, due to the absence of repulsive forces in non-contact AFM. The ability to resolve atomic rows or step on flat semiconductor materials

brought AFM on par with the STM^(86,87). The total force between the tip and the sample using the non-contact AFM is really low (10 pN to 12 pN)⁽⁸⁸⁾ providing sample topographic measurements with little or no contact of the sample, favouring studies of soft and elastic samples. Due to the oscillation of the cantilever and the minimal tip interaction yields improving image resolution over contact AFM.

2.4.2.3.2. Contact AFM imaging

Contact AFM imaging mode system is also known as “repulsive mode”, where the tip is in constant contact with the sample during the scanning. The nature of the interaction forces in this case is primarily repulsive, but also other two forces are normally present in contact AFM capillary and forces acting on the cantilever. Capillary force is due to the presence of contaminant layer over the sample surface and is an attractive force and remains constant along the sample, if it is assumed homogeneous layer⁽⁸⁸⁾. The cantilever forces used on the sample surface are directly dependent on the deflection and spring constant of the cantilever. Two operating modes can be used to generate the surface profile in contact AFM: constant height mode where the piezo laterally scans the surface without moving the z direction, in constant force mode where the force acting between the tip and the sample is kept constant. Using constant height mode any steps presented on the surface can damage the tip revealing surface irregularities during the scanning, for this reason the constant force mode is normally used as operating mode in contact AFM

imaging. The topographic image obtained using contact AFM system is formed by registering the voltage applied to the piezo, maintaining the deflection at a fixed set point value. Two major problems can be registered using this system: the presence of lateral forces from the scanning can produce damage on sample and the variations in the zero force level due to thermal drift material creeps.

2.4.2.3.3. Tapping AFM imaging

Tapping AFM system is used for high resolution imaging of soft samples, which are not easy to get using a contact AFM imaging system. Problems like friction or adhesions that normally are problems using conventional AFM imaging systems are overcome. The cantilever is oscillating near the resonant frequency, where the piezo actuator applies a force on the cantilever that permits the tip to vibrate at amplitudes that will change with the surface topography of the sample. During the tapping on the sample surface the oscillation frequency is kept constant.

2.4.2.3.4. Force spectroscopy

To obtain nano-mechanical information on the sample using AFM technique, force spectroscopy analysis can be used as extension of AFM based technique^(89,90). In force spectroscopy the AFM probe is positioning to a desired x,y position and brought in contact with the surface, until the cantilever deflects,

and pulled away again. In the first instance the cantilever is too distant from the surface and there are no forces acting on the cantilever (Region A Figure 2.8). During the approaching on the surface van der Waals and electrostatic forces are registered due to the interaction between atoms on the probe and atoms on the surface (Region B Figure 2.8). When the probe is in contact with the substrate the cantilever is bended away from the surface due to repulsive forces between probe and sample, where elastic and /or plastic deformations can be registered providing nano-mechanical information of the surface (Region C Figure 2.8). Using Hook's law a quantitative study ^(91,92) of the probe-sample forces can be done if the properties of the cantilever are determined.

$$F = -Kc * X$$

F is the force applied; X is the cantilever's deflection and Kc the spring constant. Adhesion forces between the probe and the sample are calculated from the retract curve ⁽⁹³⁾.

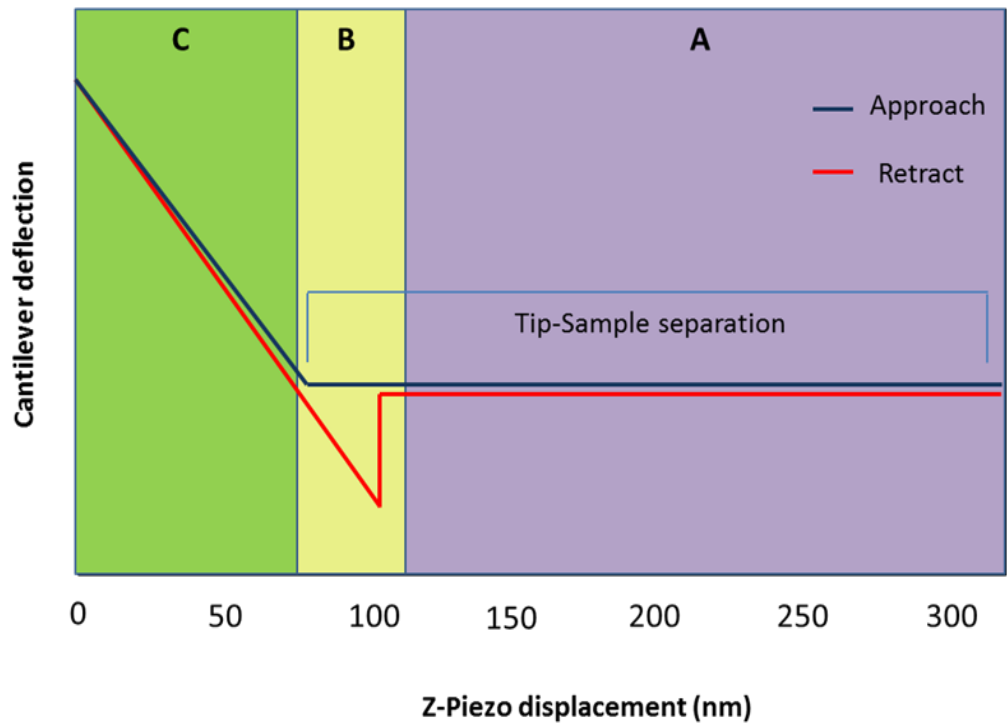


Figure 2.8: Schematic deflection vs z-piezo displacement curve. In Region A, no deflection occurs. In Region B, probe adheres to the surface and in Region C the probe is in contact with the surface and the cantilever deflects

2.4.3. Fluorescence microscopy

2.4.3.1. Applications and instrumental information

The principle of the fluorescence microscopy consists in the use of fluorophores (molecules with fluorescent properties), with high absorption at a specific wavelength (shorter) and emission at a longer wavelength. Briefly when a fluorophore absorbs light there is an alteration “excitation” of the molecular state (high energy state) and very quickly with fluorescence emission. The time that the fluorophore spends in the excited state before come back to the “normal” state (lower energy) represents the lifetime of the fluorescence.

The ability of the fluorescent molecules to be internally incorporated in living cells makes this technique useful to study fluorescent proteins in gene analysis ⁽⁹⁴⁾ and to localize proteins in living cells ⁽⁹⁵⁾. Many researchers have used fluorescence analysis to study microfluidic devices. Stroock et al. quantified the mixing of proteins in patterns using the fluorescence intensity distribution ⁽⁹⁶⁾.

2.4.3.2. Operational mode

The key component parts of a fluorescence microscope are: a light source, dichroic mirror (reflects shorter wavelengths, and emits longer wavelengths), excitation filter (preselect the exciting wavelength), emission filter (passage of longer wavelengths to the detector) and a detector (Figure 2.9) . The light

emitted from the source passes through the excitation filter where a pre-selection of the exciting wavelength is done. After this first step the light ray bounces through the dichroic mirrors that reflects shorter wavelengths from the light source and emits longer wavelengths of the fluorescence. The fluorescence light emitted from the sample passes through the dichroic mirror to the detector.

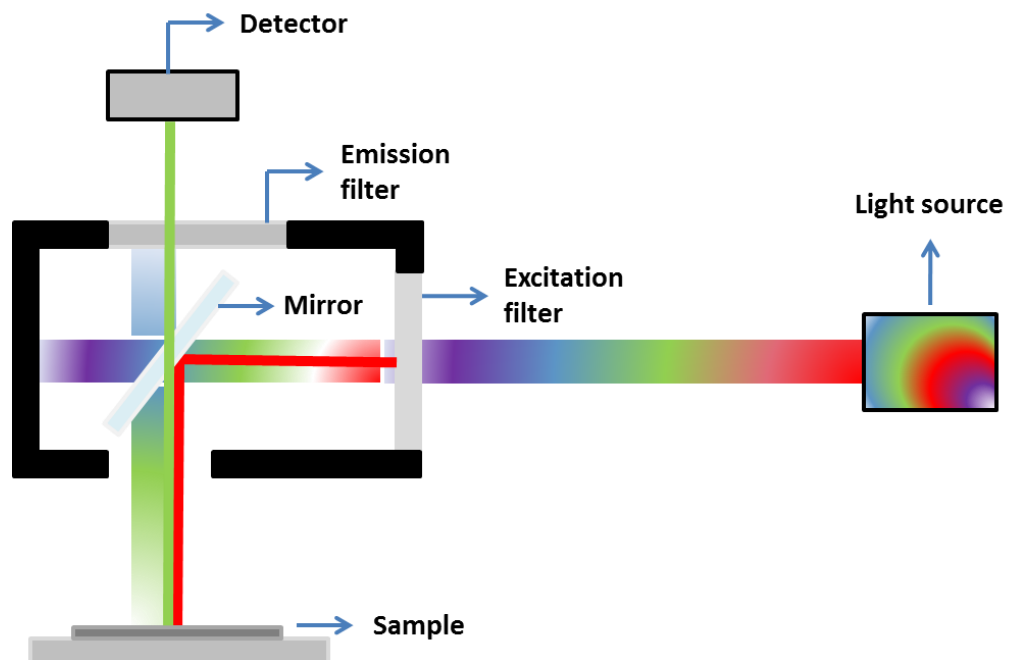


Figure 2.9: Basic principle of the fluorescence microscopy. The light source emits light that is reflected by the mirror through the objective into the sample. The excitation of the fluorophore will emit light of a longer wavelength, which will go back through the objective and form the final image on a detector.

2.4.4. Cell micro-patterning

2.4.4.1. Applications and general information

Controlling the size and the deposition of cells on a substrate using cell micro patterning has opened new frontiers for fundamental studies in cell biology. The characteristic of living cells to create mechanical connections between cells and the surrounding environment (extracellular matrix ECM), activates specific metabolic and transduction signals ⁽⁹⁷⁾ and plays a significant role in cell adhesion, migration and tissue development. Cell adhesion requires interactions between integrins and extracellular matrixes, activating signalling proteins to form focal adhesion ⁽⁹⁸⁾. It was observed using cell micro patterning that changes in shape and patterns of cell contact effects cell division, proliferation, and differentiation controlling cell-cell and cell-substrate interactions ⁽⁹⁸⁾. Some early studies to control cell spreading on substrates were conducted to prove the role of ECM in cell proliferation. It was shown that cells proliferate only when ECM was spread on the substrate, confirming the presence of an interaction between integrins and ECM ⁽⁹⁹⁾. Cell migration studies were also investigated using a substrate composed of an inert part (adhesion-resistant) and a covered ECM protein part (cell-adhesion) ⁽¹⁰⁰⁾. Both microfluidic and μ C printing are useful for the creation of these patterns. In tissue engineering studies cell-cell interactions are important to understand the physiology of organs such as the liver and skeletal muscle. The conventional methods used in this case (co-culture systems), are not able to create a substrate where two or more cell types can be highly controlled to

study the cell-cell interactions. Cell micro-patterning was used in tissue engineering to overcome such problems with conventional co-culture systems. For example, co-cultures of fibroblast and other cells like hepatocytes and micro-vascular endothelial cells have been created using cell micro-patterning technique. The ability to create patterning on biocompatible materials like gelatine was demonstrated, increasing the chance to be used it in future engineering applications for body implants ⁽¹⁰⁰⁾. The ability to control cell adhesion and development on a substrate and the possibility to co-culture different cell lines on a surface made this technique is useful in biomedical studies.

2.4.4.2. Methods to create cell patterning

Many methods have been used for the cell patterning fabrication. Photolithography was traditionally used to create a mask or master for patterning biological material on a substrate ⁽¹⁰¹⁾. Briefly photoresist patterns are created by transferring geometrical patterns from a mask to a substrate, using UV light. Due to the expensive equipment and the inconvenient for biologists to use this technique Whitesides and colleagues ⁽¹⁰²⁾ developed soft lithography ⁽¹⁰³⁾. In microfluidic patterning, as used in this thesis, the PDMS stamp is used to guide the biomolecules absorption on the substrate introducing a liquid solution in the open ends of the microfluidic channel and spontaneously for capillarity promotes the absorption of biomolecules to form patterns (Figure 2.10).

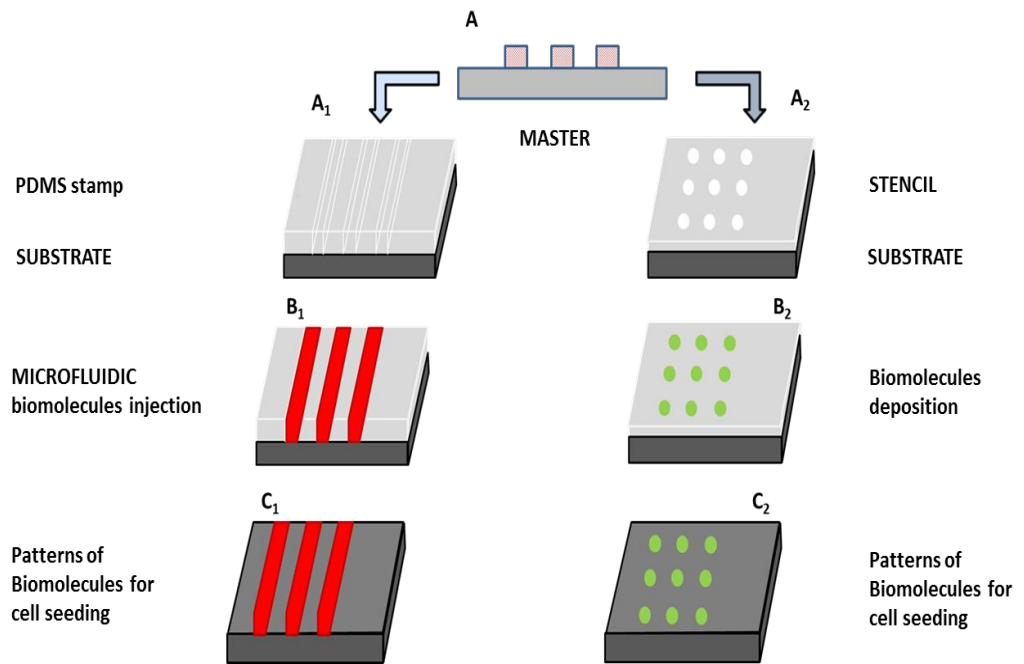


Figure 2.10: Representation of microfluidic and stencil patterning methods. In A negative photoresist pattern, in A_1 , B_1 , C_1 microfluidic patterning method showing PDMS sealing to the substrate, microfluidic technique application and patterning respectively. In A_2 , B_2 , C_2 stencil patterning method showing stencil deposition, exposure to the material and patterning realization respectively

3. Protein patterning and surface characterization

3.1. Introduction

In this chapter, the production of protein micro patterns using micro fluids is demonstrated. The distribution of the surface proteins deposited is investigated using fluorescence microscopy and AFM imaging and force spectroscopy. The AFM has been used successfully as tool for measuring inter-molecular forces in a broad spectrum of applications such as material manufacturing, polymers and biology. The ability to provide reliable measurements at the nanometre scale using an AFM provides certain advantages compared with other microscopic methods (scanning electron microscopy, SEM and transmission electron microscopy TEM) in studies of surfaces and micro-structures^(104,105). Force modulation microscopy, whereby forces of interaction are spatially mapped is also used as an AFM extension for the analysis of mechanical properties of polymers and imaging composition changes^(106,107).

3.2. Methods: AFM analysis

Additional information is provided here in addition to that already discussed in Chapter 2, where techniques or materials have been used specific to this chapter.

3.2.1. AFM Probe Functionalization

Molecular recognition studies can be conducted using force spectroscopy by attaching a suitable ligand to an AFM probe which has the potential to specifically bind sites in the target sample; in this case the proteins deposited were found in clear patterns. Probe functionalization following the attachment of ligands (such as antibodies), allows specific molecular recognition to be studied and spatially mapped ^(108,109). After antibody immobilization on the probe, force spectroscopy is used to measure specific interactions between the antibody and the protein, investigating binding kinetics, rupture forces and protein conformations ^(110,111).

Functionalization of a probe for molecular recognition requires that a biomolecule is stably attached to the probe using a linker such as a biotin-streptavidin bridge ^(112,114), or glutaraldehyde cross linking ⁽¹¹³⁾. The linker should firmly attach the ligand to the probe so that it remains on the probe throughout the study but also must allow sufficient conformation freedom so as to not inhibit binding to the target receptor. Other methods used include covalently binding the biomolecule on the probe using an amylose ^(115,116) or

PEG chain ^(117,118) between the amine reactive tip and the amine groups available on the biomolecule.

In this work the probe functionalization was carried out using an anti-fibronectin antibody. Mouse monoclonal anti-fibronectin antibody clone A22 (Antibody Shop (Denmark)) was chosen for its characteristics to specifically bind to bovine fibronectin. It is not clear where the binding site of the antibody is located, but Underwood and co-workers ⁽¹¹⁸⁾ reported that the possible binding site could be the amino-terminal Heparin1 or Heparin3 regions as showed in the picture (Figure 3.1). Underwood and co-workers ⁽¹²⁰⁾ also demonstrated that the clone A22 mimics cell adhesion to that of fibronectin coated on hydrophilic tissue culture plates as opposed to hydrophobic polystyrene substrate. Aminosilanization of the silicon tip has been used as reported in literature ^(121,122), to create the optimal condition for the binding of the amine-sulfhydryl linker.

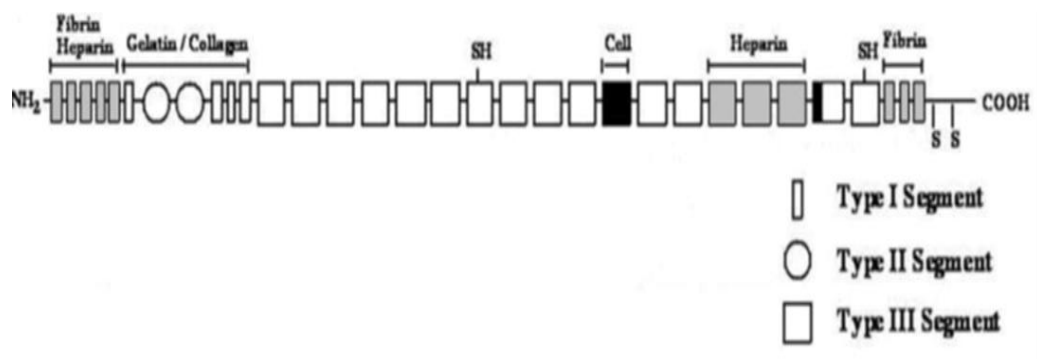


Figure 3.1: Fn monomer composition; adapted from Patel and co-workers ⁽¹²³⁾

3.3. Results and discussion

3.3.1. Patterning of proteins using the microfluidic technique

Microfluidic channels represent an effective approach for the patterning of bio molecules, guiding solutions of proteins fitted over regions of a substrate localizing their absorption.

Several requirements must be satisfied for the successful patterning of proteins on substrates. The micro-channel must be sufficiently hydrophilic to permit filling by capillary force. PDMS is natively hydrophobic which does not allow the flow of aqueous solutions through the elastomeric channels. This problem was overcome by exposing the entire PDMS mould to oxygen plasma to obtain a temporarily hydrophilic substrate, as reported in Figure 3.2. The oxygen plasma creates species which attack the silicon carbon bonds, increasing the amount of oxygen on the surface of the PDMS ⁽¹²⁴⁾. The high energy of oxidised PDMS means that it is wet by polar liquids more easily than native, hydrophobic PDMS ⁽¹²⁴⁾. In protein patterning experiments it was observed in the past that treating the entire elastomeric mould with oxygen plasma allowed leaking of deposited proteins and reduced adhesiveness ⁽⁵⁸⁾. In the work here reported a plasma etching treatment was performed on the elastomeric stamp before being put in to contact with a silica wafer or polystyrene substrate. This was found to increase the level of adhesion of the stamp to the substrate, which subsequently promoted the filling of the capillary almost instantaneously for prolonged periods of time without obvious signs of leaking. The formation of the temporary bond between the stamp

and the substrate was achieved by setting the right power and exposure time during the oxygen plasma treatment. It was observed that treating the PDMS and the substrates with oxygen plasma using a lower power for a longer period (from 50W/60W, for 1 to 2 minutes), the bond formed between the stamp and the substrate was not strong enough to permit a good level of adhesion between the elastomeric mould and substrate. In contrary using a higher power for a shorter period (100 W, for 30 seconds), the formation of a strong bond (not reversible) between the mould and the substrate was observed. A good temporary bond, strong enough to adhere on the surfaces was obtained using 80 W of power for 10 seconds. Further analysis of the substrates and the PDMS using a water contact angle technique before and after the oxygen plasma treatment clearly showed a difference in the surface wettability as summarised in **Table 2**. PDMS, a silica wafer and a polystyrene plastic plate showed a contact angle of 132°, 120.2° and 98.5° respectively confirming the hydrophobic state of the surfaces. After oxygen treatment a decreased value in the contact angle measurements were registered confirming the presence of increased levels of oxygen groups on the surface that render the surfaces temporarily hydrophilic.

Table 2: Water contact angle measurements before and after oxygen plasma treatment

SUBSTRATES	BEFORE TREATMENT w.c.a	AFTER TREATMENT w.c.a
PDMS	wca = 132.0° ± 2.5	wca = 89.4° ± 3.2
POLYSTYRENE	wca = 98.5° ± 5.4	wca = 65.6° ± 2.7
SILICA WAFER	wca = 120.2° ± 1.3	wca = 54.3° ± 1.4

A further requirement for successful patterning using micro-fluidics is the flow of solution within the micro-channels to permit a sufficient supply of proteins to the substrate and avoiding loss of proteins to the walls of the micro-channels. In this work it was observed that if the PDMS did not adhere properly to the substrate, and if the substrate is not properly cleaned problems in the visualization of patterns occurred. To avoid this problem both substrates and PDMS were treated with oxygen plasma as explained above and a clear improvement in the quality of patterns can be observed (Figure 3.3). In Figure 3.4, results of fluorescent microscopy analysis of the spatial patterns of the Texas Red BSA and Rhodamine labelled fibronectin (100 $\mu\text{g}/\text{ml}$ stock solution) at the start, middle and end point of each line formed from the micro-fluidic channels are shown. Based on fluorescent intensity higher protein deposition was observed near the point of injection, which decreased along the channel. The data shown in Figure 3.4 was acquired using a higher protein concentration of 100 $\mu\text{g}/\text{mL}$. The use of a higher protein concentration was necessary to facilitate observation of a clear difference in the intensity signal along the microfluidic channel. A screening of different concentrations from 100 $\mu\text{g}/\text{mL}$ to 1 $\mu\text{g}/\text{mL}$ was performed (data not shown) demonstrating the inability of lower concentrations 10 $\mu\text{g}/\text{mL}$ and 1 $\mu\text{g}/\text{mL}$ to give sufficient fluorescence intensity signal. Again for both proteins there is a clear decrease in the intensity from the point of injection. Whilst silicon is a commonly used substrate in micro-patterning studies due to its flatness and relative inertness it is not frequently used in cell-based studies. Hence a different substrate was also used for proteins immobilisation, namely

polystyrene based non-treated tissue culture plastic plates (non-TCPs). The same procedure used on the silicon wafer substrate was then applied to the non-TCP. In this case the fibronectin used for the experiment was green fluorescent HiLyte488 fibronectin, as the 3T3 fibroblast cells used in the biological studies were labelled with Rhodamine. As shown in Figure 3.4 recorded fluorescence microscopy images on the non-TCP substrate, highlight a different intensity of fibronectin along the channel. The results shown in Figure 3.4 are also consistent which that shown for the silicon wafer substrate.

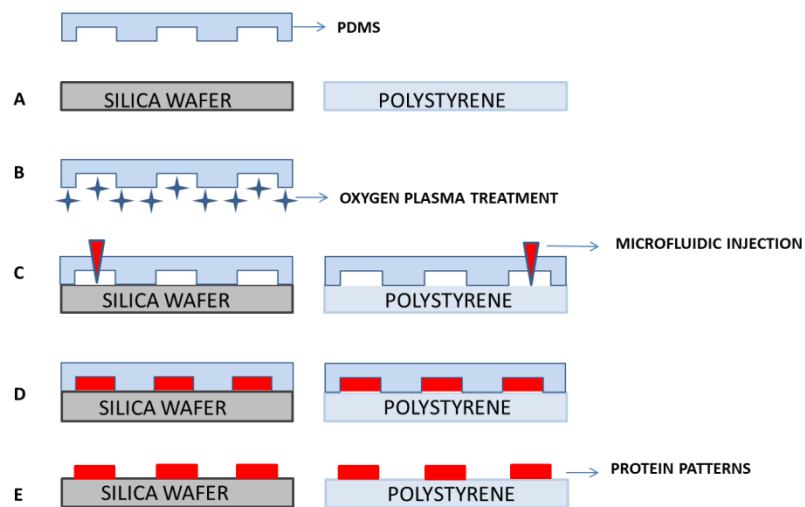


Figure 3.2: Procedure to create patterning of proteins on substrates. A) Stamp and substrates representation, B) Oxygen-Plasma treatment of PDMS, C) and D) injection of protein solutions in the microfluidic channels, and absorption, E) patterning of proteins.

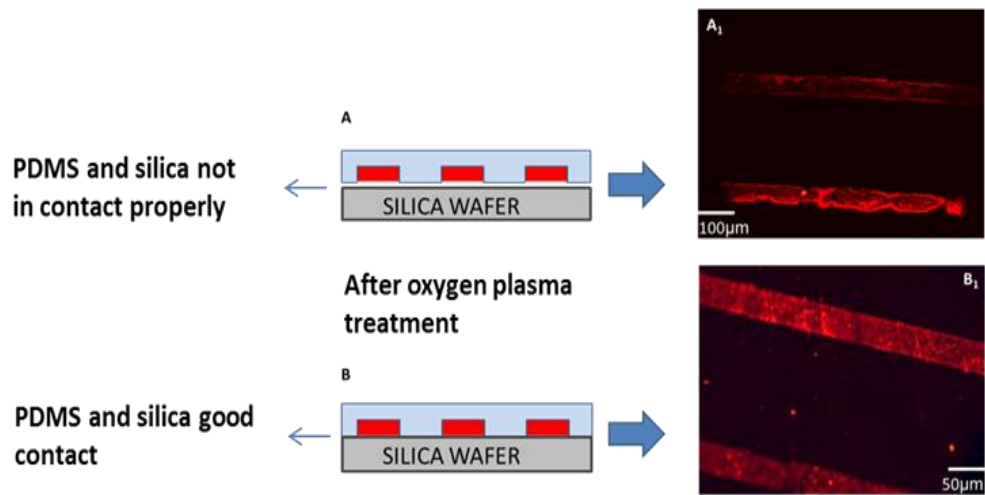


Figure 3.3: Protein patterns analysis using fluorescence microscopy technique. A) not good adhesion between PDMS and silica wafer substrate, before oxygen plasma treatment, A₁) protein pattern analysis using fluorescence microscopy, B) good adhesion between PDMS and silica wafer substrate, after oxygen plasma treatment, B₁) protein pattern analysis after oxygen plasma treatment using fluorescence microscopy technique.

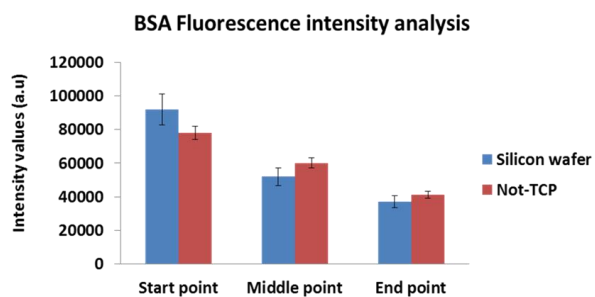
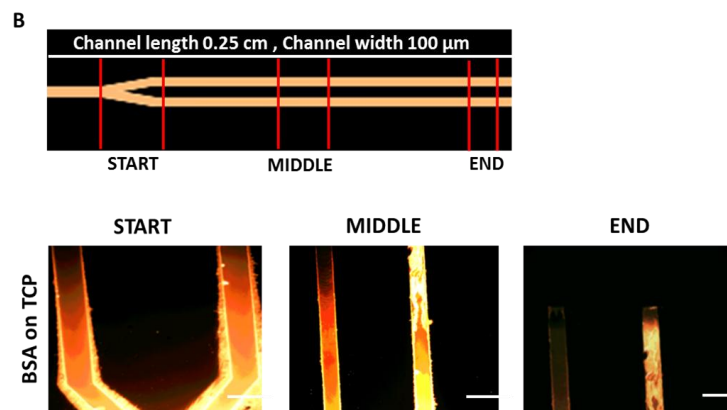
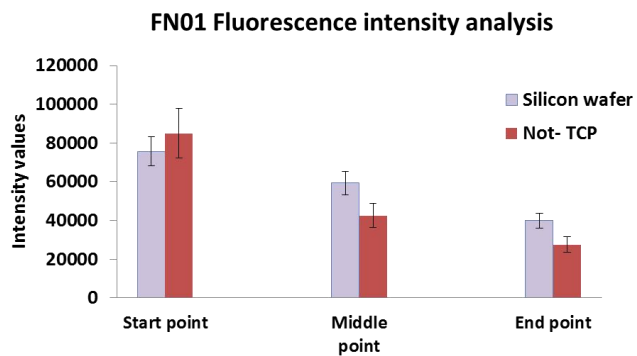
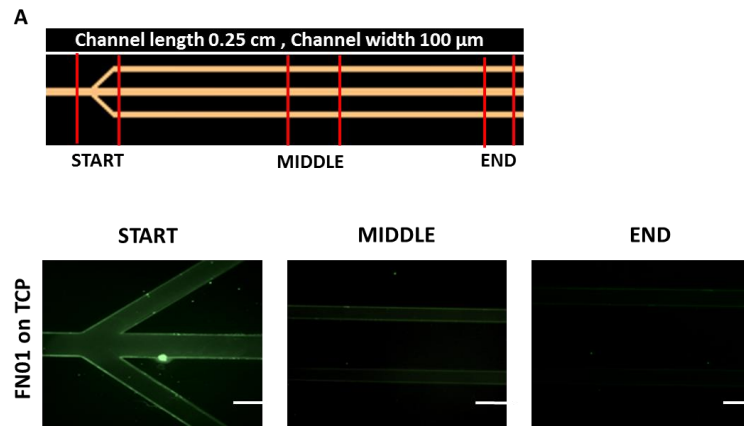


Figure 3.4: Representation of protein fluorescence surface analysis using fluorescence microscopy technique. In A and B representation of the micro-structure design, length and depth measurements used for the fibronectin and albumin deposition on substrates respectively. An example of fluorescence images of the silicon wafer after FN01 (A) and BSA (B) immobilization were reported.

Analysis of the fluorescence intensity is reported on both substrates (silicon wafer and not-TCP) using Image J programme selecting the area of interest (the channel) and an analysis of the fluorescence intensity was reported on the graph, considering three repeating measurements for every sample. The error bar reported in the fluorescence intensity graph represents the average value of \pm SD observed on three repeating measurements. Scale bar 200 μ m

3.3.2. Protein pattern AFM characterization

Characterisation of the surface before and after protein immobilisation was conducted using AFM imaging in tapping mode in air and using RTESPA probes, testing different concentrations between 1 mg/mL and 1 μ g/mL. It was observed that the fibronectin and BSA appearance on the surface depended on the concentration of the initial protein solution from which the protein is adsorbed. Using a protein concentration of 10 μ g/mL resulted in the formation of a higher density of globular protein structures and some aggregates. The preliminary screening performed using different protein concentrations from 1 mg/mL to 1 μ g/mL with an example reported in Figure 3.5, showed clearly the relationship between protein concentration and protein aggregation observed on the silicon wafer substrate. The lowest concentration (1 μ g/mL, Figure 3.6) resulted in isolated globular fibronectin and BSA molecules being distributed on the silicon wafer substrate.

The shape and size of fibronectin and serum albumin on different substrates has been extensively studied in recent literature. Elongated fibronectin molecules adsorbed on mica, Bergkvist et al. ⁽¹²⁵⁾ found a length of 121 nm \pm 25 nm, whilst Erickson et al. ⁽¹²⁶⁾ measured a length of between 110 nm and 160 nm, Chia and al. ⁽¹²⁷⁾ and Orasanu et al. ⁽¹²⁸⁾ found an average size of

serum albumin of 35 nm (diameter) on mica. Globular form of fibronectin was observed by MacDonald et al. ⁽¹²⁹⁾ on pure titanium with a molecular length of $16.5 \text{ nm} \pm 1.0 \text{ nm}$, a height of $2.5 \text{ nm} \pm 0.5 \text{ nm}$, and a width of $9.6 \text{ nm} \pm 1.2 \text{ nm}$. The lowest concentration ($1 \text{ } \mu\text{g/mL}$, Figure 3.6) resulted in isolated globular FN01 and BSA molecules distributed on the silicon wafer substrate. Particles size of proteins found using $1 \text{ } \mu\text{g/ml}$ of protein concentration is reported in **Table 3**.

Due to the aggregation of proteins the concentration was reduced to $1 \text{ } \mu\text{g/mL}$ and AFM data registered before and after protein immobilisation. Figure 3.6 shows a selection of images obtained before and after protein (Texas Red labelled BSA and Rhodamine labelled fibronectin) immobilization on the silicon wafer substrate. Comparing the images before and after protein immobilization it was observed that the surface of the silicon wafer was flat, with a R_a roughness value of $0.7 \text{ nm} \pm 0.2 \text{ nm}$ ($5 \text{ } \mu\text{m}$ by $5 \text{ } \mu\text{m}$ scan in air). After protein immobilisation a uniform surface with a R_a value of $3.2 \text{ nm} \pm 0.7 \text{ nm}$ for BSA and $2.1 \text{ nm} \pm 0.3 \text{ nm}$ fibronectin was observed for similar sized images. Hence, there were detectable changes in the surface profile and roughness due to the deposition of the proteins on the surface. AFM analysis showed a clear difference in protein adsorption along the channel, which was also confirmed by the quantitative analysis where surface coverage was also analysed (**Table 3**). In the previous experiment it was observed that after AFM imaging analysis, the appearance of proteins on the substrate is determined by the amount of proteins adsorbed on the substrate. The difference of protein coverage observed in (Figure 3.6) and reported in (**Table 3**) can be

explain considering the time that protein solution required filling the microfluidic channel. During the protein immobilisation on the substrates, it was observed that the protein solution did not fill the channels instantaneously, but takes around 50 seconds. In this case, it is reasonable to argue that during the injection and the flow of protein in the microfluidic channel the time that the protein solution spent in contact with the substrate plays a key role in the gradient formation. In fact at the injection point or start point the retention of protein solution for a longer time is likely to be a factor promoting greater deposition in this region.

Table 3: AFM images analysis after proteins immobilization on silicon wafer substrate

FN01	START(±SD)	MIDDLE(±SD)	END(±SD)
PARTICLE SIZE	144±6.1nm	78±9.3nm	47±2.0nm
ROUGHNESS	1.98±0.35nm	1.32±0.68nm	0.72±0.05nm
SURFACE COVERAGE	90%	58%	34%
BSA	START(±SD)	MIDDLE(±SD)	END(±SD)
PARTICLE SIZE	36±7.3nm	28±12.0nm	12±5.2nm
ROUGHNESS	3.08±0.75nm	2.15±0.34nm	0.75±0.05nm
SURFACE COVERAGE	70%	38%	14%

Features associated with the protein decreased from an average size of 36 nm to 12 nm for BSA and from 144 nm to 47 nm for fibronectin, when comparing the injection and end point (**Table 3**). Roughness and surface coverage also show a reduced value towards the end point, confirming the presence of varying levels of protein adsorption along the channel as previously demonstrated from fluorescence analysis. These differences are due to a

higher concentration at the injection point which reduces towards the end point due to depletion of protein in solution as it adsorbs to the substrate. Whilst silicon is a commonly used substrate in micro-patterning studies due to its flatness and relative inertness it is not frequently used in cell-based studies. Hence a different substrate was also used for protein immobilisation, namely polystyrene-based non-treated tissue culture plastic (non-TCP) plates. To characterize the non-TCP substrate water contact angle measurements were collected before and after oxygen plasma treatment. The data collected showed a hydrophobic surface with contact angle value of $98.5^\circ \pm 5.4^\circ$ before treatment with oxygen plasma, and a more hydrophilic surface after treatment (80 W for 10 seconds) with a water contact value of $65.6^\circ \pm 2.7^\circ$ (**Table 2**). Figure 3.4 shows fluorescence microscopy analysis on the non-TCP substrate, showing a different intensity along the channel as shown for the silicon wafer. In Figure 3.7 the AFM surface analysis of the not-TCP before and after plasma oxygen treatment with fibronectin deposition on plasma treated substrate is reported in Figure 3.7. Analysis of the not-TCP substrate before and after plasma oxygen treatment, revealed changes in surface profile suggesting a modification of the original substrate with a change in roughness value from $R_a = 5.23 \pm 0.71$ nm (not-TCP) to a value of $R_a = 2.89 \pm 0.51$ nm (plasma treated not-TCP) . Analysis of the sample after fibronectin immobilisation on plasma oxygen treated not-TCP substrate showed a difference in roughness value and surface profile indicating that the fibronectin was immobilised on the surface (Figure 3.7). Due to the rough nature of the non-TCP (typically not made of repeatable surface roughness in

mind) that caused difficulties in assign protein deposition using AFM image analysis, the data reported in (Figure 3.7) were collected analysing five points for every sample (three samples were analysed before and after fibronectin immobilisation) with different scan size (from 10 μm to 0.5 μm). Some variety between different areas of the control was observed (data not showed). Following fibronectin immobilisation on the substrate an increase in roughness was observed passing from $R_a = 2.89 \text{ nm} \pm 0.51 \text{ nm}$ (before protein deposition), to $R_a = 3.88 \text{ nm} \pm 0.3 \text{ nm}$ (after protein deposition) with a different level of deposition on the substrate. The difference in fibronectin assembly on the substrate can be explained with the original surface chemistry of polystyrene (not-TCP) treated with plasma oxygen as demonstrated from Kowalczyńska and al. ⁽¹³⁰⁾. In literature was reported that the deposition of fibronectin on polymeric substrates modulates surface stiffness and fibronectin deposition. Guerra and al. ⁽¹³¹⁾ demonstrated how the variation in substrates can influence the fibronectin deposition and activity, whilst work by Vallières et al. ⁽¹³²⁾ clearly shows the changing in fibronectin deposition before and after substrate modifications. The fibronectin film deposition on non-TCP substrate and the rough nature of the substrate caused difficulties in assessing protein deposition using AFM image analysis. Hence, a functionalised probe AFM technique was used to confirm the presence of varying fibronectin concentrations along the channel as previously confirmed from fluorescence analysis as well as its ability to bind to an anti-fibronectin antibody.

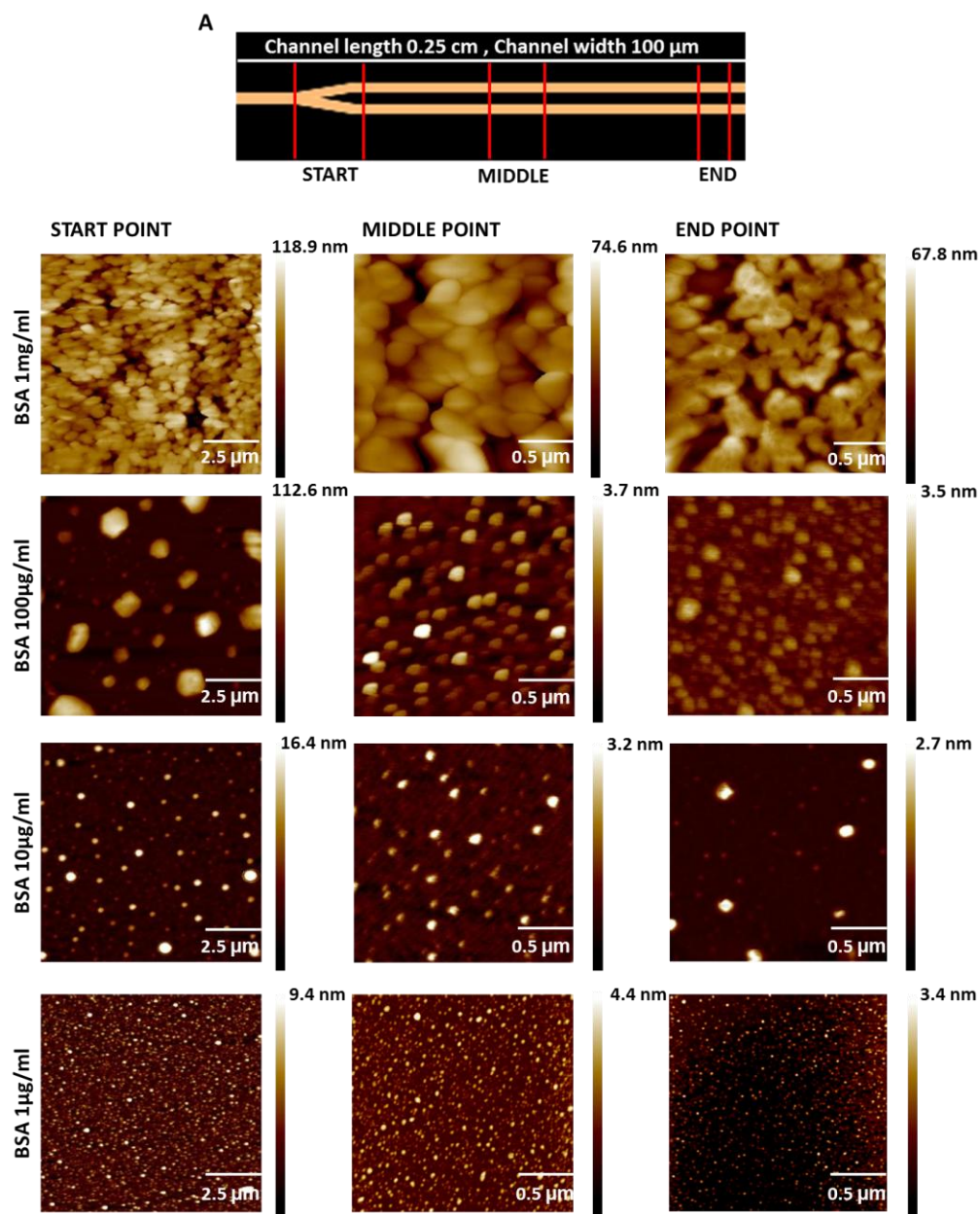


Figure 3.5: Representation of AFM images acquired along the micro-pattern considering the start, middle and end point of the pattern after albumin immobilisation on silicon wafer substrate using tapping mode AFM technique in air. In A representation of the micro-structure design, length and depth measurements used to guide the albumin deposition on silicon wafer is reported. A screening of different protein concentrations was performed to identify the ideal concentration to use in the study (from 100 $\mu\text{g}/\text{mL}$ to 1 $\mu\text{g}/\text{mL}$). The AFM images reported are an example of the representation of the surface after albumin immobilisation, showing protein aggregation when higher concentrations are used. 3 different areas for every point for a total of 9 images for every concentration using different scan size from 10 μm to 1 μm were acquired.

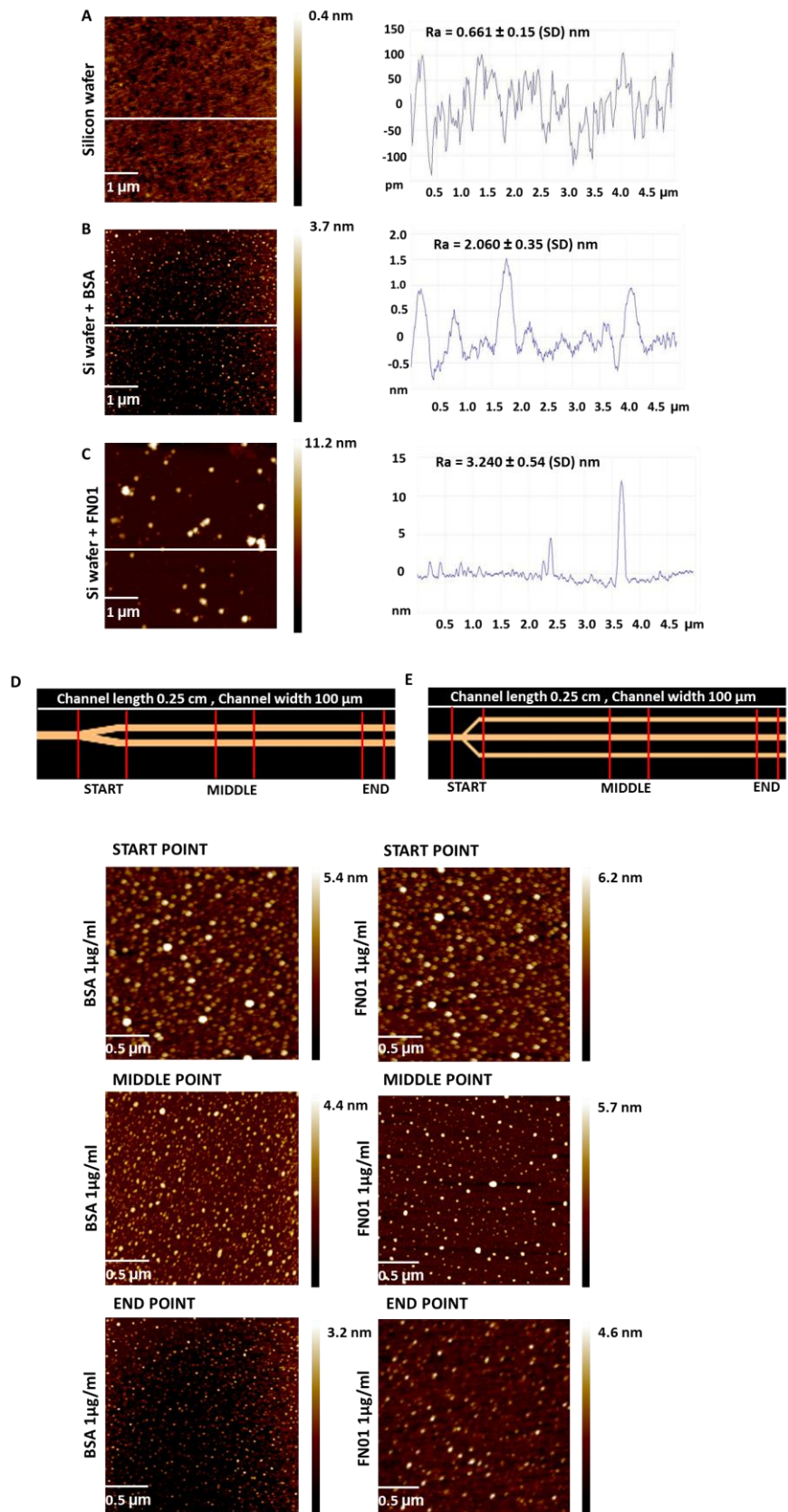


Figure 3.6: Schematic representation of AFM surface analysis conducted on the silica wafer substrate, before and after proteins immobilization. In image A, analysis of the silica wafer before proteins immobilization is reported. In image B and C analysis of the silica wafer after FN and BSA immobilisation respectively is reported. 1 $\mu\text{g}/\text{ml}$ of protein solution was deposited on the silica wafer

substrate using the micro-structure design reported in D and E for the BSA and fibronectin deposition respectively and images acquired using tapping mode AFM in air. More images were acquired to show the protein deposition along the channel and here reported. The analysis of the AFM images was conducted using the Nanoscope programme. AFM images were collected analysing three different points on the samples for a total of 12 images, using different scan size from 10 μm to 1 μm and an example reported.

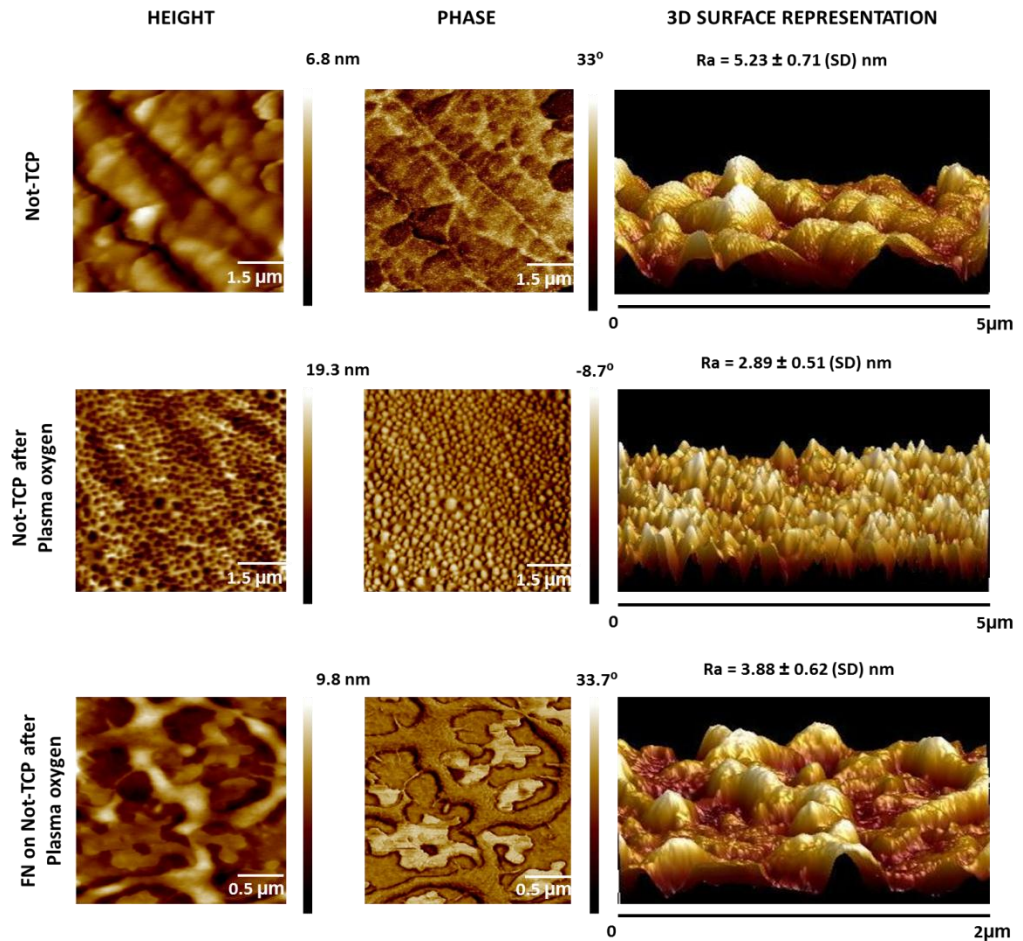


Figure 3.7: Schematic representation of AFM surface analysis conducted on the not-TCP substrate, after plasma oxygen treatment and after protein immobilisation on plasma treated not-TCP. Images were acquired using tapping mode in air. Five points for every sample were considered using different scan size from 10 to 0.5 μm , analysis of the rough value and the 3D surface representation was conducted using the Nanoscope programme.

3.3.3. AFM functional studies

The studies described above indicate that fibronectin and albumin were absorbed along the micro fluidic pattern as a gradient due to the depletion of protein in solution as it adsorbs to the substrate. To check the density of fibronectin along the patterns and confirm the presence of protein concentration inside the patterns, a functionalised probe AFM technique was used (Figure 3.8). The functionalization of the AFM tip was carried out using monoclonal anti-fibronectin antibody specifically for bovine fibronectin. The binding of the antibody to the tip was made possible by using the short chain AMAS linker. Due to the specificity of the antibody to recognise only bovine fibronectin binding to the heparin binding site⁽¹¹⁹⁾, without any cross-reactivity with other connective tissues, specific interactions between the antibody and the fibronectin receptors exposed after protein immobilisation on the substrate were registered. Force measurements were carried out with bare silicon nitride tips to assess non-specific interactions and anti-fibronectin antibody functionalised tips to assess specific interactions with fibronectin. Specificity was confirmed by measuring the forces before and after flooding the system with excess fibronectin to block binding between the antibody and the surface bound protein.

Figure 3.8 shows an example of the typical force data collected on silicon wafer and not-TCP substrates. The antibody tip force curves show clear evidence of specific interactions. In literature is well described the specific antigen/antibody interaction using a functionalized probe AFM technique. Dammer et al.⁽¹³²⁾ for the first time demonstrated that also highly structured

molecules (IgG) preserving their specificity to antigens during AFM force mode analysis. Few years later Willemsen and al. ⁽¹³³⁾ pioneers in this field demonstrated that it is possible to correlate topographical information typical of the AFM with the measure of antibody-antigen recognition. Force spectroscopy of single molecules was also used from Rief and co-workers ⁽¹³⁴⁾ to measure the elasticity of single molecules. In this work, functionalized probe AFM technique was used to confirm the presence of different protein concentration along the microfluidic channels and by checking the difference in adhesion force and numbers. A difference in the percentage of observed adhesion events was registered considering the start and end point of the microfluidic pattern, from 90% to 37% respectively on not-TCP substrate, and from 95% to 25% respectively on silicon wafer. This is likely due to the fact that at the higher surface concentration there is a higher probability of the functionalised tip interacting with multiple fibronectin molecules. With the antibody attached to the AFM tip there are three possible interactions that can occur; specific single interactions, specific multiple interactions, and no interactions. Specific interactions are when the antibody binds to fibronectin (Figure 3.8 B,C). Interestingly a correlation between protein concentration and multiple adhesions was observed. Comparing the start and end points a decrease in multiple adhesions was observed. Indeed at the end point only single adhesions were registered, as summarised in **Table 4**, compared to the start point. The use of AFM in a liquid environment to assess the force measurements in physiological conditions made it more difficult in practice to identify of the middle point along the microfluidic channel, for this reason the

measurements collected between the start and end point are indicated as “POINTS IN BETWEEN” in **Table 4**.

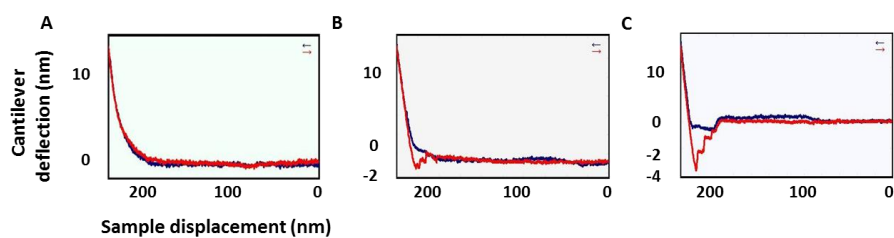
Table 4: Adhesion force analysis

FN01	ADHESION EVENTS	ADHESION ANALYSIS	F (pN) *
START POINT	90% adhesion 10% not adhesion	17% -single adhesions	82±7.4pN
POINTS IN BETWEEN	85% adhesion 15% not adhesion	45%-single adhesions	80±5.6pN
END POINT	37% adhesion 63% not adhesion	84%-single adhesions	52±3.7pN
BSA	ADHESION EVENTS	ADHESION ANALYSIS	F (pN) *
START POINT	95% adhesion 5% not adhesion	10%-single adhesions	43.5±2.3pN
POINTS IN BETWEEN	96%adhesion 4%not adhesion	25%-single adhesion	36.5±0.5pN
END POINT	25% adhesion 75%not adhesion	78%-single adhesion	19.5±1.2pN

*average force value of all adhesion measurements registered (± SD)

In recent studies concerning fibronectin interaction with the heparin subunit functionalized on glass substrate, a rupture force between 49 and 127 pN was recorded ⁽¹²²⁾. Here, a value between 52 pN ± 3.7 pN and 82 pN ± 7.4 pN was observed when analysing the rapture force at end point and start point, respectively. This is due to the deposition of fibronectin on the start point as observed from the AFM images analysis (Figure 3.5). The presence of higher concentration levels at the start point increased the probability of the antibody binding and recognises specifically more receptors on the surface, increasing the force. Further along the channel the probability that the antibody recognises multiple binding receptors on the surface decreases,

which in turn increases the possibility to find a single antibody-receptor interaction. It is important to highlight the fact that the fibronectin used in our study was a Rhodamine labelled fibronectin using a TRITC Rhodamine derivative with a dimension of 530 Daltons attached to the protein. This labels lysine randomly in the protein. The presence of a fluorophore attached to the fibronectin structure can potentially cause problems in the availability of specific binding sites due to the steric hindrance effect (amount of space occupied). It should also be noted that detection of forces of binding between the anti-fibronectin antibody and immobilised fibronectin is not necessarily direct evidence of binding to the heparin site. Differences in the binding forces (start and point) were nevertheless observed considering the silicon wafer and the not-TCP substrate (**Table 4.**), demonstrating the possibility to correlate the force measurements with fibronectin density on the surface but as stated not necessarily the Heparin binding domain. A clear decrease in binding events was observed on both substrates from the start to the end point confirming the relationship between binding events and protein density.



• **Not-TCP substrate (Section 1)**

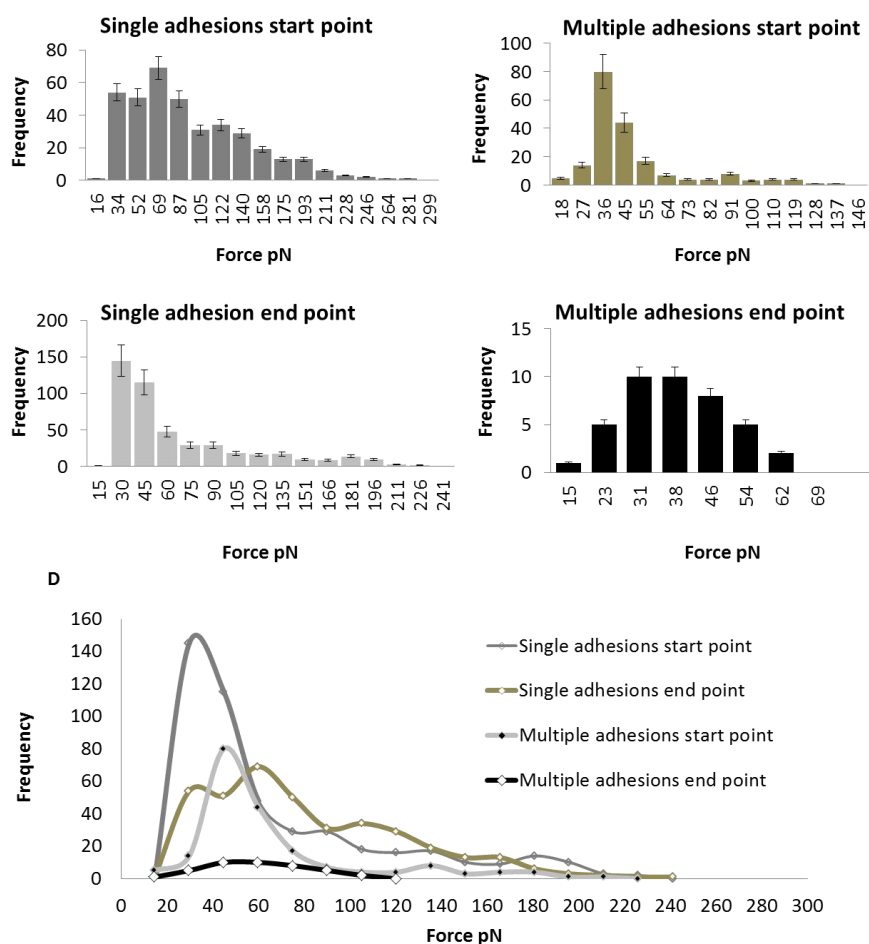
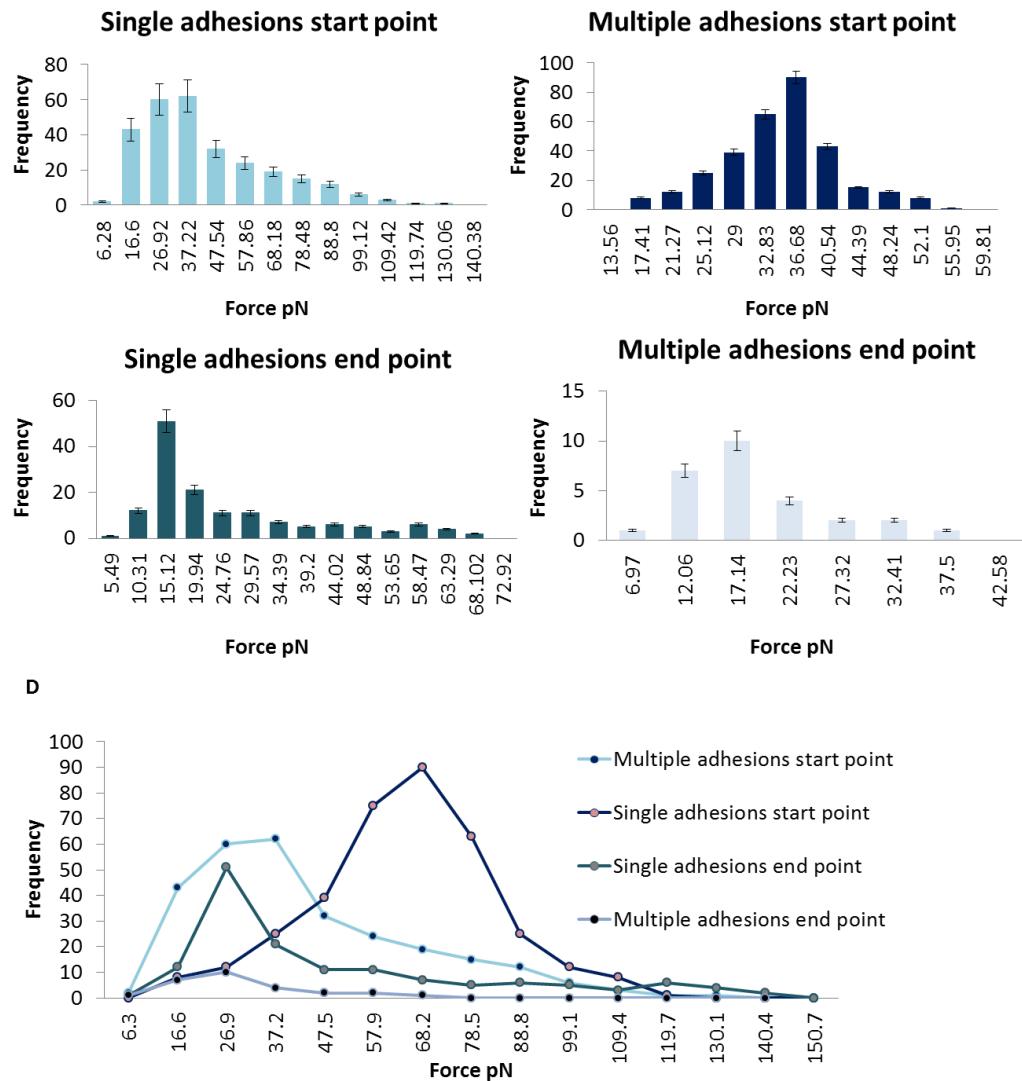


Figure 3.8: Representation of the fibronectin multiple and single unbinding events detected at the start and end point of the protein pattern on not-TCP and silicon wafer substrate. In Section 1 A, B and C an example of the no events, single and multiple unbinding events respectively registered during the analysis on not-TCP substrate are reported. The analysis of the specific unbinding events is reported showing the histograms relative to the forces registered at the start and end point. 1000 curves were analysed for every point in triplicate and an example is reported here (\pm SD). In D a correlation between the specific force detachment measurements registered at the start and end point is reported.

- Silicon wafer substrate (Section 2)



In Section 2 A, B and C an example of the no events, single and multiple unbinding events respectively registered on silicon wafer substrate during the analysis are reported. The analysis of the specific unbinding events is reported showing the histograms relative to the forces registered at the start and end point. 1000 curves were analysed for every point in triplicate and an example is reported here (\pm SD). In D a correlation between the specific force detachment measurements registered at the start and end point is reported.

3.4. Summary

In this study well-defined protein (albumin and fibronectin) gradients displaying different protein surface densities along the patterns have been formed using a microfluidic technique, on silicon wafer and not-TCP substrate. Characterization of surfaces before and after protein immobilization by AFM and fluorescence microscopy clearly defined the change in protein concentration levels along the patterned protein lines. By analyzing molecular interactions between AFM probes functionalized with antibodies and the surface bound protein *via* their force of interaction, the binding capacity and hence functionality (in the sense that the protein remains able to bind with a specific antibody) of the protein was demonstrated.

4. Micro-patterning of cells using fibronectin patterns

4.1. Introduction

The importance of cell micro-patterning in biological, cell drug screening, tissue engineering studies is due to the ability of this technique to control the placement of living cells on a substrate ⁽¹³⁵⁾. There are two general types of cell micro-patterning: the first consisting of the use of surface chemistry to generate patterns that will encourage localised cell adhesion on the substrate; second the use of physical barriers (easily removable) to limit cell adhesion. From these approaches, many micro-patterning techniques have been developed ⁽¹³⁶⁾. Cell micro patterning has become a useful method in cell-cell, cell-matrix investigation and molecular sensor development, thanks to the ability of this technique to build cell co-culture systems using two or more cell types, with accurate cell localisation on the substrate.

In this chapter a brief introduction to the cell receptors and the mechanisms of cell recognition with the ECM (extra cellular matrix) are examined. The experimental section is dedicated to the creation of cell micro-patterning using fibronectin patterns as substrate to study the cell density and morphology to confirm the creation of a bio-functional gradient. To control the cell adhesion specifically on the fibronectin patterns a functionalization of

the remaining substrate (non-TCP) was applied using Pluronics F127 as a protein-resistant layer and the findings reported here.

4.1.1. Fibronectin as a protein component of the ECM and integrins role in cell proliferation, survival and migration

4.1.1.1. Fibronectin

Fibronectin is one of the components of the ECM. Fibronectin is composed of two monomers linked by disulphide bonds. Each monomer is formed by three repeating fibronectin units: type I, II, III, representing 90% of the fibronectin used, plus two heparin, fibrin and collagen binding domains ⁽¹²³⁾. The two fibrin binding domains that are located at the ends of the molecule are important in cell adhesion and migration, due to the known interaction between fibronectin and fibrin ⁽¹³⁷⁾. Fibronectin is involved in many cellular interactions within the extracellular matrix, playing an important role in cell adhesion, migration and differentiation. The major role of fibronectin is to bind specific integrins and support other important molecules such as cadherins in cell adhesion ⁽¹³⁷⁾. Fibronectin plays an essential role in invertebrate development, guiding cell attachment and migration ⁽¹³⁸⁾. In the same study, it was observed that when inactivation of the FN gene occurs; this can lead to embryonic failure in mice.

4.1.1.2. Integrins, cell matrix receptors

Integrins are heterodimers receptors consisting of two non-covalently linked subunits α and β , collaborating together in the “inside-out” signalling from the ECM to the cell, allowing rapid and flexible responses to changes in the environment with following activation of the receptor, with change of the

conformation of the integrins ⁽¹³⁹⁾. Integrins are also involved in outside-in from receptor to the cell signalling where thanks to the association of the cytoplasmic domain with intracellular initiators like the Src family kinases and cytoskeletal components they can initiate intracellular signalling ⁽¹⁴⁰⁾. The mediation of integrins in cell-matrix and cell to cell adhesion has an influence in cell attachment, spreading, motility and cell survival ⁽¹³⁹⁾. In the literature it is reported that mammal cells have 18 α and 8 β integrins subunits that can give at least 24 different heterodimers that can bind specific cells, ECM or protein solid ligands ^(141,142,145). Integrins can be classified as FN-RGD, laminin and collagen binding and leukocyte specific receptors, depending on the cell specific expression and on the matrix ⁽¹⁴¹⁾ (Figure 4.1). However, it is important to consider that the activation of one integrin it can bind at the same time to many matrices as reported for the αV integrin ⁽¹⁴²⁾.

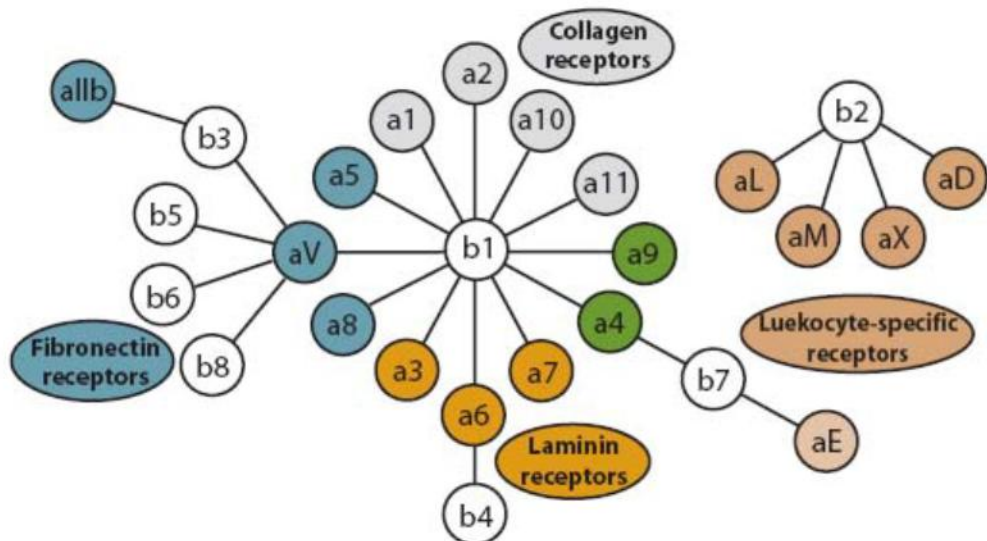


Figure 4.1 : Integrin family. Organization and grouping of the integrin subunits in mammalian cells based on their matrix affinity or cell specific expression ⁽¹⁴¹⁾

Integrins are divided into 5 groups α_V , β_1 , β_2 , β_4 , β_7 . The β_1 and α_V subunits are well studied in literature ⁽¹⁴¹⁾.

The β_1 family is important for cell development and survival and binding different proteins of the ECM ⁽¹⁴³⁾. The recognition of specific proteins on the ECM is carried out by different integrins: fibronectin ($\alpha_5\beta_1$ and $\alpha_4\beta_1$ integrins), collagen ($\alpha_1\beta_1$, $\alpha_2\beta_1$, $\alpha_{10}\beta_1$, $\alpha_{11}\beta_1$ integrins) and laminins ($\alpha_3\beta_1$, $\alpha_6\beta_1$ and $\alpha_7\beta_1$ integrins).

The α_V family are involved in placenta defects and abnormalities in central nervous system in mice ⁽¹⁴⁴⁾. The integrins included in the α_V subunit are β_1 , β_3 , β_5 , β_6 and β_8 .

4.1.1.3. Integrins control cell proliferation

Multiple steps (and not a single “checkpoint”) are involved in cell progression requiring matrix attachment ^(145,146). It was demonstrated that activation of cyclin-dependent kinases (Cdks) was important in cell progression on G1 phase of the cell cycle, and were controlled by multiple integrin events ^(147, 148). The mechanism that integrin uses to control these events include enhancement growth factor and enhancement of nuclear translocation involving transcriptional and post-transcriptional control ⁽¹⁴⁸⁾.

Other work suggests that there is a relationship between the number of adhesive contacts and the regulation of signalling and cell behaviour. It was observed that cell survival and cell proliferative capacity are influenced by the

varying of the cell spreading⁽¹⁴⁹⁾, and that cell surface and surface area are essential for cell proliferation⁽¹⁵⁰⁾.

4.1.1.4. Integrins control cell survival

Many studies have shown that cell attachment is fundamental for normal cell survival^(151,152). It was observed that suspension culture (where the cell contact with the substrate is lost) induces apoptosis of fibroblasts⁽¹⁵¹⁾, endothelial cells^(153,154) and epithelial cells^(152,155). The regulation of cell survival consists in the activation of anti-apoptotic proteins such as Bcl2 family⁽¹⁵⁶⁾ to inhibit the pro-apoptotic proteins such as caspases^(157,158). Cell death was also observed in the case that a failure occurred in cell binding the ECM ligands^(152,154). Expression of $\alpha V\beta 3$ integrin inhibits cell survival by the integrin $\alpha 2\beta 1$ presence in cells attached to collagen⁽¹⁵²⁾, whilst the $\alpha 5\beta 1$ integrin induces apoptosis of endothelial cells that are attached to the vitronectin using αV integrin family⁽¹⁵⁴⁾.

4.1.1.5. Integrins role in cell migration

Cell migration is positively or negatively regulated by the interaction of integrins within the ECM. In a previous study⁽¹⁵⁹⁾, it was observed that the inhibition of the integrin binding to the ECM actively inhibits the signal transduction to the cell essential for cell migration. An example of negative regulation of the fibroblasts and endothelial cells was observed when an

inhibitor of the $\alpha 5\beta 1$ integrin was used, obstructing the formation of stress fibres⁽¹⁵⁹⁾. Inhibition of the $\alpha 5\beta 1$ integrin enhancing the activation of PKA (membrane associate protein kinase A), was found to be responsible for cell migration^(154,159). Integrins are not the only receptor responsible for the cell migration; in fact a more complex mechanism of cross-talking between the integrin and the receptors expressed on the ECM is involved^(160,161). However integrins play an essential role in making contact with the substratum, and assisting in the promotion of the signal cascade transduction mechanism that supports cell migration.

4.1.1.6. Integrin expression on HMSC and 3T3 cells

FACS (fluorescence activating cell sorting) analysis of the HMSC cells performed by Majumdar et al. in 2003⁽¹⁶²⁾ clearly showed the expression of the following integrin subunits on the cell membrane $\alpha 1$, $\alpha 2$, $\alpha 3$, $\alpha 5$, $\alpha 6$, αV , $\beta 1$, $\beta 3$ and $\beta 4$. A previous study performed by Gronthos et al. in 2001⁽¹⁶³⁾ showed the specific binding site of the HMSC cells for the ECM proteins collagen, fibronectin, vitronectin and lamin. The analysis concluded that HMSC cells bind collagen principally with integrins $\alpha 1\beta 1$, $\alpha 2\beta 1$; lamin by $\alpha 6\beta 1$; fibronectin by $\alpha 5\beta 1$ and vitronectin by $\alpha V\beta 3$ considering cell adhesion and growth in the presence of blocking antibodies⁽¹⁶³⁾. Concerning the 3T3 mouse fibroblasts, in literature is reported that $\alpha 5\beta 1$ and $\alpha 4\beta 5$ integrins are expressed on the cell membrane, and are involved in both fibronectin and vitronectin interactions⁽¹⁶⁴⁾. Clark and co-workers⁽¹⁶⁵⁾ demonstrated that the

migration of human fibroblasts required not only the binding to the RGD complex through the $\alpha 5\beta 1$ integrin, but also the interaction with the $\alpha 4\beta 1$ integrin in the variable region ⁽¹⁶⁵⁾. Caruso et al. demonstrated the expression of $\alpha 4\beta 1$ integrin in 3T3 fibroblast cell ⁽¹⁶⁶⁾.

4.2. Results and discussion

4.2.1. Substrate functionalization using Pluronics F127

To reduce the non-specific cell adhesion on the plastic substrate and limit the cell adhesion to the fibronectin patterns a functionalization of the bare substrate was applied. As summarized in Figure 3.6 Pluronic F127 was used as a surfactant on the non-TCP substrate, to drastically reduce cell adhesion in non-fibronectin patterned substrate areas. The functionalization with Pluronic F127 showed an increase in substrate hydrophilicity that inhibited cell attachment on it. The mechanism by which Pluronics reduce cell adhesion and protein deposition on the substrate is due to interaction of the polyethylene segments and the polypropylene segment present in the structure (Figure 4.2). The polypropylene segment role is to stabilize Pluronics onto a surface using hydrophobic interactions, whilst the polyethylene segments extend to the aqueous medium protecting the surface from protein adsorption and cell adhesion⁽¹⁶⁷⁾. The stabilizing activity of the Pluronics on the substrate using hydrophobic interaction was previously observed in an earlier study by Prasad and co-workers⁽¹⁶⁸⁾. The ability of the polypropylene segment to interact with the substrate through hydrophobic interactions was also confirmed by Tan et al. where a lack of adsorption of Pluronics was observed on hydrophilic surfaces⁽¹⁶⁹⁾. A correlation between the length of the PPO (polypropylene-oxide) segment and adsorption on the substrate was also demonstrated⁽¹⁷⁰⁾. The deposition of Pluronic on hydrophobic substrates was demonstrated to use a brush like conformation (Figure 4.3 A) where the PPO is adsorbed by the

substrate using hydrophobic interaction and the PEO groups interacting with the aqueous environment blocking the cell adhesion ⁽¹⁷¹⁾. Water contact angle measurements were recorded on the sample before and after pluronics immobilisation to check for changes in the substrate hydrophobicity. As shown in **Table 5** the polystyrene substrate (non-TCP) before plasma oxygen treatment showed a value of $98.5^{\circ} \pm 5.4$ indicating a relatively hydrophobic substrate. After pluronics adsorption on the substrate for 24 hrs the water contact angle decreased to $65.3^{\circ} \pm 6.2^{\circ}$ (**Table 5**), indicating that the PPO (polypropylene-oxyde) segment stabilized the pluronics on to the substrate through hydrophobic interactions (brush like conformation) allowing the PEO segment to extend into the aqueous environment, increasing the hydrophilicity of the non-TCP substrate.

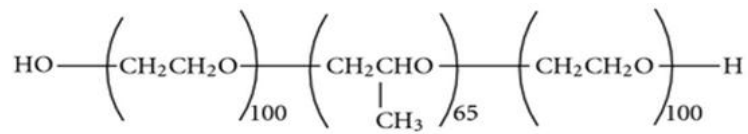
Different approaches have previously been used to block cell adhesion, such as reported from Corey et al. ⁽¹⁷²⁾ where the ability of Pluronics and BSA were tested to reduce neuroblastoma cells adhesion. In this work the use of the Pluronic F127 a preliminary investigation using BSA was also performed (data not shown) but this did not significantly reduce cell adhesion when compared to not-TCP substrate, suggesting that it would not serve effectively as an anti-adhesive surface. In the creation of cell patterning two different approaches to deposit Pluronics F127 on not-TCP substrate were applied. The first method required the creation of fibronectin pattern on the substrate (using the microfluidic technique and a concentration of $1\mu\text{g}/\text{ml}$ of FN01), then flooding this sample with Pluronics F127. As can be observed in Figure 4.3 B1 this method did not demonstrate the ability to confine cell adherence specifically

on the protein pattern as required, suggesting that the creation of an anti-adhesive substrate after protein immobilization on the not-TCP substrate was not achieved possibly due to the oxygen plasma treatment performed before the adhesion of the PDMS on the substrate. Indeed, as previously discussed a change of the hydrophilicity on the substrate (necessary to permit the adhesion of the stamp on it) can block the adhesion of the pluronics on it. The second method consists in the flood the not-TCP with Pluronic F127 before and then pattern fibronectin. Using the second method (Figure 4.3 B), plasma oxygen treatment was necessary after pluronics functionalization to permit the contact of the PDMS on it creating a temporarily hydrophilic substrate⁽³⁷⁾. It is important to highlight the fact that after plasma oxygen treatment on the functionalized substrate caused a change in the substrate (not-TCP substrate plus Pluronic F127). A measurement of the water contact angle after plasma oxygen treatment of the functionalized substrate clearly showed an increase in hydrophilicity through a reduction in contact angle from $65.3^\circ \pm 6.2^\circ$ to $42.5^\circ \pm 3.5^\circ$. As confirmed from the water contact angle analysis by treating the sample with the oxygen plasma, a more hydrophilic substrate was successfully obtained, suggesting a possible change in the conformation of the immobilized surfactant, which was sufficient to permit the adhesion of the PDMS on it. This change in hydrophilicity was proven to be only a temporary and did not interfere with the subsequent functionalization. Measurements of the contact angle after 30mins on the non-TCP treated with pluronics F127 showed an increased water contact angle to its original value from $42.5^\circ \pm 3.5^\circ$ to $64.7^\circ \pm 8.2^\circ$, suggesting a restoration of the original surface

structure of the substrate. In fact when cells were seeded on the substrate using this method adhesion of cells only on fibronectin patterns was observed, indicating that the functionalization of the substrate was achieved avoiding non-specific cell adhesion on the substrate (Figure 4.4 E). A preliminary screening of different concentration of Pluronics was conducted and it was observed that at a concentration greater than 4% by weight not only was cell adhesion avoided, but also protein adsorption was avoided, suggesting that also the concentration levels play an important role in the adhesion of cells and adsorption of proteins on the substrate.

The mechanism and the possible change of pluronics absorption after plasma treatment observed in this section, with consequent increase in cell deposition on the protein patterns and avoidance of cell deposition on the non-adhesive surface is not clear. The observation of the temporary change in the water contact angle measurements after plasma oxygen treatment suggest a reversible conformational re-arrangement of the pluronics on the substrate with a consequent change in hydrophilicity. A comparable observation has been made on the polymer PDMS with pluronic F127 embedded in its structure. When this polymer mixture was treated with an oxygen plasma it became oxidized and a hydrophilic surface was formed but was not stable in air since the hydrophobic surface recovered with time ⁽¹⁷³⁾.

The similar phenomena in this work could be further investigated in the future using cryo-x ray photoelectron spectroscopy ⁽¹⁷⁴⁾ which has the potential to reveal subtle changes in surface elemental compositions and bonding environment in hydrated systems.



HO-PEO-PPO-PEO-OH

Figure 4.2 : Pluronic F127 chemical structure, a hydrophobic polypropylene segment and two polyethylene segments MW: 126000Da

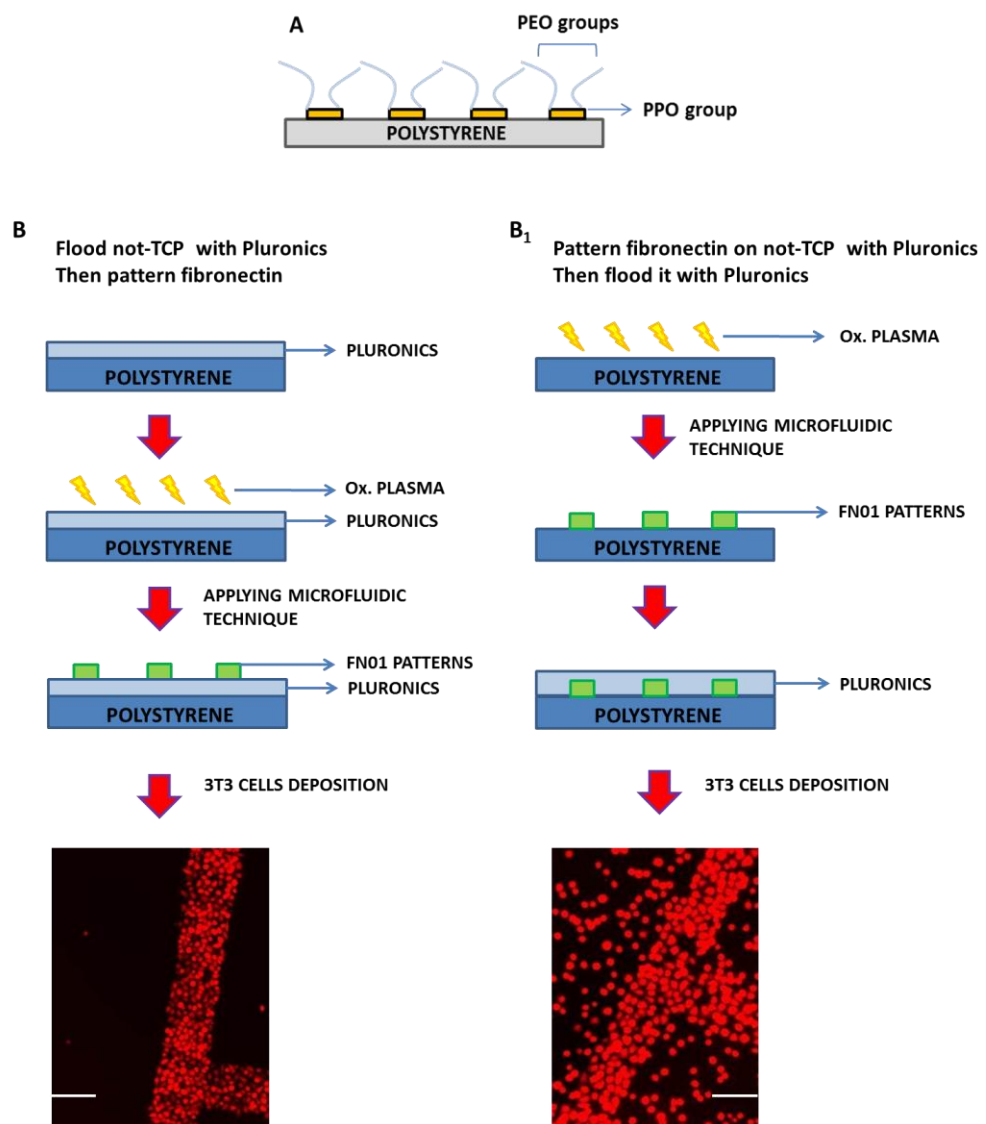


Figure 4.3 : Representation of the Pluronic brush like conformation (A) and the two approaches used to create 3T3 fibroblast cells patterning (B, B₁). The fluorescence images reported represent a selection of two images collected using the A₂ micro-channel shape reported in Figure 2.5 used for the cell micro-patterning studies. The density of cells used was 10⁶ cells/mL. Scale bar 100µm.

Table 5: Water contact angle measurements before and after functionalization with Pluronic F127

SUBSTRATES	BEFORE TREATMENT	AFTER TREATMENT
	w.c.a	w.c.a
POLYSTYRENE	wca = $98.5^{\circ} \pm 5.4$	wca = $65.6^{\circ} \pm 2.7$
POLYSTYRENE+F127	wca = $65.3^{\circ} \pm 6.2$	wca = $42.5^{\circ} \pm 3.5$

4.2.2. 3T3 mouse fibroblasts cells adhesion studies

Physiological fluids (e.g. serum) contain numerous soluble proteins that react with solid surfaces in very dynamic ways ⁽¹⁷⁵⁾. In such environments, *in vivo* and *in vitro*, cell adhesion to substrates is therefore, largely mediated by a defined layer of adsorbed serum proteins. A complex competition among over two hundreds proteins in serum results in an adsorbed layer comprising proteins facilitates cell adhesion ^(176,177). Other studies showed that the presence of FN alone is sufficient to mediate cell attachment and phenotypic expression ⁽¹⁷⁸⁾. Fibronectin gradients were selected to study cell adhesion and migration along the microfluidic patterns, to investigate the impact of the fibronectin gradient on cell behavior. The presence of fibronectin along the microfluidic channel was confirmed from the mAb binding assay, where specific interactions between the fibronectin and its heparin binding domain were found. Fibronectin gradients have already been used to study cell adhesion ⁽¹⁷⁹⁾ on protein gradients. Here non-TCP substrates were used for protein immobilization and 3T3 fibroblast cells were used for patterning. Initially 3T3 fibroblast cells were seeded on the fibronectin patterns using a concentration of 10^6 cells/mL. Fluorescence images of the sample after cells

immobilisation did not show a specific deposition of cells on the fibronectin patterns (Figure 4.4 D). To reduce the cell adhesion on the plastic substrate and limit the cell adhesion on the fibronectin patterns a functionalization of the substrate was applied. The functionalization avoided the attachment of fibroblasts on the substrate, and specific cell adhesion on the fibronectin patterns was observed (Figure 4.4 E).

In many studies concerning the behaviour of cells on non-biological substrates (polymeric substrates), the functionalization of the surface using chemical compounds and adsorbed proteins were used to affect cell adhesion and spreading ^(180,181,182,183,184). It was observed that during the absorption on polymer surfaces, protein rearrangements may occur ⁽¹⁸⁵⁾ and that the absorption depends on the orientation of protein adsorbed on the substrate ⁽¹⁸⁶⁾. Other works reported the ability of FN to change its native conformation (unfolding) to an extended shape when absorbed on the substrate ^(187,188,189), influencing the cell adhesion and spreading ^(120,190). When cells were deposited on the fibronectin patterns a correlation between fibronectin adsorption and fibroblast adhesion was observed. As confirmed in the previous experiment using a mAb binding assay, the presence of binding sites due to the fibronectin immobilisation creates a better condition for cell adhesion, in accordance with the protein concentration along the channel. In fact, as shown in Figure 4.6 E a difference in surface coverage was registered when comparing start and end point from 50% to 2% of coverage. Cells seeded on fibronectin recognized the fibronectin receptors on the surface and bound to

them. As is consistent with the mAb binding assay more adhesion events were observed at the start point with multiple adhesions.

The presence of a higher protein adsorption and the higher probability of finding receptors on the substrate increased the cell adhesion on the patterns. In contrast, the low probability of finding receptors on the substrate at the end of the channel decreased the cell adhesion on the patterns, as summarized in Figure 4.6. Horbet and Klumb⁽¹⁹¹⁾ reported that the adhesion of cells on the substrate is influenced by the amount and conformation of adsorbed proteins on the substrate. With the evidence of the data collected in this section and the evidences reported in the literature, the possible mechanism by which fibroblasts interact with the fibronectin gradient is represented in Figure 4.5. Expression of the $\alpha 5\beta 1$ integrin on the 3T3 mouse fibroblast cells is involved in the fibronectin recognition through the RGD complex⁽¹⁶⁴⁾. A higher amount of FN (as demonstrated in this study) and a favourable conformation of the protein (in this case exposure of the RGD complexes involved in cell adhesion) during the FN rearrangement as suggested in literature^(186,187), are probably involved in the 3T3 mouse fibroblast adhesion, on the substrate as observed by Horbet and Klumb⁽¹⁹⁰⁾. The cell adhesion analysis confirmed the presence of a fibronectin gradient on the patterns controlling the cell adhesions and density, through a probable mechanism involving the interaction between the $\alpha 5\beta 1$ integrin and the RGD receptor complex.

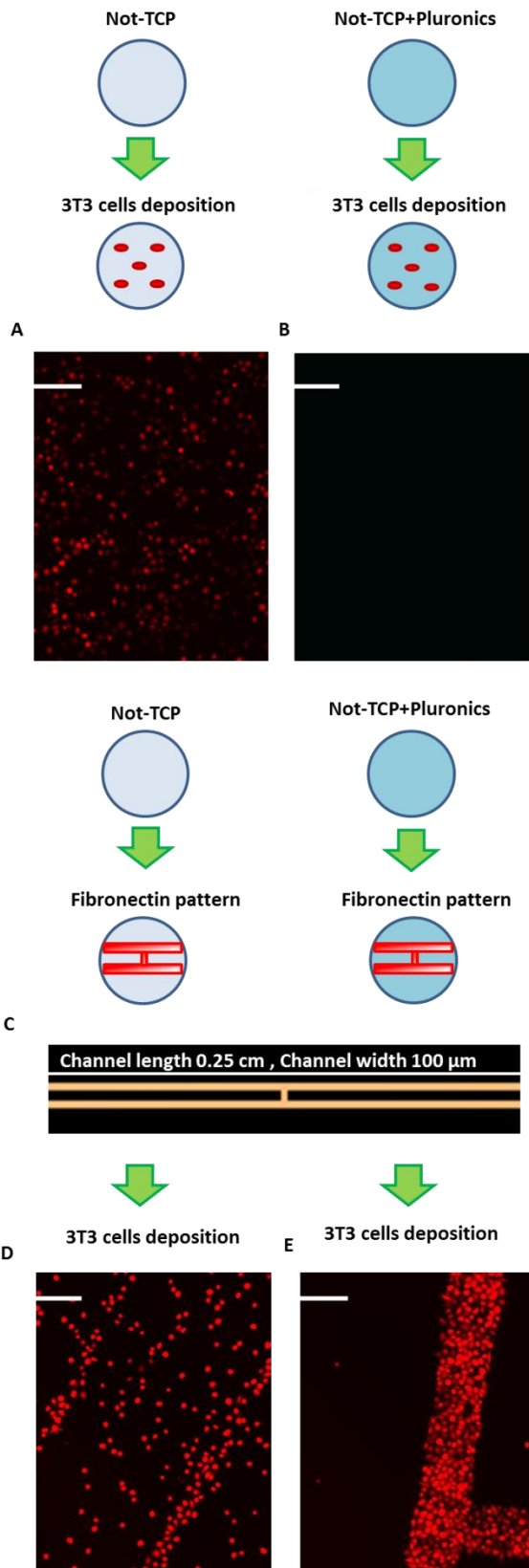


Figure 4.4 : Schematic representation of the not-TCP substrate and 3T3 cell adhesion studies performed on it. Fluorescence images of 3T3 cell deposition on the substrate before the

functionalization with Pluronics F127 surfactant is reported. In A and B cell deposition on the substrate before and after Pluronics immobilisation is reported. In C design of the micro-channel used to create the protein pattern on the not- TCP substrate, before and after functionalization with Pluronics. In D and E cell deposition on fibronectin pattern before and after Pluronics deposition respectively. The fluorescence images were acquired using a Nikon Eclipse TS100 Microscope. Analysis of the images was conducted using Volocity 5.2 software. Five Images for every point were considered and analysed.

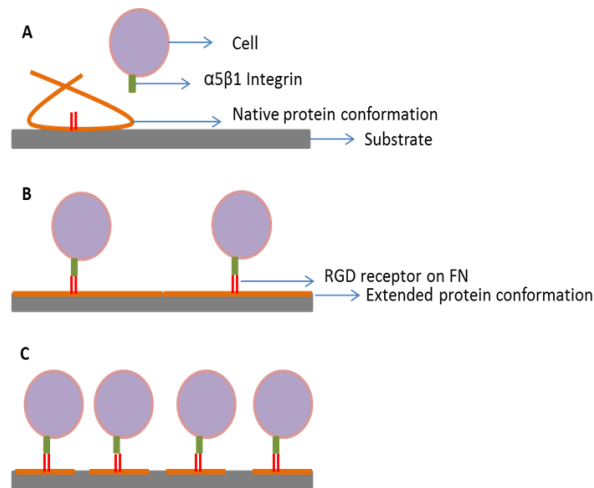


Figure 4.5: Schematic representation of the possible mechanism involved in the cell adhesion on the fibronectin. Cells adhesion on fibronectin is regulated by the integrin-receptor recognition on the FN surface. In figure A the native FN conformation (folded conformation; not integrin fibronectin receptor interaction ^(180,181,182)), before adsorption on the substrate is reported. In figure B extended FN conformation after adsorption on the substrate is reported where integrin receptor recognition occurred with cell adhesion (Integrin receptors interaction ⁽¹⁸³⁾). In figure C more fibronectin molecules on the substrate in the extended conformation, more cell adhesion is observed.

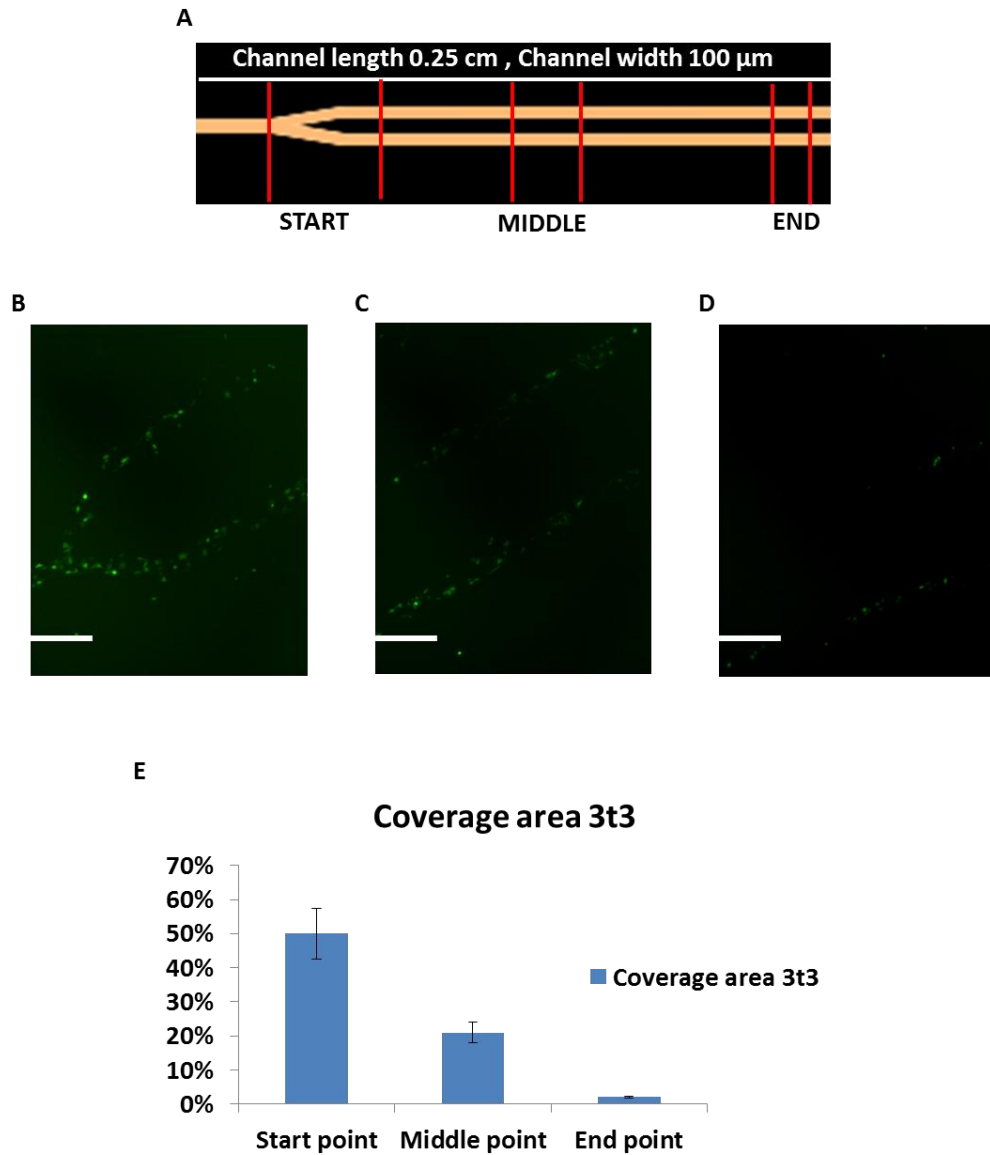


Figure 4.6 : Schematic representation of 3T3 fibroblast cells adhesion studies performed on fibronectin patterns deposited (FNO1 $1 \mu\text{g}/\text{mL}$ protein concentration used) on non-TCP substrate functionalized with Pluronics F127. In A a representation of the micro-channel design used in the study is reported. In B, C and D mesenchymal stem cell adhesion at start middle and end point respectively (fluorescent images reported). In this case due to the use of Rhodamine fibronectin for the creation of the protein patterns 3T3 fibroblast cells carrying the green fluorescent protein (mGFP) colour were used (green fluorescent images reported). In Figure E surface coverage analysis along the channel is reported. The fluorescent images were acquired using a Nikon Eclipse TS100 Microscope. Analysis of the images was conducted using Volocity 5.2 software. Five Images for every point were considered and analysed and the average value of the surface coverage reported in the graph ($\pm\text{SD}$). Scale bar 200 μm .

4.2.3. Immortalized mesenchymal stem cells (i-HMSC) adhesion studies

Previous studies have discussed the possibility that 3T3 mouse fibroblast cells can interact with the RGD complex on a fibronectin surface ^(184,185). Immortalised mesenchymal stem cells (i-HMSC) were also used for cell adhesion studies. Cell immortalisation was achieved using the protocol reported from Okamoto and co-workers in 2002 ⁽⁶³⁾ as reported in the material and method section. In literature is reported the ability of mesenchymal stem cells to recognize fibronectin through the binding of $\alpha 5\beta 1$ integrin on the RGD complex ⁽¹⁶³⁾. The ability of $\alpha 5\beta 1$ integrin to bind to the RGD complex receptor on the fibronectin surface, and the role of integrins in cell adhesion is well reported ^(159,163). The analysis of the cell adhesion reported in Figure 4.6 considering a cell density of 10^6 cells seeded on the fibronectin patterns (previously treated with the Pluronics F127 surfactant), clearly showed a correlation between protein adsorption and cell adhesion as reported for the 3T3 mouse fibroblasts. The surface coverage analysis (Figure 4.7E) showed a higher cell density 62% at the start point and a lower density at the end point 9%. The cell adhesion mechanism described for the fibroblasts cells (Figure 4.5) can be considered also valid for the mesenchymal stem cells, considering the ability of the $\alpha 5\beta 1$ integrin to bind to the RGD complex receptor on the fibronectin surface. The possibility to find more adsorbed FN on the substrate in the right conformation (exposure of the RGD complex receptor in this case), increased the chances of cells to adhere on the fibronectin substrate. In contrary a lower protein adsorption on the substrate decreased the chances of cells to adhere on it.

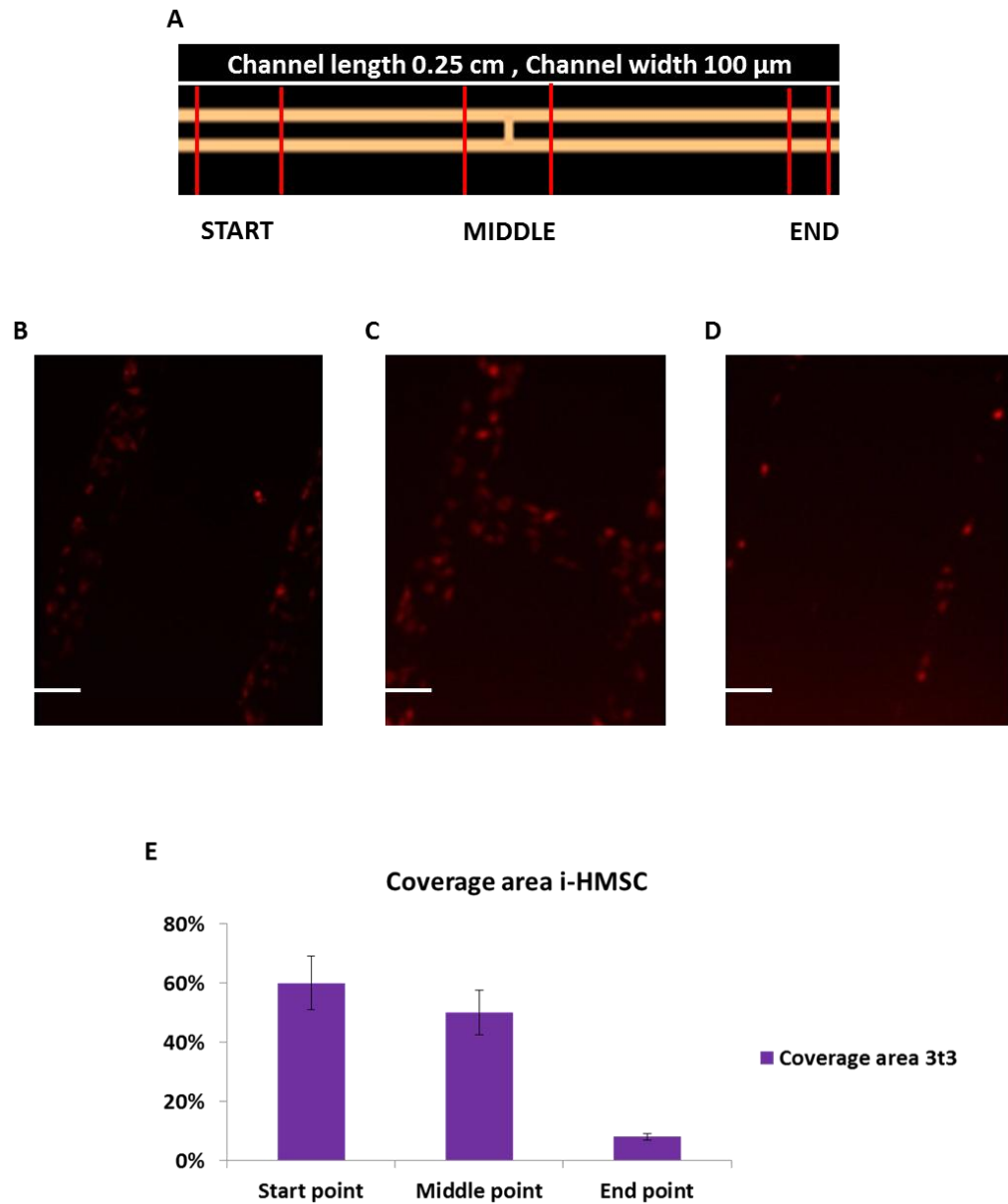


Figure 4.7 : Schematic representation of i-HMSC cells adhesion studies performed on fibronectin patterns (FND1 1 $\mu\text{g}/\text{mL}$ protein concentration used) deposited on non-TCP substrate functionalized with Pluronic F127. In A a representation of the micro-channel design used in the study is reported. In B, C and D mesenchymal stem cell adhesion at start middle and end point respectively (fluorescent images reported). In this case the use of Rhodamine fibronectin for the creation of the protein patterns was replaced by the green fluorescent HiLyte488 fibronectin due to the availability of Mesenchymal stem cells carrying the red fluorescent protein (mRFP) colour were used (red fluorescent images reported). In Figure E surface coverage analysis along the channel is reported. The fluorescent images were acquired using a Nikon Eclipse TS100 Microscope. Analysis of the images was conducted using Volocity 5.2 software. Five Images for every point were considered and analysed and the average value of the surface coverage reported in the graph ($\pm\text{SD}$). Scale bar 100 μm .

4.3. Summary

In this chapter the experimental work conducted clearly showed a strong correlation between protein adsorption density and cell adhesion. The fibronectin protein gradient was shown to control cell adhesion along the patterns, showing the possibility to use this microfluidic system for future cell behavior investigations. A possible mechanism involved in cell adhesion was also shown considering the possibility that the cell adhesion on the fibronectin patterns adsorbed on the substrate is due to the arrangement of the fibronectin receptors (probably RGD complex) on the substrate.

5. Cell migration studies: Influence of protein adsorption on cell behaviour

5.1. Introduction

Previously in this work, it was demonstrated that a fibronectin gradient can be employed to control cell adhesion. This was shown by a variance in cell distribution along the microfluidic channel in accordance with the fibronectin adsorption on the substrate. Due to the difference in cell deposition and the different cell density observed along the channel, further analysis of the cell migration was conducted to monitor changes in cell behaviour under constrains (cell density and protein adsorption). Cell migration *in vivo* studies have demonstrated that cells can migrate through 3D longitudinal paths, with bordering interfaces (channels) ⁽¹⁹⁰⁾. *In vivo* the channels used for the cells in the migration ⁽¹⁹¹⁾ were composed of connective tissue and the basal membrane of muscle, nerve and epithelium ⁽¹⁹²⁾. In other literature recent evidence suggests that physical confinement can alter cell migration mechanisms. For example, Hung et al ⁽¹⁹⁰⁾ demonstrated that when cells have an excess of space mesenchymal migration is observed with a dramatic change in cell shape with long protrusions, whilst when the space is limited amoeboid migration was observed with shorter protrusions.

In this chapter the investigation and analysis of cell migration along patterns created using microfluidic channels for fibroblasts and mesenchymal stem cells is reported. Knowledge concerning the influence of the environment (adsorption, deposition and conformation of the fibronectin on the substrate) and the space available (due to the difference in cell deposition along the microfluidic channel) in cell behaviour is important to understand how cells interact with their physical micro-environment.

5.2. Results and discussion

5.2.1. 3T3 mouse fibroblasts migration on fibronectin patterns

Cell migration plays an essential role in processes such as wound healing, cell development, cancer metastasis and tissue engineering. The cell migration mechanism is a complex system regulated by cytoplasmic protrusions, adhesion and detachment under environmental signals⁽¹⁹³⁾. In early work the role of chemical gradients was proven to be important in guiding cell migration. The role of physical cues in cell migration was demonstrated on different occasions. Groves⁽¹⁹⁴⁾ and Pillars^(195,196) research on the substrate showed the relationship between cell adhesion and migration, whilst further studies on micro-patterned adhesion areas identified that both cell shape and distribution can influence cell differentiation,⁽¹⁹⁷⁾ growth⁽¹⁹⁸⁾ and apoptosis⁽¹⁹⁹⁾. The analysis of 3T3 cells migration conducted on the functionalized non-TCP is reported in Figure 5.1. Analysis of the videos formed from pictures acquired every 10 minutes for 24 hours, showed an cell migration in the direction of the protein gradient (chemotaxis) in the lower protein density regions (end point), while with a higher protein density (start point) a random movement of the cells was observed. The substantial difference between the start and the end point of the microfluidic channel consists in the different cell density due to the influence of fibronectin adsorption along the channel (as discussed in Chapter 4). In literature the influence of cell density, and in particular the influence of confined spaces in cell migration studies has been reported^(190,191). Hung et al.⁽¹⁹⁰⁾ in particular demonstrated that changes in

cell migration and cell shape are influenced considering a confined or unconfined space. The presence of more space (where the cell density is lower and the cells have more space around which to move); in this work the end of the channel where a lower protein adsorption was observed, was shown to influence the 3T3 fibroblasts migration. In the same article Hung and co-workers⁽¹⁹⁰⁾ also demonstrated that a difference in cell shape was found to influence the density of cells deposited in a confined or an unconfined space. When analysing cells at the end point using a higher magnification (Figure 5.2) it was observed that they appeared as single elongated cells with protrusions. Moving to the start point where the cell density is higher (due to the higher protein adsorption) and the space to move is limited (confined space), 3T3 fibroblast cells assumed a compact conformation interacting with the nearest cells in a more constrained way (Figure 5.2 A). Changes in cell migration velocity were also observed both at the end and start point as reported in Figure 5.1 D, where an increase in cell velocity was observed from $0.69 \mu\text{m}/\text{min} \pm 0.21 \mu\text{m}/\text{min}$ to $1.06 \mu\text{m}/\text{min} \pm 0.43 \mu\text{m}/\text{min}$ respectively. The changes in shape and average cell velocity suggest that cell density and space available in the microfluidic channel play an important role in cell migration. Cell migration is a complex process that can be divided in to single (amoeboid or mesenchymal) cell migration or collective migration of multicellular units⁽²⁰⁰⁾. The amoeboid migration is normally referred to the movement of circular cells with a lack of focal adhesion^(201,202). Mesenchymal migration is associated with individual cells which involve cell matrix interactions and movements in a fibroblast manner^(203,204). Mesenchymal migration was

observed in fibroblasts cells with the formation of focal adhesion interactions with the ECM with a slow migration rate from 0.1 $\mu\text{m}/\text{min}$ to 1 $\mu\text{m}/\text{min}$ ^(203,205). Cell migration is regulated by integrins transducing signals across the plasma membrane. The interaction between the cytoplasmic domain of the integrin and signalling proteins is essential to activate integrin signals. The role of integrins in cell migration was simplified considering the $\alpha 4\beta 1$ pathway ⁽²⁰⁶⁾, where the $\alpha 4\beta 1$ integrin is bound to the variable chain of fibronectin playing a fundamental role in cell migration ⁽²⁰⁶⁾. Clark et al. ⁽¹⁶⁵⁾ demonstrated that human fibroblast cells migration is controlled not only by the interaction of the $\alpha 5\beta 1$ integrin interaction with the RGD complex on the fibronectin, but that also the $\alpha 4\beta 1$ bound to the variable chain of the fibronectin is necessary to permit the fibroblasts migration. The analysis of 3T3 fibroblast cells using the microfluidic system showed a different cell behaviour when a confined or unconfined space was considered. The confined and unconfined environment was considered using the higher and lower fibronectin adsorption on the substrate respectively, using cell density as a parameter of constraint. The confined space at the start point (where a higher protein deposition and cell crowding was observed), clearly showed a faster cell velocity migration with random movements, whilst the unconfined space at the end point increased the cell migration in the direction of the fibronectin gradient with a decrease in cell velocity. Hung and co-workers ⁽¹⁹⁰⁾ recently observed that by using physical confined and unconfined spaces, different cell migration was observed with the activation of distinctive signalling to modulate cell migration. Within this study, different cell shapes were observed in the

unconfined space (end point), where cells appeared more elongated and had more protrusions compare to the confined space (start point) suggesting that space influences cell distribution within the channel. Interestingly both the cell migration and the cell velocity demonstrated different behaviour patterns at the start point and the end point, suggesting that the cell density and the space available in the microfluidic channel can influence cell behaviour in this system. Further speculation on the possible explanation of the fibroblast cells behaviour using this microfluidic fibronectin system was considered. The presence of fibronectin adsorption and the consequent cell density observed along the channel can be a key influence on cell behaviour, explaining not only a physical constraint due to the channel width (as demonstrated from Hung and co-workers⁽¹⁹⁰⁾) but an “environmental” constraint due to the fibronectin adsorption on the substrate and the consequent cell density.

In fact higher protein adsorption at the start point corresponded to a higher cell density without a specific cell migration in the direction of the protein gradient, while at the end point the cell density is decreased with an increase in space and specific cell migration (Figure 5.3). Changes in cell shape were also observed during the cell migration analysis suggesting that both collective and single mesenchymal type migration is taking place. Single elongated cells with protrusions were observed at the end point (where the cells had more space), suggesting a single cell moving mechanism. Moving to the start point fibroblast cells appeared more compact, using the protrusions to interact with the nearest cells to interact each other. The less space available at the start point clearly limited the cells movements in the direction of fibronectin

gradient but seems to encourage cell-cell interaction. Single and group mesenchymal type migration were observed in fibroblast cells and reported^(204,207) in literature. To prove the presence of a mesenchymal cell type migration hypothesised here other experiments concerning the expression of integrins or specific proteins binding to the fibronectin must be conducted. This microfluidic system showed that is possible to study along the same microfluidic channel the differences in 3T3 cell behaviour and cell migration, using adsorption of fibronectin protein as substrate. The same technique can be used to study the differences in cell behaviour using different extra cellular membrane protein like collagen.

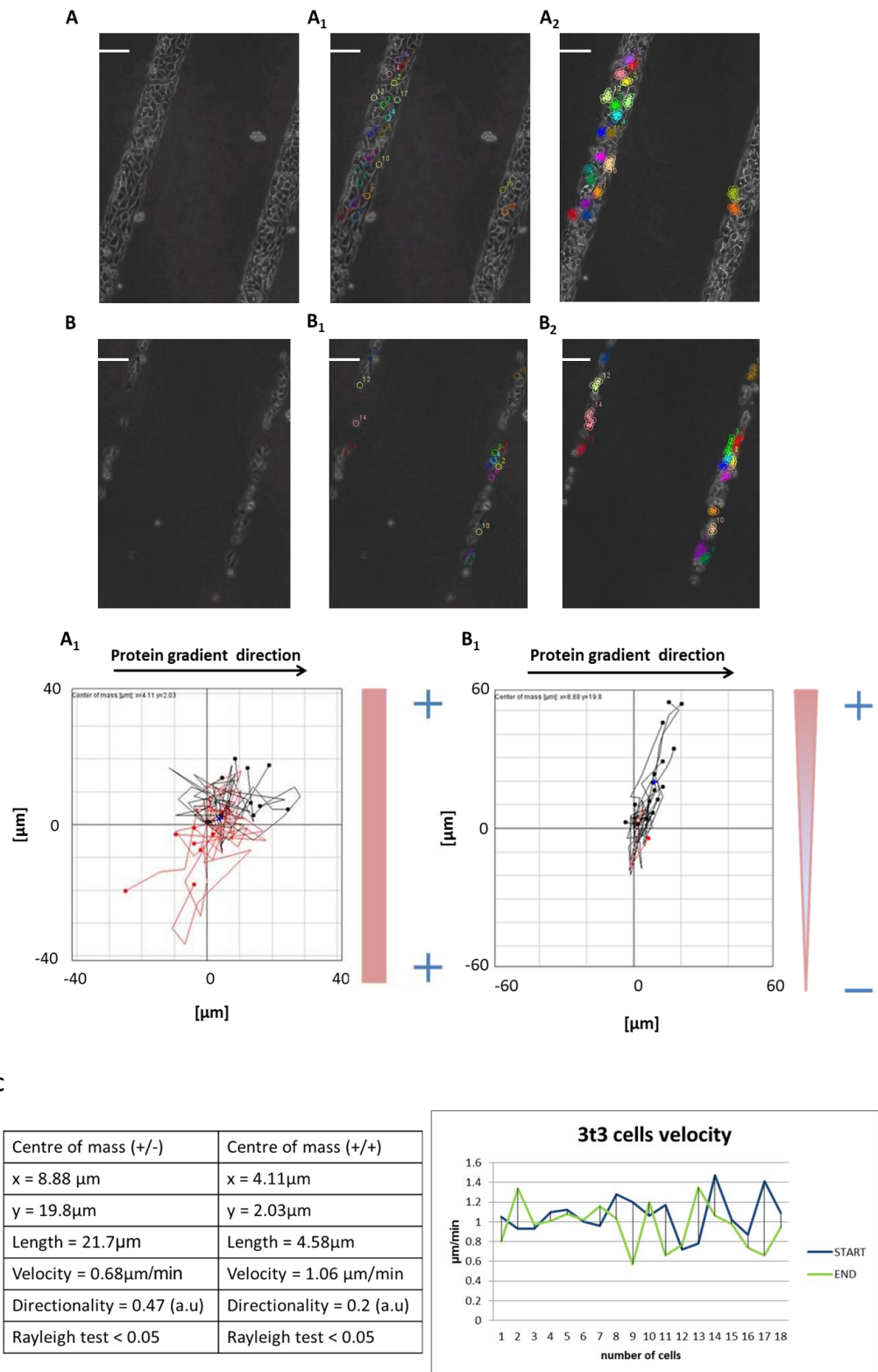


Figure 5.1: Representation of the 3T3 fibroblast cells migration. The migration analysis was conducted using the Chemotaxis tool (IBIDI) programme, using the videos obtained from picture frames acquired every 10 mins for 24 hrs. 18 cells were considered as sample in the migration analysis to have more reliable results. Data were repeated in triplicate and here an example

reported. In A and B an example of the time lapse pictures collected at start and end point showing the tracking analysis performed using the tracking programme using Image J plugs. In A₂ and B₂ the tracking migration of 18 cells is reported. In figure C an example of the analysis conducted on the sample using the IBIDI chemotaxis tool and cell velocity analysis is reported. The cell velocity analysis was repeated in triplicate. Statistical analysis using a two variable t-test was conducted to prove the statistical significance difference between start and end point cell velocity and cell migration analysis with $p < 0.05$.

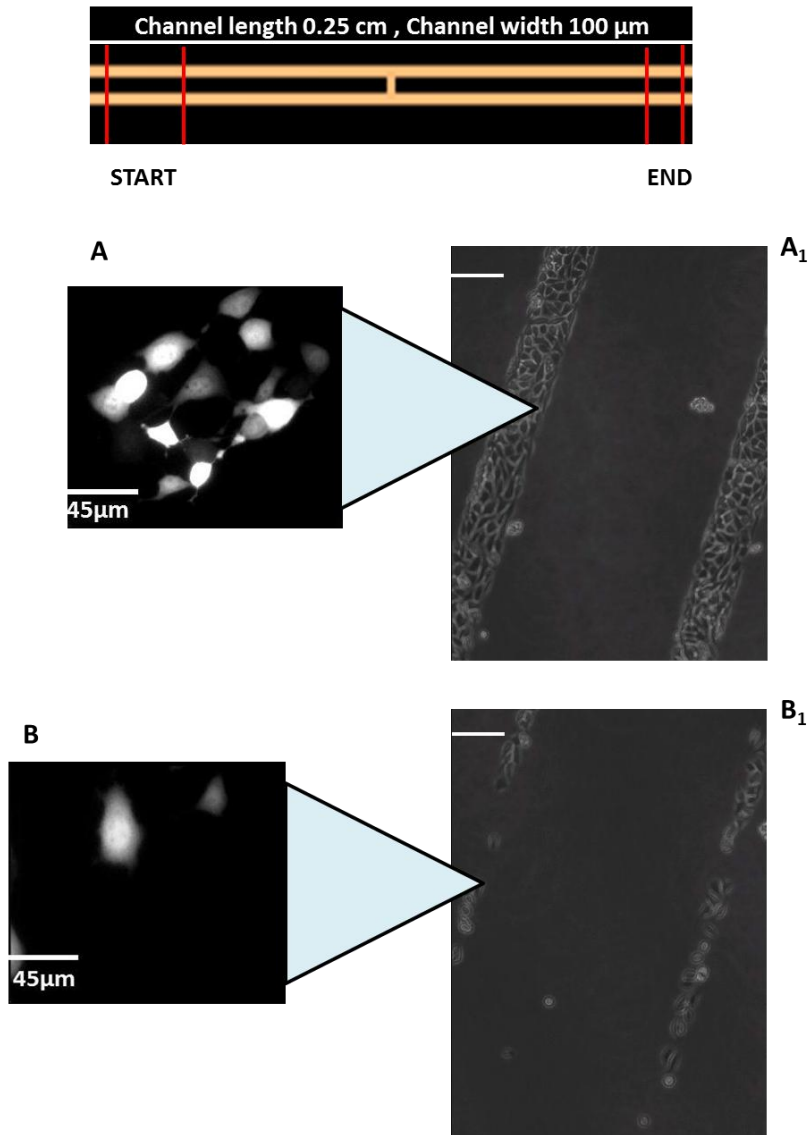


Figure 5.2: Analysis of the cell shape. Bright-field images A₁ and B₁ where acquired considering cell deposition on the fibronectin patterns using 1×10^6 3T3 fibroblast cells and incubated for two hours using a DMEM medium without FBS to avoid cell interaction with other proteins, at start and end point respectively. The fluorescent images A and B were acquired using a higher magnification. 5 images of three points along the channel for every point were acquired and here an example reported.

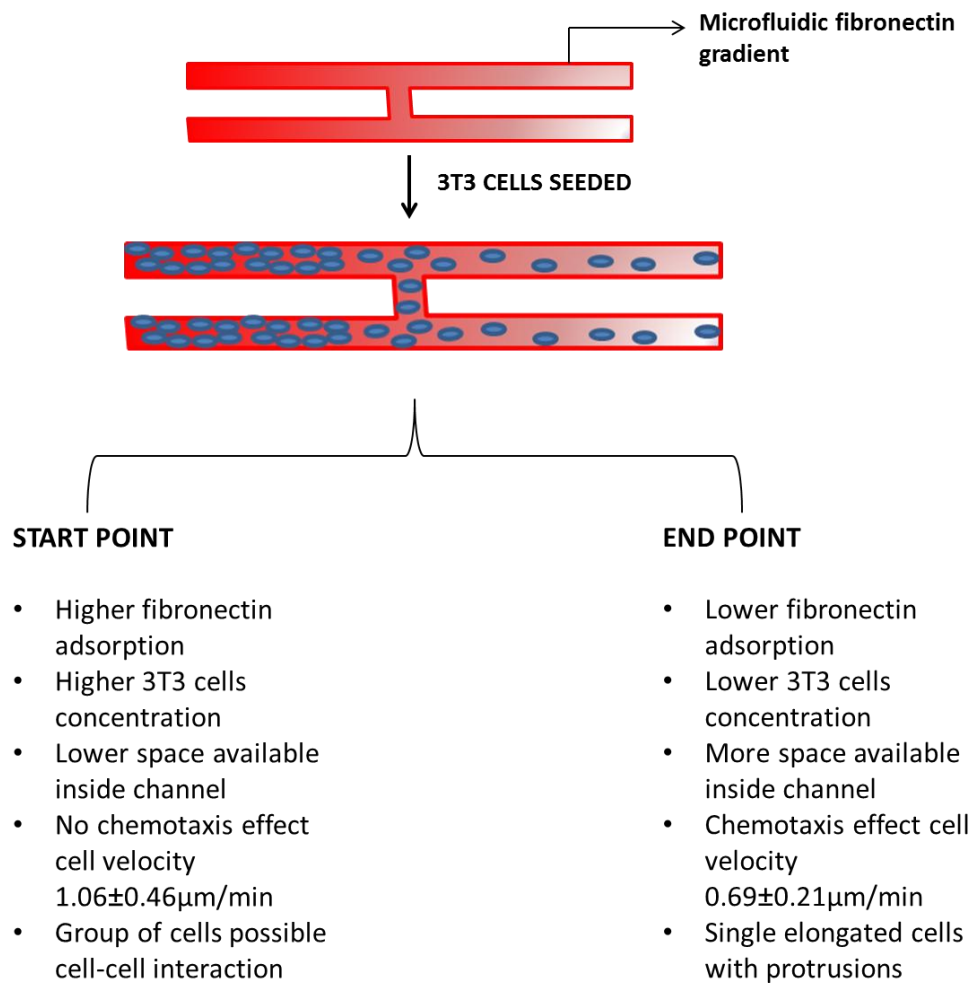


Figure 5.3: Brief summary of the 3T3 fibroblast cells behaviour using the microfluidic system. An analysis of the data obtained considering the unconfined (end point) and confined (start point) space is reported.

5.2.2. i-HMSC immortalised mesenchyme stem cells migration on fibronectin patterns

Attachment of the human mesenchyme stem cells on the substrate through the absorption of matrix proteins is principally mediated by integrins expressed on the cellular surface (as previously discussed in Chapter 4). When integrin attachment occurs, trans-membrane proteins activate signalling cascades essential in regulation of cell spreading, adhesion, migration and proliferation.

The analysis of the mesenchyme stem cells was conducted using the same procedure applied for the 3T3 fibroblast cells. The data collected using the picture frames acquired every 10 minutes for 24 hours are summarized in (Figure 5.4). Analysis of the cell migration at the start and end point of the microfluidic channel as previously observed for the 3T3 fibroblast cells, showed a random cell migration at the start point and a specific chemo-attractant effect of cells in the direction of the protein gradient at the end point (Figure 5.4 A, B). The analysis of the mesenchyme cells migration velocity reported in (Figure 5.4 D) showed a value of $0.21 \mu\text{m}/\text{min} \pm 0.02 \mu\text{m}/\text{min}$ at start point and an increase in cell velocity to $0.3 \mu\text{m}/\text{min} \pm 0.05 \mu\text{m}/\text{min}$ at the end point. The difference in cell velocity registered during the cell migration analysis, can be explained when considering the influence of RGD complex concentration in the system. In literature the effect of the RGD complex in the mesenchyme stem cells adhesion and spreading is well documented. Sawyer and co-workers⁽²¹⁶⁾ observed that when higher a density

of RGD complexes are present a reduction in HMSC cells spreading results; while a lower RGD density was observed to increase cell spreading. Keeping this in mind a theory on the possible explanation for the difference in cell migration velocity was hypothesised. The RGD complex was previously taken in consideration (Chapter 4) to explain cell adhesion on the fibronectin patterns, considering that the expression of the RGD complex in the right conformation on the fibronectin increased the possibility to find higher cell density, due to the interaction between RGD and the $\alpha 5\beta 1$ integrin expressed on the cell surface (Chapter 4, Figure 4.5). Higher cell density at the start point corresponded to a higher density of the RGD complex receptor in the correct conformation, with a possible decrease in cell spreading, whilst lower concentrations of the RGD complex receptor in the right conformation corresponded to an increase in cell spreading. The mechanism described above is summarised in Figure 5.5. In summary, lower cell spreading is associated with higher cell density at the start point in a “confined” space (inside the microfluidic channel), leading to the lower velocity in cell migration. At the same time a higher cell spreading and the “unconfined” space available at the end point can explain the higher velocity in cell migration.

Interestingly by using mesenchyme stem cells it was observed that the cell migration is not consistent with that of 3T3 fibroblast cell migration. It was observed from the video data that after 18 hours stem cells were no longer visible inside the microfluidic channel. Using green fluorescence (GFP) HMSC mesenchyme stem cells and Rhodamine labelled fibronectin, a more detailed analysis was conducted to check if changes in fibronectin adsorption were

observed during the cell migration. This was achieved by analysing the red intensity of the fluorescence protein inside the microfluidic channel over time. From a preliminary analysis as shown in the protein fluorescence during the cell migration, the intensity graph reported did not show a significant decrease in fibronectin intensity. The graph suggests a difference in protein intensity from the start and end point as expected (due to the difference in protein adsorption along the microfluidic channel), but there is not a clear decrease in protein intensity considering the single points. Considering in more detail the fluorescence intensity value over a longer period of time (0, 6, 12, 18 and 24 hrs) (Figure 5.6B) there is in fact a clear decrease in intensity. The possibility that fibronectin remodelling could be the explanation of the cell behaviour during the cell migration analysis is consistent with this decrease but clearly requires more study. Fibronectin remodelling of Human mesenchyme stem cells has been reported in literature to be due to a stretch rearrangement of the fibronectin ^(208,209). This structural rearrangement can be the result of mechanical stimuli ⁽²⁰⁸⁾ or be influenced by interaction with the environment ⁽²⁰⁹⁾. It is possible that also in this case that the interaction of mesenchyme stem cells with the environment for long time, through the generation of traction forces which leads to the stretching of Fn fibrils ⁽²¹²⁾. Stretching of Fn fibrils may activate cryptic binding sites ^(213,214,215) contributing to the fibronectin remodelling where a rearrangement of the protein structure could be explain the cell behaviour after 18 hours.

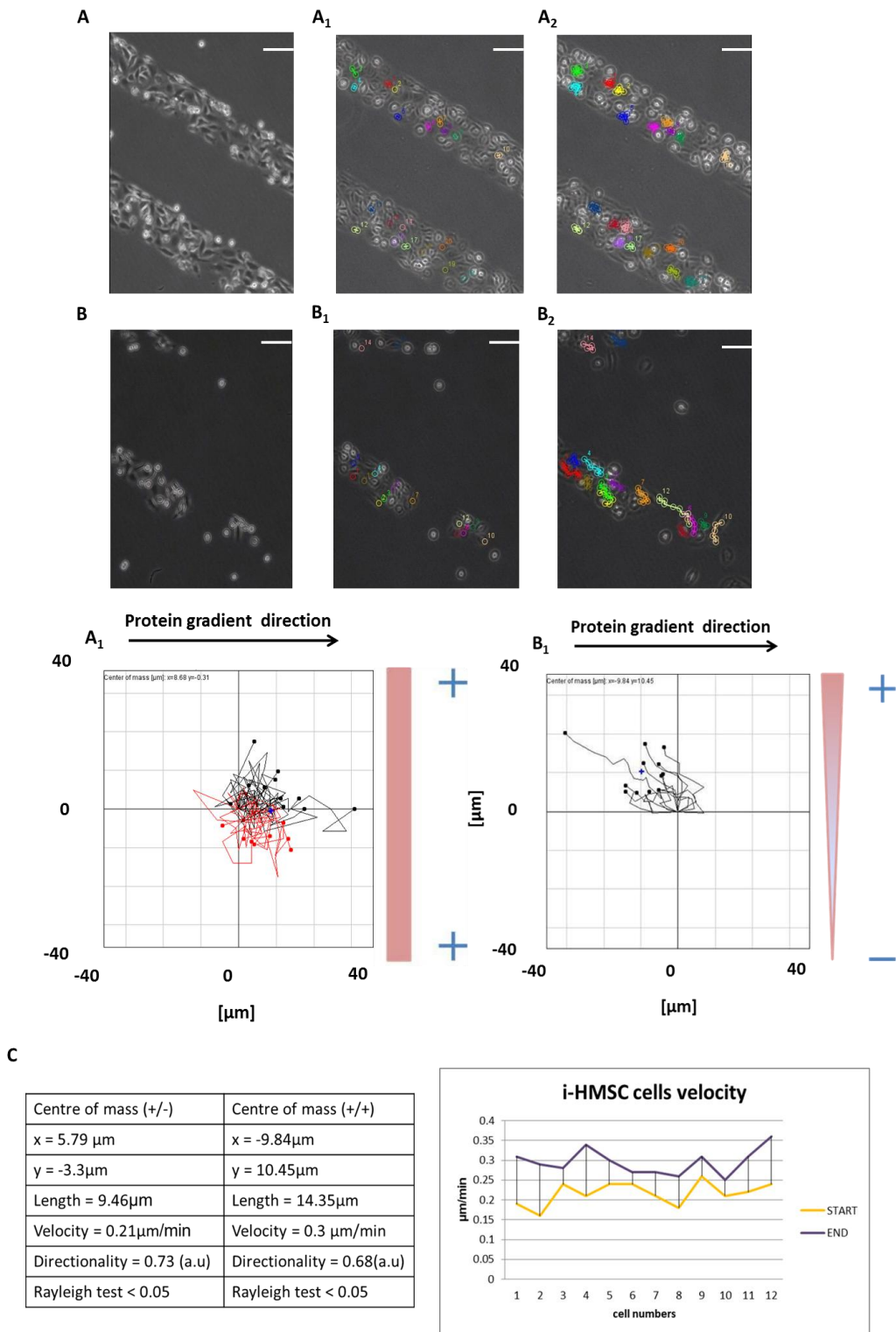
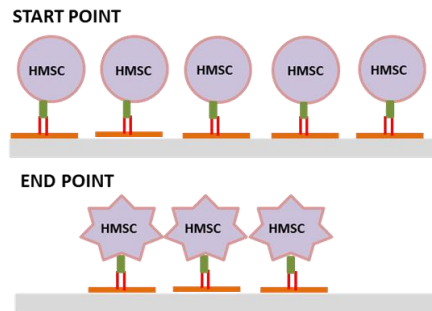


Figure 5.4: Representation of the i-HMSC mesenchymal stem cells migration. The migration analysis was conducted using the Chemotaxis tool (IBIDI) programme, using the videos obtained from picture frames acquired every 10 mins for 24 hrs. 18 cells were considered as sample in the migration analysis to have more reliable results. Data were repeated in triplicate and here an example reported. In A and B an example of the time lapse pictures collected at start and end point showing the tracking analysis performed using the tracking programme using Image J plugs. In A₂ and B₂ the tracking migration of 18 cells is reported. In figure C an example of the analysis conducted on the

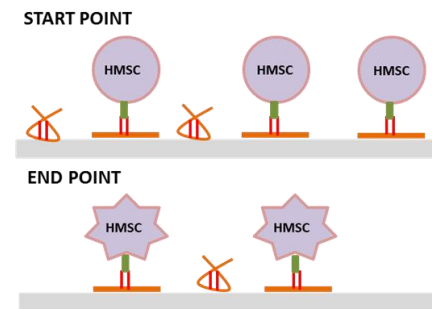
sample using the IBIDI chemotaxis tool and cell velocity analysis is reported. The cell velocity analysis was repeated in triplicate. Statistical analysis using a two variable t-test was conducted to prove the statistical significance difference between start and end point cell velocity and cell migration analysis with $p < 0.05$.

ASSUMPTION



Reported in literature:
 “Higher density RGD complex on substrate reduce i-HMSC cell spreading, cell spreading increase at lower density RGD complex”

POSSIBLE MECHANISM



Start point lower migration due to the absence of spreading of the cells at higher RGD complex

End point faster migration due to the spreading of the cells at lower RGD complex

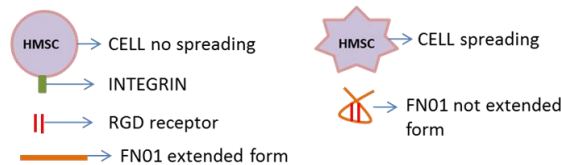


Figure 5.5: Representation of the possible mechanism involved in mesenchyme stem cells migration i-HMSC cells. The assumption that the concentration of the RGD complex expressed on the fibronectin molecules immobilised on the not-TCP substrate in the right conformation can influence the cells density and spreading, seems to be a possible explanation also to confirm difference in cell velocity migration.

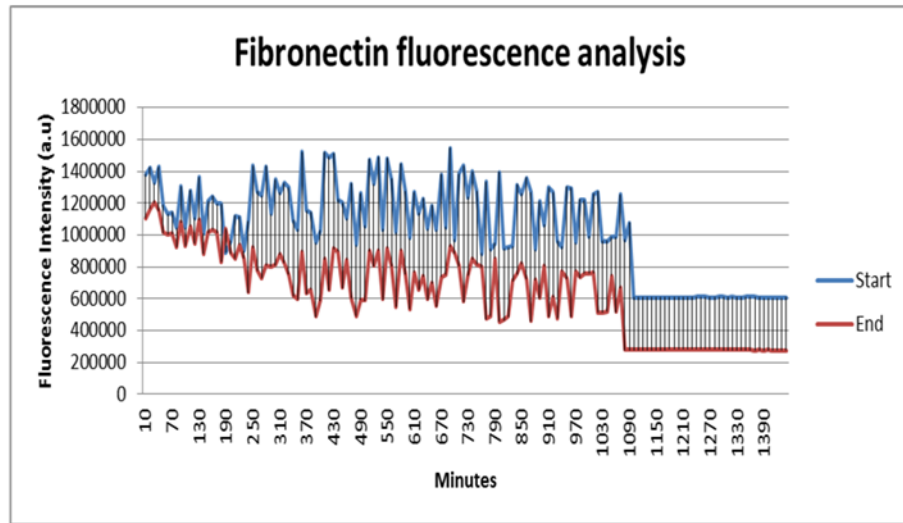
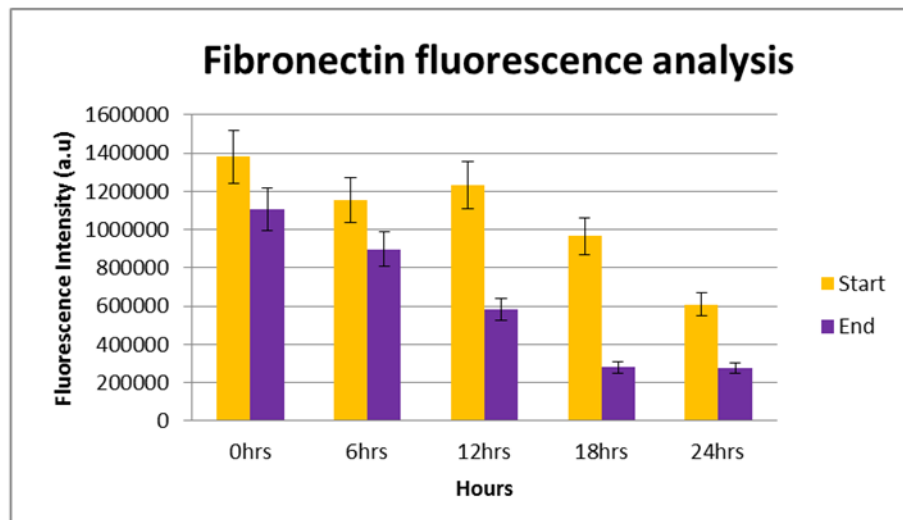
A**B**

Figure 5.6: Fibronectin fluorescence analysis during the i-HMSC stem cells migration. The analysis was conducted using the picture frames of the fibronectin taken every 10 minutes for 24 hours. In figure A and B, a representation of the fluorescence analysis is reported.

5.3. Summary

In this set of experiments it was demonstrated that the protein patterns created using the microfluidic technique could be used in cell migration and cell behaviour analysis. The particularity of this system is that along the patterns a decrease in protein adsorption on the substrate was observed (considering the injection and the end point of the channel), that can be used to encourage a range of cell behaviour as influenced by protein density and gradient. The use of two different cell lines namely 3T3 fibroblast and i-HMSC mesenchyme stem cells demonstrated that this system is sufficient to distinguish differences in cell migration and behaviour patterns between cell lines. The theory and associated mechanisms for future analysis proposed in this study have found early supporting evidence in recent literature to support, but it is clear further experiments must be carried out to confirm such mechanisms. This study has successfully demonstrated that this system can be used for biological application to monitor the cell behaviour using difference protein concentration and cell density all in the same microfluidic channel.

6. Summary

6.1. Brief overall summary of the surface characterisation and cell behaviour studies

The study of cell adhesion and functionality using a bio-functional gradient on silica and polymeric substrate was the principal scope of this work. The ability of the microfluidic patterning technique to create simple to complex bio-molecular gradients mimicking the physiological environment makes this technique well suited to cell adhesion and migration investigations. The use of the silica wafer and non-tissue culture plate substrates was not chosen randomly. The analysis technique employed such as AFM and fluorescence microscopy operate most easily on flat surfaces so as to characterize cells and of molecules. Whilst silica wafers have extensively been used in microfluidic pattern studies, it is not generally used in cell studies due to the inability of cells to adhere on this type of substrate. For this reason a polystyrene plate (non-tissue culture plate) was also used to conduct the cell studies.

The surface analysis characterisation of the substrates after immobilisation of the protein on the substrate (using the microfluidic channel to guide the protein injection), was conducted using fluorescence microscopy and AFM techniques. From the fluorescence analysis it was immediately observed that protein immobilisation on both substrates was achieved. Differences in

fluorescence intensity were also registered along the microfluidic channel suggesting a variation in protein adsorption levels along the channel.

An essential part of a good surface analysis is understanding the interaction between the protein and the corresponding substrates and monitoring the changes on the substrate surface before and after protein immobilisation. In order to understand the changes on substrate before and after protein immobilisation, and to observe protein distribution on the substrate inside the microfluidic channel AFM imaging was conducted on the samples. Analysis of the silica wafer substrate conducted using the AFM demonstrated that by using a concentration of 1 $\mu\text{g}/\text{ml}$ of protein, immobilisation on the substrate was observed. By using this microfluidic system a clear variation in particle size, density and roughness value was observed and recorded along a fibronectin pattern. On non-tissue culture plate (polystyrene) substrate AFM images analysis revealed a different fibronectin assembly on the surface, but due to rougher nature of this surface it was not possible to achieve the same level of detailed information as when using the silica wafer.

To assess protein density along the fibronectin pattern on polystyrene substrates an antibody functionalised probe AFM technique was used to monitor the molecular interactions between probes functionalised with antibody and the corresponding protein immobilised on the substrate. The resultant force curves were analysed in this study considered the injection point and the end point of the channel and revealed the presence of a density variation (in terms of functional binding) from the start to the end point due

to the change in binding frequency between the antibody and the immobilised fibronectin on the substrate. The binding capacity of fibronectin and its functionality were assessed.

The study confirmed the immobilisation of proteins on the substrates and assessed the variance in protein adsorption, considering the injection and the end point of the microfluidic channel, used for the guidance of proteins on the substrate. Attention then moved to the possible applications of this system in future cell studies. The variation of protein adsorption along the microfluidic channel suggesting the possibility to have a system where theoretically it is possible to control the cell density on it (due to the characteristics of the ECM proteins like fibronectin that can be used to bind cells on the substrate), and observe the cell behaviour under specific conditions.

Fibronectin protein was used to seed 3T3 fibroblast cells and i-HMSC immortalised human stem cells on the polystyrene (not-tissue culture plate) substrate. To avoid adhesion of the cells on the non-patterned areas of the substrate and hence have a clear cell deposition on the fibronectin pattern the substrate was coated with a surfactant (Pluronic F₁₂₇). Analysis of the consequent cell adhesion demonstrated that the cell density on the substrate is influenced by the protein adsorption on it, in fact at the higher protein adsorption start point a higher cell density was observed, whilst a lower protein adsorption end point yielded a lower cell density.

The presence of a variation in cell density along the microfluidic channel was investigated further to check the behaviour patterns of cells during the

migration from the end point (lower protein adsorption) to the injection point (higher protein adsorption). It was observed via recording cell motility that the cell behaviour is clearly influenced by the presence of higher or lower cell density as recorded.

It was demonstrated that by using this system future cell behaviour studies can be conducted. The system used in this research, detected differences in cell behaviour along the fibronectin pattern suggesting that the cells behaviour is influenced by the cell density on the substrate.

6.2. Surface characterization and protein functionality

6.2.1. Fluorescence microscopy versus AFM functionalised probe technique.

To ensure the protein immobilisation and to characterise the observed deposition of protein on the substrates, a surface analysis was conducted as discussed in Chapter 3.

To assess the protein adsorption along the patterns on the non-tissue culture plate substrate an AFM functionalised probe technique was used in addition to the fluorescence microscopy. The use of AFM functionalised probe technique to investigate the adsorption of protein on substrates is a new research concept that was not investigated before in literature.

The aim of this experiment was to understand and prove if there is a correlation between the fluorescence signals registered along the fibronectin pattern and the antibody-fibronectin receptor binding forces registered on the polystyrene substrate.

The combination of atomic force microscopy and force spectroscopy can be used to detect specific interaction forces between two molecules with pN sensitivity ^(210,211).

The experiment described schematically in (Figure 6.1) illustrates how fluorescence measurements can be associated to the presence of specific force measurements detectable by an AFM tip. The AFM tip functionalised with an anti-fibronectin antibody has the ability to recognise specific bovine fibronectin on the surface using the heparin binding sites expressed on the immobilised fibronectin ⁽¹¹⁶⁾. Specific binding events were registered during

this study with a range of $82 \text{ pN} \pm 7.4 \text{ pN}$ at the observed higher fluorescence intensity region (start point) and $52 \text{ pN} \pm 3.7 \text{ pN}$ at the lower fluorescence intensity region (end point).

The unbinding events between the antibody and the heparin receptor expressed on the immobilised fibronectin were at an increased concentration at the start point and decreased level of concentration at the end point. This is consistent with the presence of a higher protein deposition levels (Figure 6.1 C) as indicated by the higher fluorescence intensity registered after protein immobilisation on the substrate. This increased the possibility to find increased levels of receptor expressed on the fibronectin surface. In fact higher unbinding frequency events were registered at the start point along with an increase of the multiple adhesions due to the pull of multiple molecules immobilised on the substrate. The presence of a lower fluorescence intensity (Figure 6.1 D) along the fibronectin pattern corresponded to a decrease in unbinding frequency events due to the lower protein deposition on the substrate and hence the limited probability of finding heparin receptors expressed on the fibronectin coated surface.

Through combining AFM binding force technique with fluorescence microscopy it was possible within this study to confirm a difference in protein density and concentration of functional groups.

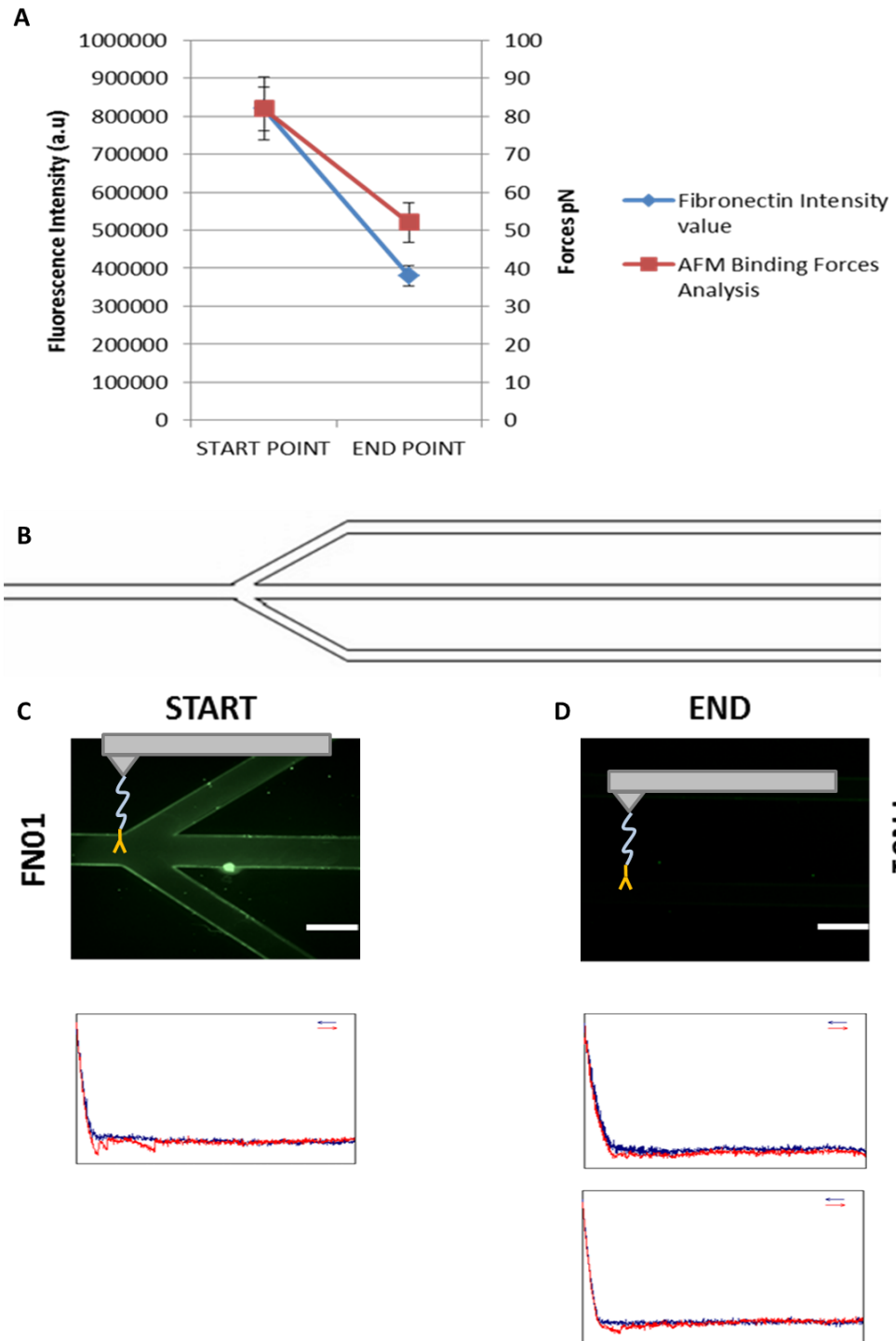


Figure 6.1: Correlation between fluorescence intensity and specific AFM force measurements (A) on fibronectin pattern (B) created on not-tissue culture plate substrate. A tip was functionalized with an anti-fibronectin antibody able to target the histamine groups exposed on the fibronectin surface. Fluorescent fibronectin at the start point (C) exhibits a higher number of specific multiple unbinding events (red line) whereas for most of the lower fluorescent fibronectin at the end point (D), no events or some few specific single unbinding events can be detected confirming the presence of a lower protein deposition along the pattern. Scale bar 200 μ m.

6.2.2. Assessment of fibronectin influence in cell behaviour

The influence of fibronectin functionality and density on cell culture behaviour was investigated. The presence of a concentration gradient along the fibronectin micro-pattern was used to check if changes in protein density are responsible for specific changes in cell adhesion and migration.

The difference in fibronectin density recorded at the start and end point revealed a difference in cell density using both fibroblasts and mesenchyme stem cells. The presence of a higher protein density appears to increase the possibility of finding an increased number of receptors in the right conformation on the functionalised surface with a corresponding higher level of cell adhesion, whilst lower protein density decreased the cell adhesion.

Changes in the cell shape were also observed when comparing the injection and the end point of the pattern, suggesting that the space available inside the micro-pattern plays an important role in fibroblast cell behaviour.

When undertaking cell migration analysis both cell lines showed a distinctive chemo-attractant behaviour in the direction of the protein gradient. This behaviour was observed at the end point where a lower cell density was recorded, whilst random cell movement was observed at higher cell density levels (injection point) presumably due to increased cell-cell interactions.

Interestingly a difference in cell migration velocity was registered when analysing the i-HMSC stem cells at the higher and lower cell densities, i.e. injection and end point respectively.

The cell density and the space available along the micro-pattern clearly showed that it is possible to investigate cell behaviour (fibroblasts and

mesenchyme stem cells) under specific conditions along the same fibronectin pattern. The adhesion and migration mechanisms of fibroblasts and mesenchyme stem cells reviewed and observed in this study have close similarities with previous work reported in wider research literature.

The control of cell growth and density on defined areas of surface would be important for potential application in tissue engineering studies to understand how the presence of a particular microenvironment and the presence of confined or unconfined space can influence the cell behaviour.

7. Conclusions and future work

The key aim of this thesis was to create protein concentration gradients on surfaces using microfluidic approaches for possible biological application – inclusive of cell adhesion and migration studies - and to utilise AFM as a tool for protein imaging and force spectroscopy investigations. Initially a review of microfluidic systems and their applications in biological studies, inclusive of gradient generation was discussed. A detailed discussion concerning the application of the AFM in conjunction with other analytical techniques such as, fluorescence microscopy and cell adhesion studies were reviewed. The design and production of silicon masters and the subsequent production of PDMS microfluidic channels was described. Overall this approach has allowed the generation and characterisation of well-defined protein gradients on a variety of substrates including uniquely non-tissue culture plastic as typically used in a variety of standard cell-based studies.

The use of the protein microfluidic systems is of growing interest for a variety of applications, including but not limited to tissue engineering, drug delivery and biosensors. The facility it provides to spatially control chemistries on substrates for biological and medical applications is in high demand. The characterisation of the protein deposition using tapping mode AFM allowed for conformational elucidation of protein deposition on the substrate. Both protein deposition and the surface characterisation were also investigated

using fluorescence microscopy in parallel with AFM. Changes in fluorescence intensity along the protein pattern and the quantitative analysis conducted on the AFM images identified a clear difference in protein density observed along the protein patterns produced from a high to low surface density.

The use of suitably functionalized AFM probes allowed the study of specific molecular interactions in a simulated between patterned fibronectin molecules and anti-fibronectin in a physiological environment. This technique was used to show that the immobilized protein remained able to interact in a specific manner (ie. conformation had been conserved) and to relate this to the protein density observed along the fibronectin pattern using AFM and fluorescence imaging. The difference in protein binding registered by the AFM functionalized probe technique at the injection and the end point of the pattern on substrate was used to rationalise the influence of both protein deposition and space available inside the pattern on subsequent cell based studies. The spatially patterned fibronectins affinity was tested by investigating cell adhesion, shape and migration on the protein patterns. This involved the use of different cell lines, including human mesenchymal stem cells and human fibroblasts.

The ability to control cell adhesion and migration on substrates could be of significant interest when researching possible applications in future tissue engineering and biological studies. The combination of AFM and fluorescence microscopy techniques for the protein density investigation allowed a deeper

insight into protein deposition and rearrangement on a substrate; essential understanding for future biological applications.

The complex multi-step process involved in cell migration from the coordination of biochemical and biomechanical signals to the modulation of cell morphology by rearranging cytoskeletal filaments ⁽²¹⁷⁾, reveals the importance of further bio-molecular studies to understand the changes observed in cell migration here reported. The role of specific Rho and GTPase signalling proteins in the regulation of cytoskeleton-dependent processes, and the activation of specific GTPase ⁽²¹⁷⁾ and Rho/ROK signalling patterns ⁽²¹⁸⁾ in mesenchymal and amoeboid cell type migration respectively has been reported in literature.

The ability of cells to assume different cell behaviour when a difference in protein density and space available is detected in the surrounding micro-environment could be further investigated in the future considering the activation of different signalling proteins (Rho and GTPase) in the regulation of cell contractility and consequent cell migration mechanisms using a cell fluorescent vector transfection technique ⁽²¹⁸⁾.

The activation of different signalling protein patterns could explain the ability of cells to detect changes in the surrounding micro-environment with consequent changes in cell behaviour (cell migration and shape).

The possibility that changes in the physical microenvironment can alter the mechanisms of cell migration when a crowd or open space is considered (as suggested in this study), opens new frontiers concerning the study of cell

migration under physiological conditions, where confined spaces are more physiologically relevant⁽¹⁹²⁾.

Ideally, this system could be used in future to establish and understand further the relationship between the cells (for example tumour or stem cells) and the influence of physical microenvironment in terms of the impact on cell behaviour. The ability to study cells in a near physiological environment where the presence of a constrained space with higher protein deposition, or the presence of a larger space with lower protein concentration allow more elucidations concerning the cell growth, migration and proliferation in the *in vivo* environment. The development of this system could therefore have a great impact in areas of tissue engineering and advance material research.

Reference List

- [1]. J. Gurdon, P. Bourillot, "Morphogen gradient interpretation" *Nature* (2001), 413, 797–803.
- [2]. T.M. Keenan, A. Folch, "Biomolecular gradient in cell culture systems" *Lab Chip* (2008), 8, 34–57.
- [3]. A.L. Paguirigan, D.J. Beebe, "Microfluidics meet cell biology: bridging the gap by validation and application of microscale techniques for cell biological assays" *Bioessays* (2008), 30, 811–821.
- [4]. D. Rogulja, K.D. Irvine, "Regulation of cell proliferation by a morphogen gradient" *Cell* (2005), 123, 449–461.
- [5]. M. Baggiolini, B. Dewald, B. Moser, "Human chemokines: An update" *Annu. Rev. Immunol.* (1997), 15, 675-705.
- [6]. E. Stein, M. Tessier-Lavigne, "Hierarchical organization of guidance receptors: silencing of netrin attraction by slit through a Robo/DCC receptor complex" *Science* (2001), 291, 1928–1938.
- [7]. H.J. Song, G.L. Ming, M.M. Poo, "cAMP-induced switching in turning direction of nerve growth cones" *Nature* (1997), 388, 275–279.
- [8]. V.H. Hopker, et al., "Growth-cone attraction to netrin- 1 is converted to repulsion by laminin-1" *Nature* (1999), 401, 69–73.
- [9]. R.A. Firtel, C.Y. Chung, "The molecular genetics of chemotaxis: sensing and responding to chemoattractant gradients" *Bioessays* (2000), 22, 603–615.
- [10]. H.J. Song, M.M. Poo, "Signal transduction underlying growth cone guidance by diffusible factors" *Neurobiol.* (1999), 9, 355–363.
- [11]. A.D. Lander, "Morpheus unbound: Reimagining the morphogen gradient" *Cell* (2007), 128, 245–256.
- [12]. E.F. Foxman, E.J. Kunkel and E.C. Butcher, "Integrating conflicting chemotactic signals. The role of memory in leukocyte navigation" *J. Cell Biol.* (1999), 147, 577-588.
- [13]. B. Heit, et al., "An intracellular signaling hierarchy determines direction of migration in opposing chemotactic gradients" *J. Cell Biol.* (2002), 159, 91–102.
- [14]. H. Chen, et al., "Semaphorin-neuropilin interactions underlying sympathetic axon responses to class III semaphorins" *Neuron* (1998), 21, 1283–1290.

- [15]. W.J. Rosoff, "A new chemotaxis assay shows the extreme sensitivity of axons to molecular gradients" *Nat. Neurosci.* (2004), 7, 678–682.
- [16]. S. Boyden, "The chemotactic effect of mixtures of antibody and antigen on polymorphonuclear leucocytes" *J. Exp. Med.* (1962), 115, 453–466.
- [17]. S.H. Zigmond, "Ability of polymorphonuclear leukocytes to orient in gradients of chemotactic factors" *J. Cell Biol.* (1977), 75, 606–616.
- [18]. D. Zicha, G. Dunn, G. Jones, "Analyzing chemotaxis using the Dunn direct-viewing chamber" *Methods Mol. Biol.* (1997), 75, 449–457.
- [19]. T. Bogenrieder, M. Herlyn, "Axis of evil: Molecular mechanisms of cancer metastasis" *Oncogene* (2003), 22, 6524–6536.
- [20]. C.S. Goodman, "Mechanisms and Molecules that Control Growth Cone Guidance" *Annu. Rev. Neurosci.* (1996), 19, 341–377.
- [21]. T.M. Keenan, C.H. Hsu, A. Folch, "Microfluidic "jets" for generating steady-state gradients of soluble molecules on open surfaces" *Appl. Phys. Lett.* (2006), 89.
- [22]. A.P. Quist, E. Pavlovic, S. Oscarsson, "Recent advances in microcontact printing" *Anal. Bioanal. Chem.* (2005), 381, 591–600.
- [23]. A. Bernard, et al., "Microcontact Printing of Proteins" *Adv. Mater.* (2000), 12, 1067–1070.
- [24]. C.W. Frevert, et al., "Measurement of cell migration in response to an evolving radial chemokine gradient triggered by a microvalve" *Lab Chip* (2006), 6, 849–856.
- [25]. B.G. Chung, F. Lin, N.L. Jeon, "A microfluidic multi-injector for gradient generation" *Lab Chip* (2006), 6, 764–768.
- [26]. J.Q. Zheng, M. Felder, J.A. Connor, M.M. Poo, "Turning of nerve growth cones induced by neurotransmitters" *Nature* (1994), 368, 140–144.
- [27]. S. Lang, A.C. Von Philipsborn, A. Bernard, F. Bonhoeffer, M. Bastmeyer, "Growth cone response to ephrin gradients produced by microfluidic networks" *Anal. Bioanal. Chem.* (2008), 390, 809–816.
- [28]. F. Lin, et al., "Effective neutrophil chemotaxis is strongly influenced by mean IL-8 concentration" *Biochem. Biophys. Res. Commun.* (2004), 319, 576–581.
- [29]. F. Lin, et al., "Neutrophil migration in opposing chemoattractant gradients using microfluidic chemotaxis devices" *Ann. Biomed. Eng.* (2005), 33(4), 475–482.

- [30]. S.J. Wang, W. Saadi, F. Lin, C.M.C. Nguyen, N.L. Jeon, "Differential effects of EGF gradient profiles on MDA-MB-231 breast cancer cell chemotaxis" *Exp. Cell Res.* (2004), 300, 180–189.
- [31]. P. Kourilsky, P. Truffa-Bachi, "Cytokine fields and the polarization of the immune response" *Trends Immunol.* (2001), 22, 502–509.
- [32]. F. Lin, E.C. Butcher, "T cell chemotaxis in a simple microfluidic device" *Lab Chip* (2006), 6, 1462–1469.
- [33]. T.M. Keenan, C.W. Frevert, A. Wu, V. Wong, A. Folch, "A new method for studying gradient-induced neutrophil desensitization based on an open microfluidic chamber" *Lab Chip* (2010), 10, 116–122.
- [34]. A.J. Engler, S. Sen, H.L. Sweeney, D.E. Discher, "Matrix elasticity directs stem cell lineage specification" *Cell* (2006), 126, 677–689.
- [35]. D.E. Discher, D.J. Mooney, P.W. Zandstra, "Growth factors, matrices, and forces combine and control stem cells" *Science* (2009), 324, 1673–1677.
- [36]. B.G. Chung, L.A. Flanagan, S.W. Rhee, P.H. Schwartz, A.P. Lee, E.S. Monuki and N. L. Jeon, "Human neural stem cell growth and differentiation in a gradient-generating microfluidic device" *Lab Chip* (2005), 5, 401–406.
- [37]. J.C. McDonald, G.M. Whiteside, "Poly-(dimethylsiloxane) as a material for fabricating microfluidic devices" *Acc. Chem. Res.* (2002), 35, 491–499.
- [38]. J.M.K. Ng, I. Gitlin, A.D. Stroock, G.M. Whitesides, "Components for integrated poly(dimethylsiloxane) microfluidic systems" *Electrophoresis* (2002), 23, 3461–3473.
- [39]. J.N. Lee, C. Park, G.M. Whitesides, "Solvent Compatibility of Poly (dimethylsiloxane)-Based Microfluidic Devices" *Anal. Chem.* (2003), 75, 6544–6554.
- [40]. G.T. Roman, T. Hlaus, K. J. Bass, T. G. Seelhammer, C. T. Culbertson, "Sol-gel modified poly (dimethylsiloxane) microfluidic devices with high electroosmotic mobilities and hydrophilic channel wall characteristics" *Anal. Chem.* (2005), 77, 1414–1422.
- [41]. J.N. Lee, X. Jiang, D. Ryan, G.M. Whitesides, "Compatibility of mammalian cells on surfaces of poly (dimethylsiloxane)" *Langmuir* (2004), 20, 11684–11691.
- [42]. R. Mukhopadhyay, "When PDMS isn't the best" *Anal. Chem.* (2007), 79, 3248–3253
- [43]. H.A. Stone, S. Kim, "Microfluidics: Basic issues, applications, and challenges" *AI. Ch. E. J.* (2001), 47, 1250–1254.

- [44]. T. M. Squires, S. R. Quake, "Microfluidics: Fluid physics at the nanoliter scale" *Rev. Mod. Phys.* (2005), 77, 977–1026.
- [45]. A. Sawano, S. Takayama, M. Matsuda, A. Miyawaki, "Lateral propagation of EGF signaling after local stimulation is dependent on receptor density" *Dev. Cell.* (2002), 3, 245.
- [46]. S. Takayama, E. Ostuni, P. LeDuc, K. Naruse, D.E. Ingber, G.M. Whitesides, "Laminar flows - subcellular positioning of small molecules" *Nature* (2001), 411, 1016.
- [47]. C.A. Parent, P.N. Devreotes, "A cell's sense of direction" *Science* (1999), 284, 765.
- [48]. I. Barkefors, S. Le Jan, L. Jakobsson, E. Hejll, G. Carlson, H. Johansson, "Endothelial cell migration in stable gradients of vascular endothelial growth factor A and fibroblast growth factor 2: effects on chemotaxis and chemokinesis" *J. Biol. Chem.* (2008), 283, 13905.
- [49]. C.R Terenna, T. Makushok, G. Velve-Casquillas, D. Baigl, Y. Chen, M. Bornens, "Physical mechanisms redirecting cell polarity and cell shape in fission yeast" *Curr. Biol.* (2008), 18, 1748.
- [50]. G. Faure-Andre, P. Vargas, M.I. Yuseff, M. Heuze, J. Diaz, D. Lankar, "Regulation of dendritic cell migration by CD74, the MHC class II-associated invariant chain" *Science* (2008), 322, 1705.
- [51]. J.M. Higgins, D.T. Eddington, S.N. Bhatia, L. Mahadevan, "Sickle cell vasoocclusion and rescue in a microfluidic device" *Proc. Natl. Acad. Sci. USA* (2007), 104, 20496.
- [52]. J. Guck, S. Schinkinger, B. Lincoln, F. Wottawah, S. Ebert, M. Romeyke, "Optical Deformability as an Inherent Cell Marker for Testing Malignant Transformation and Metastatic Competence" *Biophys. J.* (2005), 88, 3689.
- [53]. A.E. Kamholz, B.H. Weigl, B.A. Finlayson, P. Yager, "Quantitative Analysis of Molecular Interaction in a Microfluidic Channel: The T-Sensor" *Anal. Chem.* (1999), 71, 5340.
- [54]. H. Mao, P.S. Cremer, M.D. Manson, "A sensitive, versatile microfluidic assay for bacterial chemotaxis" *Proc. Natl. Acad. Sci. USA* (2003), 100, 5449.
- [55]. N.L. Jeon, H. Baskaran, S.K. Dertinger, G.M. Whitesides, L. Van De Water, M. Toner, "Neutrophil chemotaxis in linear and complex gradients of interleukin-8 formed in a microfabricated device" *Nat. Biotechnol.* (2002), 20, 826.
- [56]. V.V. Abhyankar, M.A. Lokuta, A. Huttenlocher, D.J. Beebe, "Characterization of a membrane-based gradient generator for use in cell-signaling studies" *Lab Chip* (2006), 6, 389.

- [57]. W. Saadi, S.W. Rhee, F. Lin, B. Vahidi, B.J. Chung, N.L. Jeon, "Generation of stable concentration gradients in 2D and 3D environments using a microfluidic ladder chamber" *Biomed. Microdev.* (2007), 9, 627.
- [58]. E. Delamarche, A. Bernard, H. Schmid, B. Michel, H. Biebuyck, "Patterned Delivery of Immunoglobulins to Surfaces Using Microfluidic Networks" *Science* (1997), 276, 779.
- [59]. X. Jiang, Q. Xu, S.K. Dertinger, A.D. Stroock, T. Fu, G.M. Whitesides, "A General Method for Patterning Gradients of Biomolecules on Surfaces Using Microfluidic Networks" *Anal. Chem.* (2005), 77, 2338.
- [60]. K.A. Fosser, R.G. Nuzzo, "Fabrication of patterned multicomponent protein gradients and gradient arrays using microfluidic depletion" *Anal. Chem.* (2003), 75, 5775.
- [61]. O.A. Saleh, L.L. Sohn, "An Artificial Nanopore for Molecular Sensing" *Nano Letters* (2003), 1, 37-38.
- [62]. J.E. Dixon, E. Dick, D. Rajamohan, K.M. Shakesheff, C. Denning "Directed differentiation of human embryonic stem cells to interrogate the cardiac gene regulatory network" *Mol. Ther.* (2011), 19, 1695–1703.4
- [63]. T. Okamoto, T. Aoyama, T. Nakayama, T. Nakamata, T. Hosaka, K. Nishijo, T. Nakamura, T. Kiyono, J. Toguchida "Clonal heterogeneity in differentiation potential of immortalized human mesenchymal stem cells" *Biochemical and Biophysical research communications* (2002), 295, 354-361.
- [64]. W. Wang, H. Liang, A.L. Cheikh, R. Ghanami, L. Hamilton, M. Fraylich, K.M. Shakesheff, B. Saunders, C. Alexander. "Biodegradable Thermoresponsive Microparticle Dispersions for Injectable Cell Delivery Prepared Using a Single-Step Process" *Adv. Mater.* 2009, 21, 1809–1813.
- [65]. P. Suraneni, B. Rubinstein, J. R. Unruh, M. Durnin, D. Hanein, R. Li. "The Arp2/3 complex is required for lamellipodia extension and directional fibroblast cell migration" *J. Cell Biol.* 2012, 2, 248-251.
- [66]. C. O. Morgner, P. Reichardt, M. Chopin, S. Braungart, C. Wahren, M. Gunzer, R. Jessberger "Sphingosine 1-Phosphate-Induced Motility and Endocytosis of Dendritic Cells Is Regulated by SWAP-70 through RhoA" *J. of Immunology* 2011, 186, 5351-5355.
- [67]. P. J. Hanley, Y. Xu, M. Kronlage, K. Grobe, P. Schön, J. Song, L. Sorokin, A. Schwab, M. Bähler "Motorized RhoGAP myosin IXb (Myo9b) controls cell shape and motility" *PNAS* 2010, 107,12147-12150.
- [68]. G.M. Whitesides, "The 'right' size in nanobiotechnology" *Nat. Biotech.* (2003), 21, 1161–1165.

- [69]. N.L. Tourovskaia, A. Folch, "Biology on a chip: microfabrication for studying the behavior of cultured cells" *A. Crit. Rev. Biomed. Eng.* (2003), 31, 423–488.
- [70]. S.P. Fodor, "Light-directed, spatially addressable parallel chemical synthesis" *Science* (1991), 251, 767–73.
- [71]. Y. Xia, G.M. Whitesides, "Replica molding with a polysiloxane mould provides this patterned microstructure" *Angew. Chem. Int. Ed. Engl.* (1998), 37, 551–575.
- [72]. A. Kumar, G.M. Whitesides, "Features of gold having micrometer to centimeter dimensions can be formed through a combination of stamping with an elastomeric stamp and an alkanethiol "ink" followed by chemical etching" *Appl. Phys. Lett.* (1993), 63, 2002–2004.
- [73]. Y. Xia, et al., "Replica molding using polymeric materials: A practical step toward nanomanufacturing" *Adv. Mater.* (1997), 9, 147–149.
- [74]. R.A. Lewis, A.R. Leach, "Current methods for site-directed structure generation" *J Computer-Aided Mol. Des.*, (1994), 8, 467–75.
- [75]. E. Sun, F.E. Cohen, "Computer-assisted drug discovery a review" *Gene* (1993), 137, 127–32.
- [76]. N.A. Peppas, A. Langer, "New challenges in biomaterials" *Science* (1994), 263, 1715–20.
- [77]. T. Boland, B.D. Ratner, "Direct measurement of hydrogen bonding in DNA nucleotide bases by atomic force microscopy" *Proc. Nat. Acad. Sci. USA* (1995), 92, 5297.
- [78]. M. Ludwig, M. Rief, L. Schmidt, H. Li, F. Oesterhelt, M. Gautel, "AFM, a tool for single- molecule experiments" *Appl. Phys. Mater. Sci. Process* (1999), 68, 173–176.
- [79]. M. Rief, M. Gautel, F. Oesterhelt, J.M. Fernandez, H.E. Gaub, "Reversible Unfolding of Individual Titin Immunoglobulin Domains by AFM" *Science* (1997), 276, 1109–12.
- [80]. T.A. Camesano, K.J. Wilkinson, "Single molecule study of xanthan conformation using atomic force microscopy" *Biomacromolecules* (2001), 2, 1184–91.
- [81]. M. Ashhab, M.V. Salapaka, M. Dahleh, I. Mezić, "Dynamical analysis and control of microcantilevers" *Nonlinear Dyn.* (1999), 20, 197–220.
- [82]. R. Fung, S. Huang, "Dynamic modeling and vibration analysis of the Atomic Force Microscope" *ASME J. Vib. Acoust.* (2001), 123, 502–9.
- [83]. F.M. Serry, E.Y. Strausser, J. Magonov, S.J. Thornton, L. Ge, "Surface characterisation using atomic force microscopy" *Surf. Eng.* (1999), 15, 285–90.

- [84]. K.D. Costa, "Single-cell elastography: probing for disease with atomic force microscope" *Dis Markers*. (2003), 19, 139–154.
- [85]. M. Radmacher, "Studying the mechanics of cellular processes by atomic force microscopy" *Cell. Mech.* (2007), 347–372.
- [86]. P. Geuthner, "Simultaneous imaging of Si(111) 7×7 with atomic resolution in scanning tunneling microscopy, atomic force microscopy, and atomic force microscopy noncontact mode" *J. Vacuum Sci. Technol. B.* (1996), 14, 2428.
- [87]. F.J. Giessibl, "Atomic Resolution of the Silicon (111)-(7x7) Surface by Atomic Force Microscopy" *Science* (1995), 267-68.
- [88]. J. Nader, L. Karthik, "A Review of Atomic Force Microscopy Imaging Systems: Application to Molecular Metrology and Biological Sciences" *Mechatronics* (2004), 14, 907-945.
- [89]. J. Tansock, C. Williams, "Force measurement with a piezoelectric cantilever in a scanning force microscope" *Ultramicroscopy* (1992), 44, 1464-9.
- [90]. B. Cappella, G. Dietler, "Force-distance curves by atomic force microscopy" *Surface Science Reports* (1999), 34, 1-104.
- [91]. C.T. Gibson, G.S. Watson, S. Myrha, "Determination of the spring constants of probes for force microscopy/spectroscopy" *Nanotechnology* (1996), 7, 259-62.
- [92]. C.T. Gibson, G.S. Watson, S. Myrha, "Scanning force microscopy—calibrative procedures for 'best practice'" *Scanning* (1997), 19, 564-81.
- [93]. J. Zlatanova, S.M. Lindsay, S.H. Leuba, "Single molecule force spectroscopy in biology using the atomic force microscope" *Progress in Biophysics and Molecular Biology* (2000), 74, 37-61.
- [94]. Jarvik JW, Adler SA, Telmer CA, Subramaniam V, Lopez AJ. CD-Tagging: "A new approach to gene and protein discovery and analysis" *BioTechniques* (1996), 5, 896–904
- [95]. Habeler G, Natter K, Thallinger GG, Crawford ME, Kohlwein SD, Trajanoski Z. "YPL. db: the Yeast Protein Localization database" *Nucleic Acids Research* (2002), 30, 80–83.
- [96]. A. D. Stroock, S. K. W. Dertinger, A. Ajdari, I. Mezi, H. A. Stone, and G. M. Whitesides, "Chaotic mixer for microchannels" *Science* (2002), 295, 647 2002.
- [97]. M.B. Gumbiner, "Cell adhesion: the molecular basis of tissue architecture and morphogenesis" *Cell* (1996), 84, 345-357
- [98]. M.A. Schwartz, M.H. Ginsberg "Networks and crosstalk: integrin signalling spreads" *Nat. Cell. Biol.*, (2002), 4, 65–68

- [99]. J. Folkman, A. Moscona "Role of cell shape in growth control" *Nature* (1978), 273, 345–349
- [100]. X.Y. Jiang, R. Ferrigno, M. Mrksich, G.M. Whitesides, "Electrochemical desorption of self-assembled monolayers noninvasively releases patterned cells from geometrical confinements" *J. Am. Chem. Soc.* (2003), 125, 2366–2367
- [101]. F.L. Yap, Y. Zhang, "Protein and cell micropatterning and its integration with micro/nanoparticles assembly" *Biosens. Bioelectron.* (2007), 22, 775–788
- [102]. Y. Xia, G.M. Whitesides, "Replica molding with a polysiloxane mould provides this patterned microstructure" *Angew. Chem. Int. Ed. Engl.* (1998), 37, 551–575.
- [103]. M. Elisa, P. Dario, "Nanobiotechnology: soft lithography" *Prog. Mol. Subcell Biol.* (2009), 47, 341–358
- [104]. K.L. Westra, D.J. Thomson, "The microstructure of thin films observed using atomic force microscopy" *Thin Solid Films* (1995), 251, 15–21.
- [105]. Y. Yang, W. Hong, D.A. Erie, "Quantitative characterization of biomolecular assemblies and interactions using atomic force microscopy" *Quantitative Methods* (2003), 29, 175–87.
- [106]. V. Scherer, B. Bhushan, U. Rabe, W. Arnold, "Local elasticity and lubrication measurements using atomic force and friction force microscopy at ultrasonic frequencies" *IEEE Trans Mag* (1997), 33, 4077–9.
- [107]. S. Amelio, A.V. Goldade, U. Rabe, V. Scherer, B. Bhushan, W. Arnold, "Measurements of elastic properties of ultra-thin diamond-like carbon coatings using atomic force acoustic microscopy" *Thin Solid Films* (2001), 392, 75–84.
- [108]. A. Ebner, L. Wilding, R. Zhu, C. Rankl, T. Haselgrubler, P. Hinterdorfer, H.J. Gruber, "Functionalization of Probe Tips and Supports for Single-molecule Recognition Force Microscopy STM and AFM Studies on Biomolecular Systems" *STM and AFM Studies* (2008)
- [109]. R. Barattin, N. Voyer, "Chemical modifications of AFM tips for the study of molecular recognition events" *Chemical Communications* (2008), 7, 1513-32
- [110]. H. Clausen-Schaumann, M. Seitz, R. Krautbauer, H.E. Graub, "Force spectroscopy with single bio-molecules" *Current Opinion in Chemical Biology* (2000), 4, 524-30
- [111]. E. Evans, K. Ritchie, "Dynamic strength of molecular adhesion bonds" *Biophysical Journal* (1997), 72, 1541-55
- [112]. S. Izrael, S. Stepaniant, M. Balsara, Y. Oono, K. Schulten, "Molecular dynamics study of unbinding of the avidin–biotin complex" *Biophysical journal* (1997), 72, 1568-81

- [113]. J. Wong, A. Chiljoti, V.T. Moy, "Direct force measurements of the streptavidin–biotin interaction" *Biomolecular engineering* (1999), 16, 45-55
- [114]. A. Chen, V.T. Moy, "Cross-linking of cell surface receptors enhances cooperativity of molecular adhesion" *Biophysical journal* (2000), 78, 2814-20
- [115]. M. Grandbois, M. Beyer, M. Rief, H. Clausen-Schaumann, H. Gaub, "How strong is a covalent bond?" *Science* (1999), 283, 1727-30
- [116]. A. Touhami, M.H. Jericho, T.J. Beveridge, "Atomic Force Microscopy of Cell Growth and Division in *Staphylococcus aureus*" *Langmuir* (2007), 23, 2755-60
- [117]. C. Riener, "Simple test system for single molecule recognition force microscopy" *Analytica Chimica Acta* (2003), 479, 59-75
- [118]. J.A. Wieland, A.A. Gewirth, D.E. Leckband, "Single molecule adhesion measurements reveal two homophilic neural cell adhesion molecule bonds with mechanically distinct properties" *The Journal of Biological Chemistry*, (2005), 280, 41037-46
- [119]. P.A. Underwood, B.A. Dalton, J.G. Steele, F.A. Bennett, P. Strike, "Anti-fibronectin antibodies that modify heparin binding and cell adhesion: evidence for a new cell binding site in the heparin binding region" *Journal of Cell Science* (1992), 102, 833-845.
- [120]. P.A. Underwood, J.G. Steele, B.A. Dalton, "Effects of polystyrene surface chemistry on biological activity of solid phase fibronectin and vitronectin, analysed with monoclonal antibodies" *Journal of Cell Science* (1993), 104, 793-803.
- [121]. T.V. Ratto, K.C. Langry, R.E. Rudd, R.L. Balhorn, M.J. Allen, M.W. McElfresh, "Force spectroscopy of the double-tethered concanavalin-A mannose bond" *Biophysics Journal* (2004), 86, 2430
- [122]. R. Ros, F. Schwesinger, D. Anselmetti, M. Kubon, R. Schafer, A. Pluckthun, L. Tiefenauer, "Antigen binding forces of individually addressed single-chain Fv antibody molecules" *Proc. Natl. Acad. Sci. USA* (1998), 95, 7402
- [123]. R.S. Patel, E. Odermatt, J.E. Schwarzbauer, R.O Hynes, "Organization of the fibronectin gene provides evidence for exon shuffling during evolution" *EMBO J* (1987), 6, 2565-2572.
- [124]. M.K. Chaudbury, G.M. Whitesides, "Direct Measurement of Interfacial Interactions between semispherical lenses and flat sheets of poly(dimethylsiloxane) and their chemical derivatives" *Langmuir* (1991), 7, 1013-1025
- [125]. M. Bergkvist, J. Carlsson, S. Oscarsson, "Surface-dependent conformations of human plasma fibronectin adsorbed to silica, mica, and hydrophobic surfaces,

- studied with use of Atomic Force Microscopy" *S. J. Biomed. Mater. Res.* (2003), 64, 349-356
- [126]. H.P. Erickson, N.A. Carrell, "Fibronectin in extended and compact conformations. Electron microscopy and sedimentation analysis" *J. Biol. Chem.* (1983), 258, 14539-14544
- [127]. D. Chiea, R. Chiea, L.M. Chiea, "HAS particle size characterization by afm" *Romanian reports in physics* (2013), 65, 178-185
- [128]. A. Orasanu, R.H. Bradley, "AFM and XPS study on albumin adsorption onto graphite surfaces" *European Cells and Materials*, (2003), 6, 46-48.
- [129]. D.E. MacDonald, B. Markovic, M. Allen, P. Somasundaran, A.L. Boskey, "Surface analysis of human plasma fibronectin adsorbed to commercially pure titanium materials" *J. Biomed. Mater. Res.* (1998), 41, 120-130.
- [130]. H.M. Kowalczyńska, R. Kolos, M.N. Wyrzykowska, J. Dobovsky, D. Elbaum, A. Szczepankiewicz, J. Kaminski, "Atomic force microscopy evidence for conformational changes of fibronectin adsorbed on unmodified and sulfonated polystyrene surfaces" *Journal of Biomedical Materials Research* (2009), 01, 1239-51
- [131]. N.B. Guerra, C.G. Garcia, V. Llopis, J. C. R. Hernandez, D. Mortal, P. Rico, M.S. Sanchez, "Subtle variations in polymer chemistry modulate substrate stiffness and fibronectin activity" *Soft Matter* (2010), 6, 4847-55.
- [132]. U. Dammer, M. Hegner, D. Anselmetti, P. Wagner, M. Dreier, W. Huber, H.J. Guntherodt "Specific Antigen/Antibody Interactions Measured by Force Microscopy" *Biophysical Journal* (1996), 70, 2437-41.
- [133]. O.H. Willemsen, M.M.E. Snel, K.O. van der Werf, B.G. de Grooth, Jan Greve, "Simultaneous height and adhesion imaging of antibody-antigen interactions by atomic force microscopy" *Biophysical Journal* (1998), 75, 2220-28.
- [134]. M. Rief, F. Oesterhelt, B. Heymann, H.E. Gaub P., "Single Molecule Force Spectroscopy on Polysaccharides by Atomic Force Microscopy" *Science* (1997), 275, 1295-97.
- [135]. D. Falconnet, G. Csucs, H. M. Grandin, and M. Textor, "Surface engineering approaches to micropattern surfaces for cell-based assays" *Biomaterials* (2006), 27, 3044-3046.
- [136]. X.Y. Jiang, G.M. Whitesides, "Soft lithography in biology and biochemistry" *Engineering in Life Science* (2003), 3, 475-480
- [137]. R. Pankov, K.M. Yamada, "Fibronectin at a glance" *J. Cell. Sci.* (2002), 115, 3861-3863.

- [138]. E.L. George, E.N. Georges-Labouesse, R.S. Patel-King, H. Rayburn, R.O. Hynes, "Defects in mesoderm, neural tube and vascular development in mouse embryos lacking fibronectin" *Development* (1993), 119, 1079-1091.
- [139]. D. Docheva, F. Haasters, M. Schieker, "Mesenchymal Stem Cells and Their Cell Surface Receptors" *Current Rheumatology Reviews* (2008), 4, 113-116
- [140]. D.M. Beauvais, A.C. Rapraeger, "Syndecans in tumor cell adhesion and signaling" *Reprod. Biol. Endocrinol.* (2004), 2, 3.
- [141]. R.O. Hynes, "Integrins: bidirectional, allosteric signaling machines" *Cell* (2002), 110, 673-687.
- [142]. D.A. Calderwood, "Integrin activation" *J. Cell. Sci.* (2004), 117, 657-666.
- [143]. A. De Arcangelis, E. Georges-Labouesse, "Integrin and ECM functions: roles in vertebrate development" *Trends Genet.* (2000), 16, 389-395.
- [144]. D. Bouvard, C. Brakebusch, E. Gustafsson, A. Aszodi, T. Bengtsson, A. Berna, R. Fassler, "Functional consequences of enhanced by a better understanding of the trans-membrane integrin gene mutations in mice" *Circ. Res.* (2001), 89, 211-223.
- [145]. M.A. Schwartz, R.K. Assoian, "Integrins and cell proliferation: regulation of cyclin-dependent kinases via cytoplasmic signaling pathways" *J. Cell. Sci.* (2001), 114, 2553-2560.
- [146]. R.K. Assoian, M.A. Schwartz, "Coordinate signaling by integrins and receptor tyrosine kinases in the regulation of G1 phase cell-cycle progression" *Curr. Opin. Genet. Dev.* (2001), 11, 48-53.
- [147]. T.M. Guadagno, M. Ohtsubo, J.M. Roberts, R.K. Assoian, "A link between cyclin A expression and adhesion-dependent cell cycle progression" *Science* (1993), 262, 1572-1575.
- [148]. C.K. Miranti, J.S. Brugge, "Sensing the environment: a historical perspective on integrin signal transduction" *Nat. Cell. Biol.* (2002), 4, 83-90.
- [149]. C.S. Chen, D.E. Ingber "Tensegrity and mechanoregulation: from skeleton to cytoskeleton" *Osteoarthritis Cartilage* (1999), 7, 81-94.
- [150]. C. O'Neill, P. Jordan, G. Ireland, "Evidence for two distinct mechanisms of anchorage stimulation in freshly explanted and 3T3 Swiss mouse fibroblasts" *Cell* (1986), 44, 489-496.
- [151]. J.E. Meredith, B. Fazeli, M.A. Schwartz, "The extracellular matrix as a cell survival factor" *Mol. Biol. Cell* (1993), 4, 953-961.

- [152]. D.G. Stupack, X.S. Puente, S. Boutsaboualoy, C.M. Storgard, D.A. Cheresh, "Apoptosis of adherent cells by recruitment of caspase-8 to unligated integrins" *J. Cell Biol.* (2001), 155, 459-470.
- [153]. M.M. Bakre, Y. Zhu, H. Yin, D.W. Burton, R. Terkeltaub, L.J. Deftos, J.A. Varner, "Parathyroid hormone-related peptide is a naturally occurring, protein kinase A-dependent angiogenesis inhibitor" *Nat. Med.* (2002), 8, 995-1003.
- [154]. S. Kim, M. Bakre, H. Yin, J.A. Varner, "Inhibition of endothelial cell survival and angiogenesis by protein kinase A" *J. Clin. Invest.* (2002), 110, 933-941.
- [155]. N. Boudreau, C. Andrews, A. Srebrow, A. Ravanpay, D.A. Cheresh, "Induction of the angiogenic phenotype by Hox D3" *J. Cell. Biol.* (1997), 139, 257-264.
- [156]. Z. Zhang, K. Vuori, J.C. Reed, E. Ruoslahti, "The alpha 5 beta 1 integrin supports survival of cells on fibronectin and up-regulates Bcl-2 expression" *Proc. Natl. Acad. Sci. U S A* (1995), 92, 6161-6165.
- [157]. N. Boudreau, C.J. Sympson, Z. Werb, M.J. Bissell, "Suppression of ICE and apoptosis in mammary epithelial cells by extracellular matrix" *Science* (1995), 267, 891-893.
- [158]. M. Rytomaa, L.M. Martins, J. Downward, "Involvement of FADD and caspase-8 signalling in detachment-induced apoptosis" *Curr. Biol.* (1999), 9, 1043-1046.
- [159]. S. Kim, M. Harris, J.A. Varner, "Regulation of integrin alpha5beta1-mediated endothelial cell migration and angiogenesis by integrin alpha5beta1 and protein kinase A" *J. Biol. Chem.* (2000), 275, 33920-33928.
- [160]. L. Moro, M. Venturino, C. Bozzo, L. Silengo, F. Altruda, L. Beguinot, G. Tarone, P. Defilippi, "Integrins induce activation of EGF receptor: role in MAP kinase induction and adhesion-dependent cell survival" *EMBO J* (1998), 17, 6622-6632.
- [161]. A. Danilkovitch-Miagkova, D. Angeloni, A. Skeel, S. Donley, M. Lerman, E.J. Leonard, "Integrin-mediated RON growth factor receptor phosphorylation requires tyrosine kinase activity of both the receptor and c-Src" *J. Biol. Chem.* (2000), 275, 14783-14786.
- [162]. M.K. Majumdar, M. Keane-Moore, D. Buyaner, W.B. Hardy, M.A. Moorman, K.R. McIntosh, J.D. Mosca, "Characterization and functionality of cell surface molecules on human mesenchymal stem cells" *J. Biomed. Sci.* (2003), 10, 228-241.
- [163]. S. Gronthos, P.J. Simmons, S.E. Graves, P.G. Robey, "Integrin-mediated interactions between human bone marrow stromal precursor cells and the extracellular matrix" *Bone* (2001), 28, 174-181.
- [164]. K.M. Kowalzynska, M.N. Wyrzykoska, "Modulation of adhesion, spreading and cytoskeleton organization of 3T3 fibroblasts by sulfonic groups present on polymer surfaces" *Cell biology international* (2003), 27, 101-114.

- [165]. R.A.F. Clark, A.J. Qiang, D. Greiling, A. Khan, J.E. Schwarzbauer, "Fibroblast migration on fibronectin requires three distinct functional domains" *The journal of investigative dermatology* (2003), 121, 4-8.
- [166]. M. Caruso, L. Belloni, O. Sthandler, P. Amati, M.I. Garcia, " $\alpha 4\beta 1$ integrin acts as a cell receptor for murine polyomavirus at the post-attachment level" *Journal of virology* (2003), 77, 3913-3921
- [167]. M. Amiji, K. Park, "Prevention of protein adsorption and platelet adhesion on surfaces by PEO/PPO/PEO triblock copolymers" *Biomaterials* (1992) 13, 682
- [168]. K.N. Prasad, T.T. Luong, A.T. Florence, J. Paris, C. Vaution, M. Seiller, F. Puisieux, "Surface activity and association of ABA polyoxyethylene-polyoxypropylene block copolymers in aqueous solution" *J. Colloid Interface Sci.* (1979) 69, 225-230
- [169]. J.L. Tan, W. Liu, C.M. Nelson, S. Raghavan, C.S. Chen, "Simple approach to micropattern cells on common culture substrates by tuning substrate wettability" *Tissue Engineering* (2004), 5, 865-872
- [170]. S.L. McGurk, R.J. Green, G.H.W. Sanders, M.C. Davies, C.J. Roberts, S.J.B. Tendler, P.M. Williams, "Molecular interactions of biomolecules with surface-engineered interfaces using atomic force microscopy and surface plasmon resonance" *Langmuir* (1999) 15, 5134-5136.
- [171]. M.R. Nejadnik, A.L. J. Olsson, P.K. Sharma, H.C. van der Mei, W. Norde, H.J. Busscher, "Adsorption of Pluronic F-127 on Surfaces with Different Hydrophobicities Probed by Quartz Crystal Microbalance with Dissipation" *Langmuir* (2009), 25, 6245-6249.
- [172]. J.M. Corey, C.C. Gertz, T.J. Sutton, Q. Chen, K.B. Mycek, B.S. Wang, A.A. Martin, S.L. Johnson, E.L. Feldman, "Patterning N-type and S-type Neuroblastoma Cells with Pluronic F108 and ECM Proteins" *Journal of biomedical materials research Part A* (2010), 93, 673-686.
- [173]. Z. Wu, K. Hjort, "Surface modification of PDMS by gradient-induced migration of embedded Pluronic" *Lab on Chip* (2009), 9, 1500-1503.
- [174]. M. Ramstedt, R. Nakao, S. N. Way, B.U Uhlin, J.F Boliv, "Monitoring surface chemical changes in the bacterial cell wall: multivariate analysis of cryo-x-ray photoelectron spectroscopy data" *J. Biol. Chem.* (2011), 8, 12389-96.
- [175]. D. Docheva, C. Popov, M. Mutschler, M. Schieker, "Human mesenchymal stem cells in contact with their environment: surface characteristics and the integrin system" *J Cell Mol Med* (2007), 11, 21-38.
- [176]. M.A. Mooney, D.E. Ingber, "Extracellular matrix controls tubulin monomer levels in hepatocytes by regulating protein turnover" *Mol. Biol. Cell.* (1994), 5, 967-979.

- [177]. Y. Yamada, H.K. Kleinman, "Functional domains of cell adhesion molecules" *Curr. Opin. Cell. Biol.* 1992, 4, 819–823.
- [178]. K. Lewandowska, N. Balachander, C.N. Sukenik, L.A. Culp, "Modulation of fibronectin adhesive functions for fibroblasts and neural cells by chemically derivatized substrata" *J. Cell Physiol.* (1989), 141, 334–345.
- [179]. M.D. Pierschbacher, E. Ruoslahti, "Variants of the cell recognition site of fibronectin that retain attachment-promoting activity" *Proc. Natl. Acad. Sci. USA* (1984), 81, 5985–5988
- [180]. D.R. Absolom, W. Zingg, A.W. Neumann, "Protein adsorption to polymer particles: role of surface properties" *J. Biomed. Mater. Res.* (1987), 21, 161–71.
- [181]. G. Altankov, T. Groth, N. Krasteva, W. Albrecht, D. Paul, "Morphological evidence for a different fibronectin receptor organization and function during fibroblast adhesion on hydrophilic and hydrophobic glass substrata" *J. Biomater. Sci. Polym.* (1997), 8, 721–40.
- [182]. T.A. Haas, E.F. Plow, "Integrin–ligand interactions: a year in review" *Curr Opin Cell Biol* (1994), 6, 656–62.
- [183]. M.J. Humphries, "Integrin activation: the link between ligand binding and signal transduction" *Curr Opin Cell Biol* (1996), 8, 632–40.
- [184]. R.C. Liddington, L.A. Bankston, "The structural basis of dynamic cell adhesion: heads, tails, and allostery" *Exp Cell Res* (2000), 261, 37–43.
- [185]. W. Norde, C.A. Haynes, "Thermodynamics of protein adsorption" Brash JL, Wojciechowski PW, editors. *Interfacial phenomena and bioproducts* New York: Marcel Dekker (1996), 123–44
- [186]. S.J. Lee, K. Park "Statistical mechanics of protein adsorption" Brash JL, Wojciechowski PW, editors. *Interfacial phenomena and bioproducts* New York: Marcel Dekker (1996), 173–207
- [187]. C.S. Lai, C.E. Wolff, D. Novello, L. Griffone, C. Cuniberti, F. Molina et al. "Solution structure of human plasma fibronectin under different solvent conditions. Fluorescent energy transfer, circular dichroism and light-scattering studies" *J Mol Biol* (1993), 230, 625–40.
- [188]. E. Odermatt, J. Engel, "Physical properties of fibronectin" Mosher DF, editor. *Fibronectin*. San Diego: Academic Press, 1989;25–45.
- [189]. T.P. Ugarova, C. Zamarron, Y. Veklich, R.D. Bowditch, M.H. Ginsberg, J.W. Weisel et al. "Conformational transitions in the cell binding domain of fibronectin" *Biochemistry* (1995), 34, 4457–66.

- [190]. E K.B. McClary, T. Ugarova, D.W. Grainger, "Modulating fibroblast adhesion, spreading, and proliferation using self-assembled monolayer films of alkylthiolates on gold" *J Biomed Mater Res* (2000), 50, 428–39.
- [191]. T.A. Horbett, L.A. Klumb, "Cell culturing: surface aspects and considerations" Brash JL, Wojciechowski PW, editors. *Interfacial phenomena and bioproducts* New York: Marcel Dekker (1996), 351–445.
- [192]. W.C. Hung, S.H. Chen, C.D. Paul, K.M. Stroka, Y.C. Lo, J.T. Yang, K. Konstantopoulos, "Distinct signaling mechanisms regulate migration in unconfined versus confined spaces" *Journal of cell biology* (2013), 202, 807–824
- [193]. S. Alexander, G.E. Koehl, M. Hirschberg, E.K. Geissler, P. Friedl, "Dynamic imaging of cancer growth and invasion: a modified skin-fold chamber model" *Histochem. Cell Biol.* (2008) 130:1147–1154.
- [194]. P. Friedl, S. Alexander, "Cancer invasion and the microenvironment plasticity and reciprocity" *Cell* (2011), 147, 992–1009.
- [195]. A.J. Ridley, M.A. Schwartz, A.R. Horwitz, "Cell migration: integrating signals from front to back" *Science* (2003), 302, 1704–1709.
- [196]. A. Curtis, C. Wilkinson, "Topographical control of cells" *Biomaterials* (1997), 18, 1573–1583.
- [197]. M. Ghibaudo, L. Trichet, B. Ladoux, "Substrate topography induces a crossover from 2D to 3D behavior in fibroblast migration" *Biophys. J.* (2009), 97, 357–368.
- [198]. S.J. Han, K.S. Bielawski, N.J. Sniadecki, "Decoupling substrate stiffness, spread area, and micropost density: a close spatial relationship between traction forces and focal adhesions" *Biophys. J.* (2012), 103, 640–648.
- [199]. R. McBeath, D.M. Pirone, C.S. Chen, "Cell shape, cytoskeletal tension, and RhoA regulate stem cell lineage commitment" *Dev. Cell* (2004), 6, 483–495.
- [200]. R. Singhvi, A. Kumar, D.E. Ingber, "Engineering cell shape and function" *Science* (1994), 264, 696–698.
- [201]. C.S. Chen, M. Mrksich, D.E. Ingber, "Geometric control of cell life and death" *Science* (1997), 276, 1425–1428.
- [202]. P. Friedl, K. Wolf, "Plasticity of cell migration: a multiscale tuning model" *J. Cell Biol.* (2009), 188, 11–19.
- [203]. P. Friedl, S. Borgmann, E.B. Bröcker, "Amoeboid leukocyte crawling through extracellular matrix: lessons from the Dictyostelium paradigm of cell movement" *J. Leukoc. Biol.* (2001), 70, 491–509.

- [204]. T. Lämmermann, M. Sixt, "Mechanical modes of 'amoeboid' cell migration" *Curr. Opin. Cell Biol.* (2009), 21, 636–644.
- [205]. G.I. Kaye, L.F. Siegel, R.R. Pascal, "Cell replication of mesenchymal elements in adult tissues. I. The replication and migration of mesenchymal cells in the adult rabbit dermis" *Anat. Rec.* (1971), 169, 593–611.
- [206]. F. Grinnell, "Fibroblast mechanics in three-dimensional collagen matrices" *J. Bodyw. Mov. Ther.* (2008), 12, 191–193.
- [207]. K. Paňková, D. Rösel, M. Novotný, J. Brábek, "The molecular mechanisms of transition between mesenchymal and amoeboid invasiveness in tumor cells" *Cell. Mol. Life Sci.* (2010), 67, 63-71.
- [208]. N. Nishiya, W.B. Kiosses, J. Han, M.H. Ginsberg, "An alpha4 integrin-paxillin-Arf-GAP complex restricts Rac activation to the leading edge of migrating cells" *Nat. Cell Biol.* (2005), 7, 343-352.
- [209]. P.M. Kulesa, S.E. Fraser, "In ovo time-lapse analysis of chick hind brain neural crest cell migration shows cell interactions during migration to the branchial arches" *Development* (2000), 127, 1161–1172.
- [210]. E.K. Lee, J.S. Lee, H.S. Park, C.H. Kim, Y.J. Gin, Y. Son, "Stretch-stimulated cellular rearrangement and alteration of fibronectin matrix assembly, α -smooth muscle actin, and CD44 expression in human mesenchymal stem cells" *Tissue Engineering and Regenerative Medicine* (2005), 2, 94-99.
- [211]. B. Li, C. Moshfegh, Z. Lin, J. Albuschies, V. Vogel, "Mesenchymal stem cells exploit extracellular matrix as mechanotransducer" *Scientific reports* (2013), 3, 1-8
- [212]. R. Merkel, P. Nassoy, A. Leung, K. Ritchie, E. Evans, "Energy landscapes of receptor–ligand bonds explored with dynamic force spectroscopy," *Nature* (1999), 397, 50-53.
- [213]. J. Fritz, A.G. Katopodis, F. Kolbinger, D. Anselmetti, "Force-Mediated Kinetics of Single P-selectin/Ligand Complexes Observed by Atomic Force Microscopy," *Proc. Nat. Acad. Sci. USA* (1998), 95, 12283-12289.
- [214]. G. Baneyx, L. Baugh, V. Vogel, "Fibronectin extension and unfolding within cell matrix fibrils controlled by cytoskeletal tension" *Proc. Natl. Acad. Sci. U. S. A.* (2002) 99, 5139–5143.
- [215]. C. Zhong, *et al.* "Rho-mediated contractility exposes a cryptic site in fibronectin and induces fibronectin matrix assembly" *J. Cell Biol.* (1998) 141, 539–551.
- [216]. A.A. Sawyer, K.M. Hennessy, S.L. Bellis, "The effect of adsorbed serum proteins, RGD and proteoglycan-binding peptides on the adhesion of mesenchymal stem cells to hydroxyapatite" *Biomaterials* (2007) 28, 383-392.

- [217]. M.A. Schwartz, A.R. Horwitz, "Integrin adhesion, protrusion, and contraction during cell migration" *Cell* (2006) 125, 1223-5.
- [218]. F. Guo, M. Debidda, D.A. Williams, Y. Zheng, "Genetic deletion of Rac1 GTPase reveals its critical role in actin stress fibre formation and focal adhesion complex assembly" *J. Biol. Chem.* (2006) 281, 18652-59.